Raman Spectral Studies on Stereochemistry of Cobalt(III) Complexes with Maltidentate Ligands

A thesis submitted in partial fulfilment
of the requirements for
the degree of
Doctor of Science

Tatsuya Kawamoto
University of Tsukuba
1988

Contents

	Page
Chapter I. Introductory Remarks	1
Chapter II. General Background	4
II-A. Stereochemistry of Cobalt(III) complexes	4
II-A-1. Cobalt(III) Complexes with Bidentate Ligands Containing N and O Donor Atoms ..	4
II-A-2. Cobalt(III) Complexes with Linear Terdentate Ligands Containing N and O Donor Atoms	4
II-A-3. [Co(quadridentate)(bidentate)]-Type Complexes	5
II-A-4. Cobalt(III) Complexes with Sulfur-containing Bidentate ligands	6
II-A-5. $[Co(DL\text{-}asp)(dien)]^+$ and $[Co(\text{branched terdentate})_2]$-Type Complexes ..	6
II-B. Theory of Normal Vibration	15
II-B-1. Kinetic and Potential Energies	15
II-B-2. Normal Coordinates	16
II-B-3. Group Theoretical Treatment of Normal Coordinates	17
II-B-4. Number of Normal Vibrations for Each Species	18
II-B-5. Use of Internal Coordinates	20
II-B-6. Principle of GF Matrix Method	22
II-B-7. Potential Fields and Force Constants	24
II-B-8. Depolarization of Raman Bands	27

Chapter III. Experimental 31
III-A. Preparation of Complexes 31
III-A-1. Tris(bidentate)cobalt(III) Complexes with Six and/or Five-Membered Chelate Rings 31
III-A-2. Cobalt(III) Complexes with Linear Terdentate Ligands Containing N and O Donor Atoms 33
III-A-3. Cobalt(III) Complexes with Terdentate Ligands Containing N-Methyl Group 35
III-A-4. Cobalt(III) Complexes with Quadridentate Ligands 37
III-A-5. Cobalt(III) Complexes with Sulfur-containing Ligands 40
III-A-6. Cobalt(III) Complexes with Branched Terdentate Ligands 41
III-B. Measurements 42
III-C. Calculation 44
III-D. Elemental Analytical Data 44
III-E. Absorption Spectra 44
Chapter IV. Normal Coordinate Analysis of $[Co(en)_3]^{3+}$ and $[Co(tn)_3]^{3+}$ 50
IV-A. Introduction 50
IV-B. Results 51
IV-B-1. Normal Coordinate Analysis of $[Co(en)_3]^{3+}$ 51
IV-B-2. Normal Coordinate Analysis of $[Co(tn)_3]^{3+}$ 52
IV-C. Discussion 65

Chapter V. Raman Spectral Characteristics of Cobalt(III) Complexes 67
V-A. Introduction 67
V-B. Results and Discussion 68
V-B-1. Raman Spectra of Cobalt(II) Complexes with Bidentate Ligands Containing N and/or O Donor Atoms 68
V-B-2. Raman Spectral Characteristics of the Geometrical Isomers of Cobalt(III) Complexes with Five- and Six-membered Chelate Rings 78
V-B-3. Raman Spectra of Cobalt(III) Complexes with Linear Terdentate Ligands Containing N and O Donor Atoms 86
General Aspects 89
Raman Spectral Characteristics of the Geometrical Isomers of Cobalt(III) Complexes with Linear Terdentate Ligands 92
Influence of Coordinated Atoms and Ligands on Raman Spectral Characteristics of Cobalt(III) Complexes with Linear Terdentate Ligands 111
V-B-4. Raman Spectra of Cobalt(III) Complexes with Terdentate Ligands Containing N-Methyl Group 116
V-B-5. Raman Spectral Characteristics of Cobalt(III) Complexes with Quadridentate Ligands 131
General Aspects 131
Raman Spectra of [Co(trien)(bidentate)]- and

[Co(tren)(bidentate)]-Type Complexes 138
Raman Spectra of [Co(edda)(bidentate)]-Type and $[Co(aeida)(en)]^+$ Complexes 142
Role of Bidentate Ligands 143
V-B-6. Raman Spectra of the Cobalt(III) Complexes with Sulfur-containing Ligands 144
V-B-7. Raman Spectra of the Cobalt(III) Complexes with Branched Terdentate Ligands 154
Chapter VI. Concluding Remarks 165
References 171
Acknowledment 177

Abbreviation of ligands

en	1,2-ethanediamine	$NH_2CH_2CH_2NH_2$
Hgly	glycine	NH_2CH_2COOH
H_2ox	oxalic acid	HOOCCOOH
tn	1,3-propanediamine	$NH_2CH_2CH_2CH_2NH_2$
β-Hala	β-alanine	$NH_2CH_2CH_2COOH$
dien	3-azapentane-1,5-diamine	$NH_2CH_2CH_2NHCH_2CH_2NH_2$
Hedma	ethylenediamine-N-acetic acid	$NH_2CH_2CH_2NHCH_2COOH$
H_2ida	iminodiacetic acid	$NH(CH_2COOH)_2$
mdien	3-methyl-3-azapentane-1,5-diamine	$NH_2(CH_2)_2N(CH_3)(CH_2)_2NH_2$
H_2mida	N-methyliminodiacetic acid	$CH_3N(CH_2COOH)_2$
trien	triethylenetetramine	$NH_2(CH_2)_2NH(CH_2)_2NH(CH_2)_2NH_2$
tren	tris(2-aminoethyl)amine	$N(CH_2CH_2NH_2)_3$
H_2edda	ethylenediamine-N,N'-diacetic acid	$HOOCCH_2NH(CH_2)_2NHCH_2COOH$
H_2aeida	N-(2-aminoethyl)iminodiacetic acid	$NH_2(CH_2)_2N(CH_2COOH)(CH_2COOH)$
Haet	2-aminoethanethiol	$NH_2CH_2CH_2SH$
Haese	aminoethanesulfenic acid	$NH_2CH_2CH_2SOH$
Haesi	aminoethanesulfinic acid	$NH_2CH_2CH_2SO_2H$
mea	2-(methylthio)ethylamine	$NH_2CH_2CH_2SCH_3$
DL-H_2asp	DL-aspartic acid	$HOOCCH_2\overset{*}{C}H(NH_2)COOH$
L-Hsmc	S-methyl-L-cysteine	$CH_3SCH_2\overset{*}{C}H(NH_2)COOH$
L-Hmet	L-methionine	$CH_3S(CH_2)_2\overset{*}{C}H(NH_2)COOH$

Chapter I. Introductory Remarks

I-A. General Features of Raman Spectroscopy.

In recent years, the applicable areas for chemical analysis of Raman spectroscopy became dramatically wide by the use of photomultiplier and lasers. The utilization of photomultiplier as a detector made it feasible to directly record Raman spectra, and that of lasers removed the restriction on sample of the Raman spectral measurements. In contrast with the Raman spectral measurements by using the mercury arc as an excitation source in early studies, a high power and a selectivity of excitation line of the laser afforded us to facilitate the Raman spectral measurements of colored materials such as transition metal complexes, which have d-d absorption in the visible region.

Raman and infrared spectroscopies are regarded as complementary methods for investigation of molecular vibrations. The vibration which causes a change of the dipole moment of the molecule is infrared active, while the vibration which causes a change of the polarizability of the molecule is Raman active. It may be seen from the group theoretical consideration that in the character table a totally symmetric vibration is Raman active in any point groups and the infrared and Raman active vibrations always belong to u and g types, respectively, when the point group has a center of symmetry, thereby holding the "mutual exclusion rule". Therefore, Raman spectral studies are absolutely necessary and important for a full assignment of

the normal vibrations of the molecule.

Furthermore, Raman spectroscopy has the following characteristic features compared with infrared spectroscopy: (1) The Raman spectra of an aqueous solution can be easily mesured. Accordingly, the vibration spectra can be obtained that have no lattice vibrations and no coupling between intramolecular and lattice vibrations. Moreover, in the low frequency region, solute molecule in the aqueous solution does not give any overlapped Raman spectrum with that of solvent (water) because water molecule exhibit no Raman bands in that region; the Raman spectra of the aqueous solution are not complicated compared with those of solid state because it is thought that the solute molecule in the aqueous solution generally have higher symmetry property owing to relaxation of the restriction in molecular structures. These spectral features make it easy to assign the observed Raman bands. (2) The polarization measurements of the Raman lines in liquids and solutions give an indication of the symmetry property of the normal vibration; Raman bands due to totally symmetric vibrations appear as polarized bands ($0 \leqq \rho < 3/4$, ρ: depolarization ratio) and bands due to nontotally symmetric vibrations appear as depolarized bands ($\rho = 3/4$). (3) Localized vibrations of the molecule appear as strong bands in the infrared spectra. This feature is widely used for qualitative analysis. On the other hand, vibrations as a whole molecule appear as strong bands in the Raman spectra. This suggests that the

molecular symmetry will be reflected more definitely on the Raman spectra than on the infrared spectra. Especially, it seems that the Raman spectra of octahedral complexes in the skeletal vibration region, which appear in the low frequency region, considerably reflect their structural characteristics and are suitable for the vibrational study of geometrical isomers of the complexes. And, (4) combination bands and overtones are scarcely observed in normal Raman spectra of the octahedral complexes.

I-B. Purpose of This Work.

This work was undertaken for the following purposes:

(a) To assign the Raman spectra of the cobalt(III) complexes in the skeletal vibration region.

(b) To elucidate the Raman spectral features for differentiating the coordinated atoms and ligands of the cobalt(III) complexes.

(c) To investigate the influence on the Raman spectra of the size of chelate rings and the number of link of chelate rings.

(d) To find any vibrational criteria for differentiating the geometrical isomers of the cobalt(III) complexes.

(e) To apply the vibrational criteria for new isomeric pairs prepared in this work.

(f) To obtain a transferable set of force constants to reproduce the vibrational frequencies of a series of cobalt(III) complexes.

Chapter II. General Background

II-A. Stereochemistry of Cobalt(III) Complexes.

II-A-1. Cobalt(III) Complexes with Bidentate Ligands Containing N and O Donor Atoms.

Three geometrical isomers are possible for each of $[Co(gly)_2(en)]^+$, $[Co(\beta\text{-ala})_2(en)]^+$, and $[Co(\beta\text{-ala})_2(tn)]^+$ and their isomers are denoted by C_1-cis(O), C_2-cis(O), and trans(O) with respect to the arrangements of the chelate rings and the coordinated oxygen atoms (Fig. 1).

Likewise, $[Co(gly)_2(ox)]^-$ may be expected to have three geometrical isomers and their isomers are denoted by C_1-cis(N), C_2-cis(N), and trans(N) with respect to the arrangements of the chelate rings and the coordinated nitrogen atoms (Fig. 1).

On the contrary, two geometrical isomers are possible for each of $[Co(gly)_3]$, $[Co(\beta\text{-ala})_3]$, and [Co(gly)(ox)(en)] and their isomers are denoted by fac(N) and mer(N) with respect to the arrangement of the coordinated nitrogen atoms (Fig. 1).

II-A-2. Cobalt(III) Complexes with Linear Terdentate Ligands Containing N and O Donor Atoms.

Three geometrical isomers are possible for each of $[Co(dien)_2]^{3+}$, $[Co(ida)(dien)]^+$, and $[Co(ida)_2]^-$ and their isomers are designated as sym-fac, unsym-fac, and mer with respect to the arrangement of the chelate rings (Fig. 2).

There are four possible geometrical isomers for

[Co(edma)(dien)]$^{2+}$ (Fig. 3) and for [Co(edma)(ida)] (Fig. 4). The four isomers of [Co(edma)(dien)]$^{2+}$ are designated as sym-fac, unsym-fac-fac(N_t), unsym-fac-mer(N_t), and mer with respect to the arrangements of the chelate rings and the coordinated terminal nitrogen atoms (where N_t stands for the terminal nitrogen atom). The four isomers of [Co(edma)(ida)] are analogously designated as sym-fac, unsym-fac-mer(N), unsym-fac-fac(N), and mer with respect to the arrangements of the chelate rings and the coordinated nitrogen atoms.

[$Co(edma)_2$]$^+$ has six possible geometrical isomers and their isomers are denoted by sym-fac-trans(N_t), sym-fac-cis(N_t), unsym-fac-cis(N_t)trans(O), unsym-fac-cis(N_t)cis(O), unsym-fac-trans(N_t), and mer with respect to the arrangements of the chelate rings and the coordinated atoms, N_t and O (Fig. 5).

II-A-3. [Co(quadridentate)(bidentate)]-Type Complexes.

Two geometrical isomers are possible for each of the [Co(trien)(bidentate)]-type and [Co(edda)(bidentate)]-type complexes and their isomers are denoted by cis-α and cis-β with respect to the arrangement of the quadridentate ligands (Fig. 6).

Likewise, two geometrical isomers are possible for [Co(aeida)(en)]$^+$ and their isomers are denoted by trans(O) and cis(O) with respect to the arrangement of the coordinated oxygen atoms (Fig. 6).

On the contrary, possible geometrical isomer of the [Co(tren)(bidentate)]-type complexes is only one (Fig. 6).

II-A-4. Cobalt(III) Complexes with Sulfur-Containing Bidentate Ligands.

For all these types of complexes, which belong to the $[Co(N-S)(en)_2]$- or $[Co(S-O)(en)_2]$-type, the possible geometrical isomer is restricted to only one, as shown in Fig. 7.

II-A-5. $[Co(DL-asp)(dien)]^+$ and $[Co(branched\ terdentate)_2]$-Type Complexes.

Three geometrical isomers are possible for $[Co(DL-asp)(dien)]^+$ and their isomers are designated as sym-cis, $unsym^1$-cis, and $unsym^2$-cis as depicted in Fig. 8.

$[Co(DL-asp)_2]^-$ has five geometrical isomers and their isomers are designated as trans·trans·trans, trans(N), cis(N)trans(O_5), cis·cis·cis, and cis(N)trans(O_6) with respect to the arrangement of the coordinated atoms, N, O (where O_5 and O_6 stand for oxygen atoms in five- and six-membered chelate rings, respectively) (Fig. 9).

Three geometrical isomers are possible for each of $[Co(L-smc)_2]^+$ and $[Co(L-met)_2]^+$ and their isomers are denoted by trans(N), trans(O), and trans(S) with respect to the arrangement of the coordinated atoms, N, S, and O (Figs. 10 and 11).

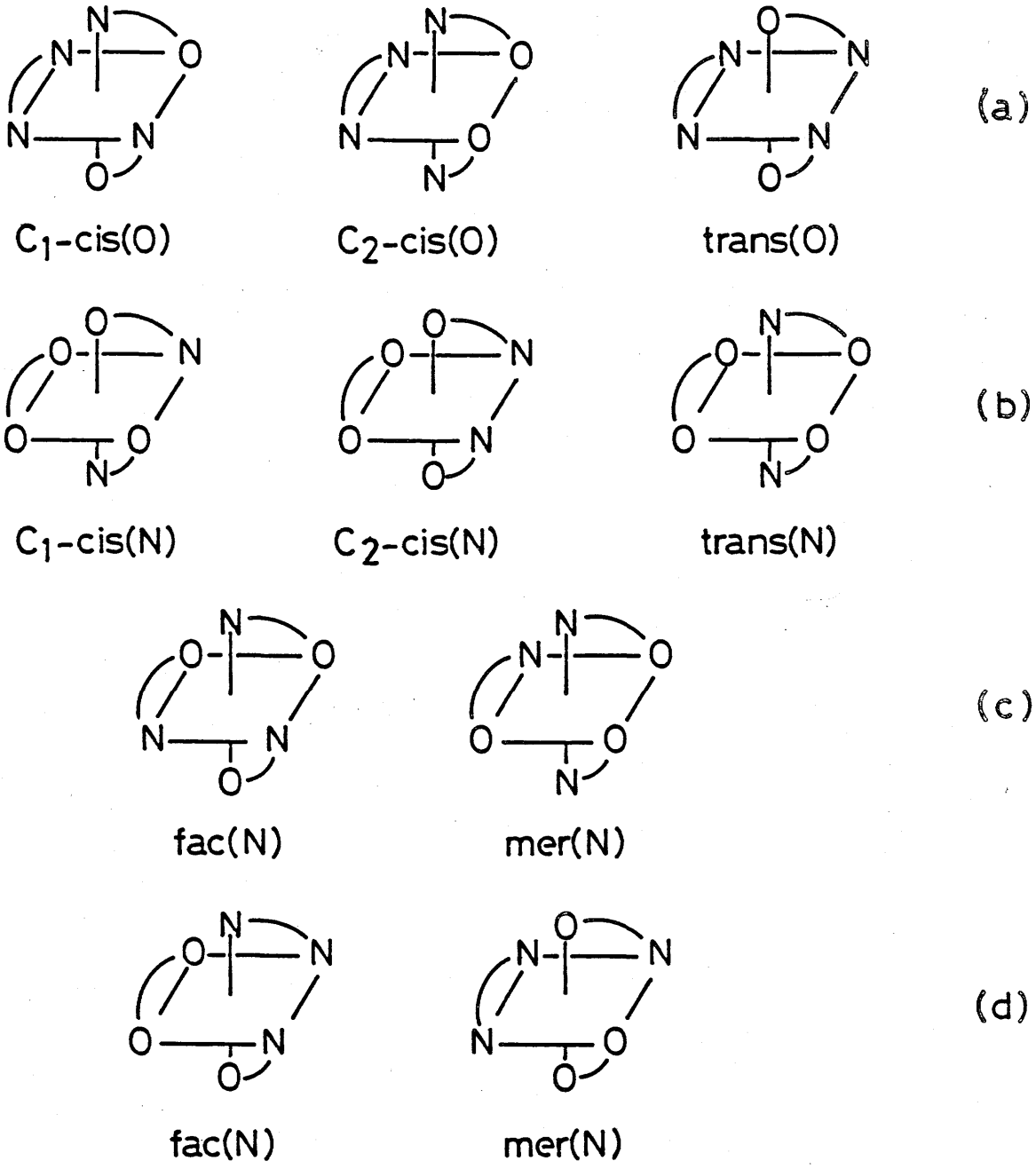

Figure 1. Three geometrical isomers of $[Co(gly)_2(en)]^+$, $[Co(\beta\text{-ala})_2(en)]^+$, $[Co(\beta\text{-ala})_2(tn)]^+$ (a), and $[Co(gly)(ox)_2]^-$ (b). Two geometrical isomers of $[Co(gly)_3]$, $[Co(\beta\text{-ala})_3]$ (c) and [Co(gly)(ox)(en)] (d).

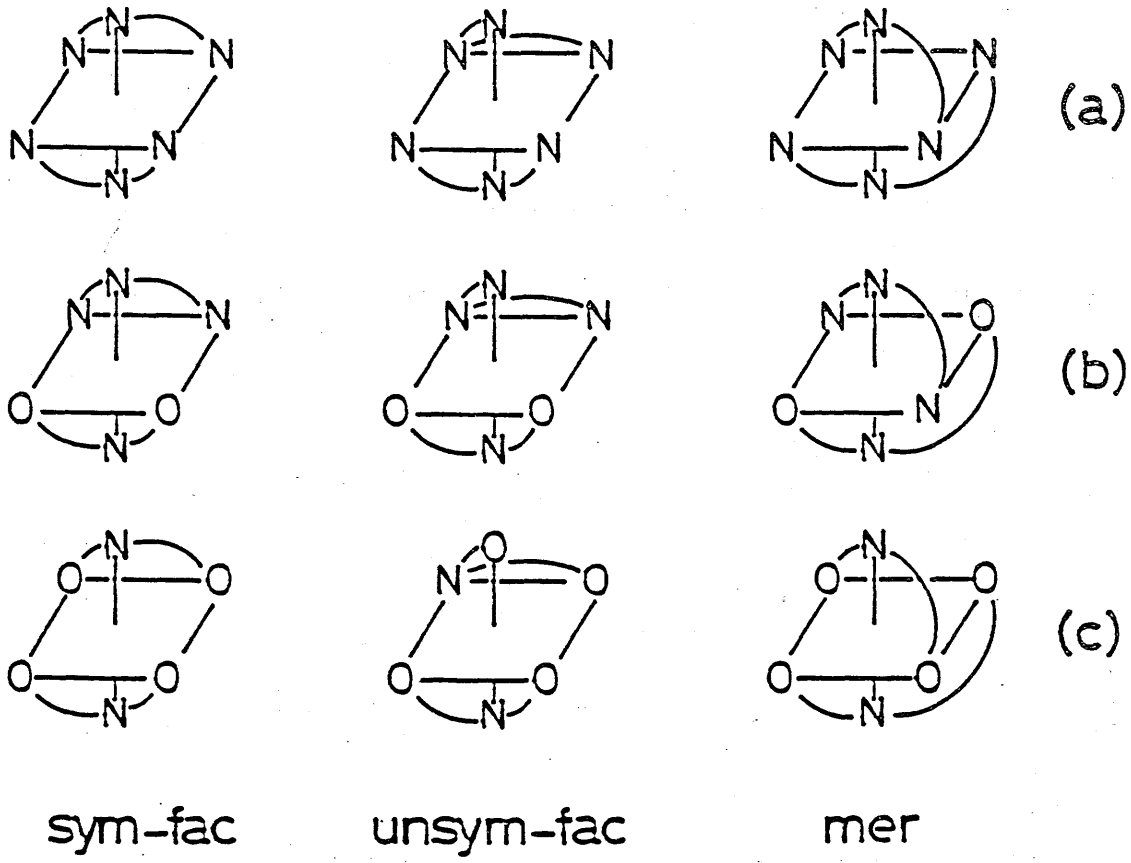

Figure 2. Three geometrical isomers of $[Co(dien)_2]^{3+}$ (a), $[Co(ida)(dien)]^{+}$ (b), and $[Co(ida)_2]^{-}$ (c).

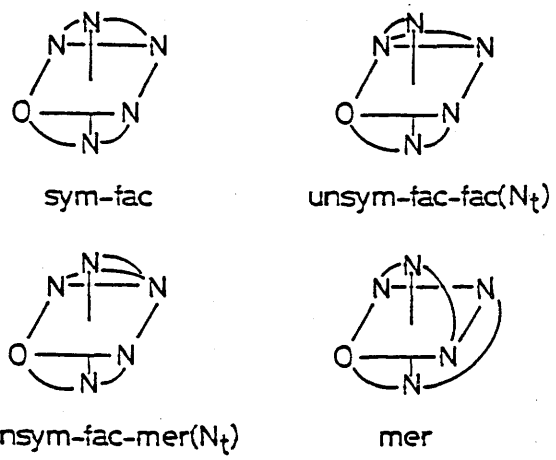

Figure 3. Four geometrical isomers of $[Co(edma)(dien)]^{2+}$.

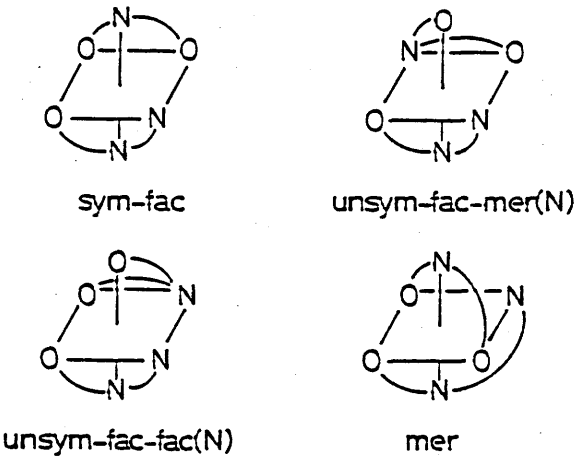

Figure 4. Four geometrical isomers of $[Co(edma)(ida)]$.

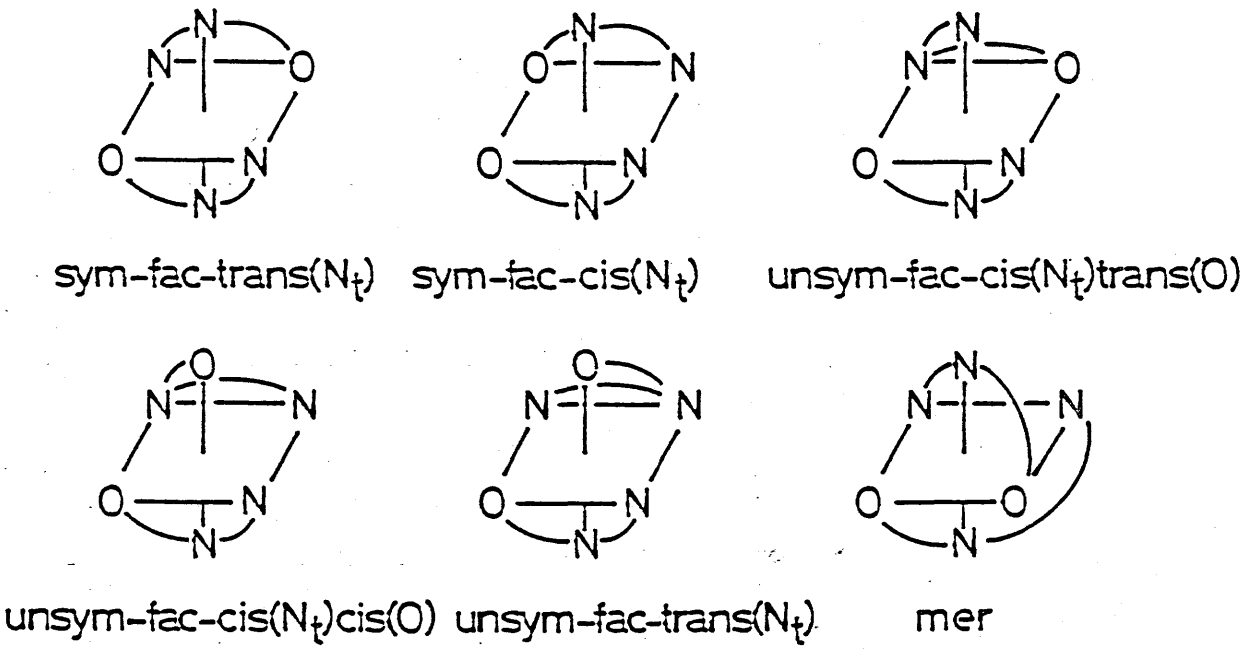

Figure 5. Six geometrical isomers of $[Co(edma)_2]^+$.

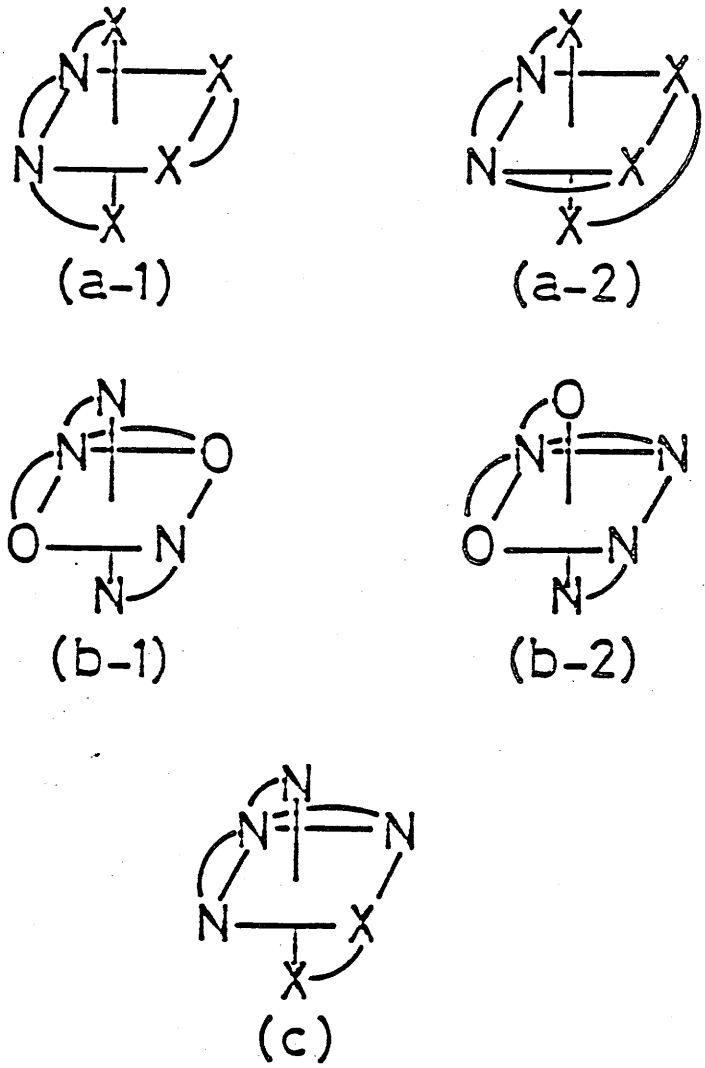

Figure 6. Structures of [Co(quadridentate)(bidentate)]-type complexes. Cis-α (a-1) and cis-β (a-2) isomers of the complexes with trien (X = N) and edda (X = O), trans(O) (b-1) and cis(O) (b-2) isomers of $[Co(aeida)(en)]^+$, and the complexes with tren (c).

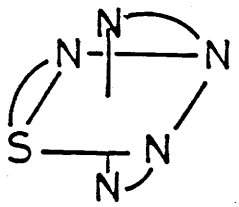

[Co(N-S)(en)$_2$]-type

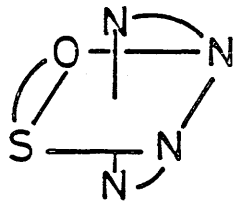

[Co(S-O)(en)$_2$]-type

Figure 7. Structures of [Co(N-S)(en)$_2$]- and [Co(S-O)(en)$_2$]-type complexes.

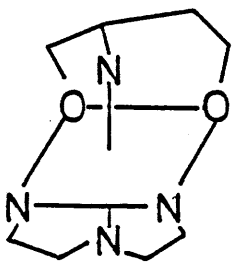

sym-cis

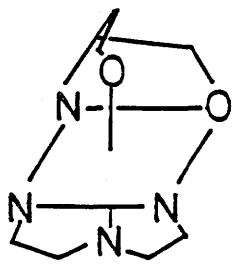

unsym^1-cis

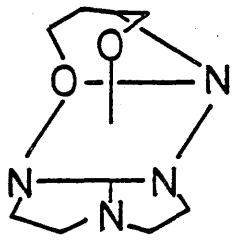

unsym^2-cis

Figure 8. Three geometrical isomers of [Co(DL-asp)(dien)]$^+$.

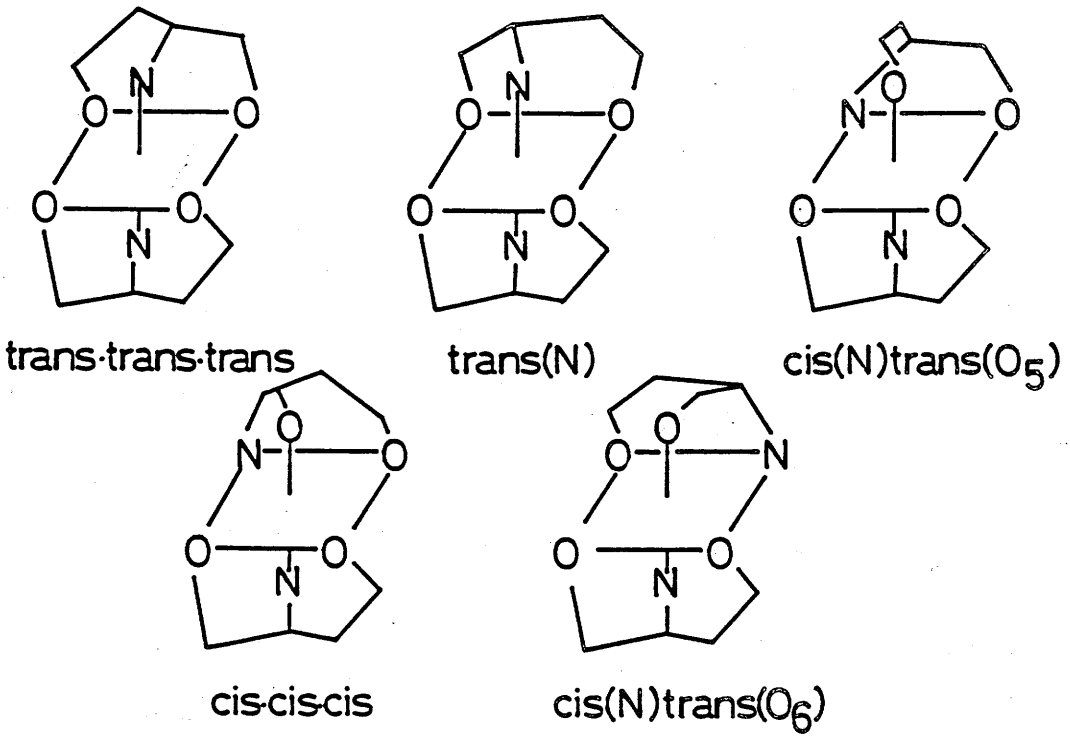

Figure 9. Five geometrical isomers of $[Co(DL\text{-}asp)_2]^-$

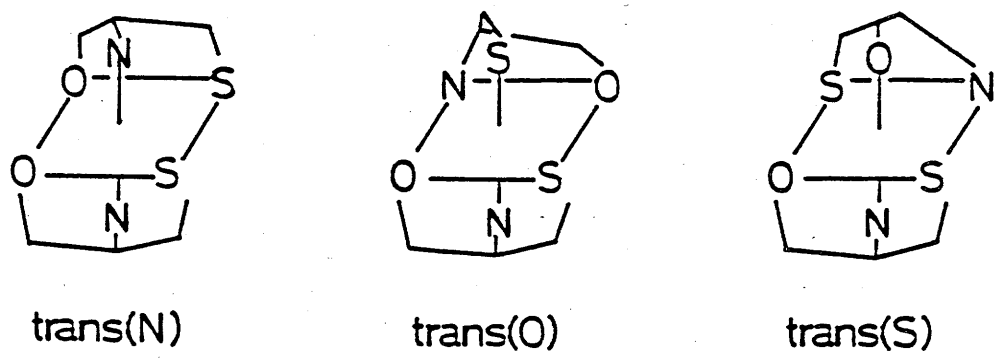

Figure 10. Three geometrical isomers of $[Co(L\text{-}smc)_2]^+$.

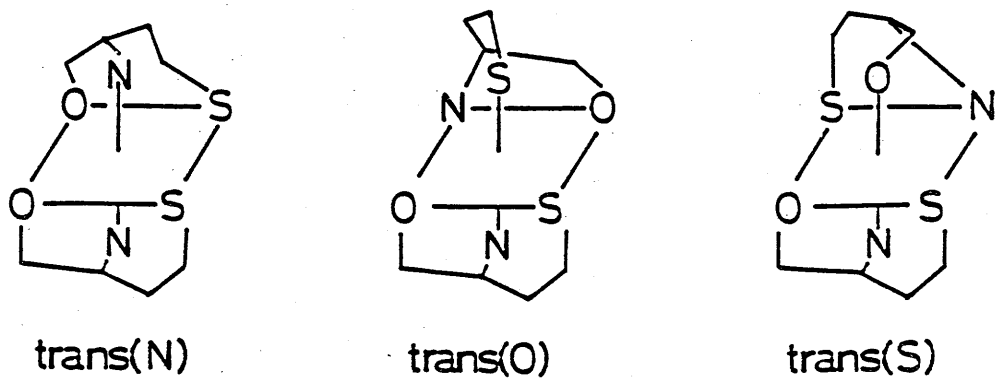

Figure 11. Three geometrical isomers of $[Co(L\text{-}met)_2]^+$.

II-B. Theory of Normal Vibration.

II-B-1. Kinetic and Potential Energies.

Frequency of the normal vibration can be determined by the kinetic and the potential energies of the system. Since classical mechanics yields a solution of the problem of small vibrations which is easier to visualize than the quantum mechanical solution, it will be employed first.

The kinetic energy is given by

$$2T = \sum_{\alpha=1}^{N} m_\alpha [(d\Delta x_\alpha/dt)^2 + (d\Delta y_\alpha/dt)^2 + (d\Delta z_\alpha/dt)^2] \qquad (1\text{-}1)$$

If generalized coordinates, such as

$$q_1 = \sqrt{m_1}\Delta x_1,\ q_2 = \sqrt{m_1}\Delta y_1,\ q_3 = \sqrt{m_2}\Delta x_2,\ \text{etc} \qquad (1\text{-}2)$$

are used, the kinetic energy is simply written as Eq.1-3.

$$2T = \sum_{i=1}^{3N} \dot{q}_i^2 \qquad (1\text{-}3)$$

The potential energy will be some function of the displacements and therefore of the q's. For small values of the displacements, the potential energy V may be expressed as a power series in the displacement q_i:

$$2V = 2V_0 + 2\sum_{i=1}^{3N}(\partial V/\partial q)q_i + \sum_{i,j=1}^{3N}(\partial^2 V/\partial q_i \partial q_j)q_i q_j + \text{higher terms}$$

$$= 2V_0 + 2\sum_{i=1}^{3N} f_i q_i + \sum_{i,j=1}^{3N} f_{ij} q_i q_j + \text{higher terms} \qquad (1\text{-}4)$$

If the potential energy at $q_i = 0$, the equilibrium position, is taken, V_0 may be eliminated. Furthermore, when all the q's are zero, the atoms are all in their equilibrium positions so that the energy must be a minimum for $q_i = 0$ ($i = 1,2,3,\cdots$).

$$(\partial V/\partial q_i) = f_i = 0 \qquad i = 1, 2, \cdots, 3N$$

For sufficiently small amplitudes of vibration, the higher

terms (cubic, quadratic, etc., in the q's) can be neglected, so that Eq.1-5 are derived from Eq.1-4.

$$2V = \sum_{i,j=1}^{3N} f_{ij} q_i q_j \qquad (1\text{-}5)$$

where the f_{ij}'s are constants given by Eq.1-6

$$f_{ij} = (\partial^2 V/\partial q_i \partial q_j)_0 \qquad (1\text{-}6)$$

with $f_{ij} = f_{ji}$.

Newton's equation of motion can be written in the form of Eq.1-7.

$$d/dt\,\partial T/\partial q_j + \partial V/\partial q_j = 0 \quad j = 1, 2, \cdots, 3N \qquad (1\text{-}7)$$

From Eqs.1-3, 1-5, and 1-6, Eq.1-7 is written as Eq.1-8

$$q_j + \sum_{i=1}^{3N} f_{ij} q_i = 0 \quad j = 1, 2, \cdots, 3N \qquad (1\text{-}8)$$

This is a set of 3N simultaneous second-order linear differential equations. One possible solution is

$$q_i = A_i \cos(\lambda^{1/2} t + \varepsilon) \qquad (1\text{-}9)$$

where A_i, λ, and ε are properly chosen constants.

II-B-2. Normal Coordinates.

In order to carry out quantum mechanical treatment of the molecular vibrations, it is necessary to introduce a new set of coordinates Q_k, k = 1, 2, • • •, 3N, called normal coordinates. It will be shown that there is one normal coordinate associated with each normal mode of motion, and vice versa. The normal coordinates are defined in terms of the mass-weighted cartesian displacement coordinates q_i by the linear equations,

$$Q_k = \sum_{i=1}^{3N} l''_{ki} q_i \quad k = 1, 2, \cdots, 3N \qquad (2\text{-}1)$$

where the coefficients l''_{ki} have been chosen so that in

terms of the new coordinates the kinetic and potential energies have the forms given in Eq.2-2.

$$2T = \sum_{k=1}^{3N} \dot{Q}^2 \qquad 2V = \Sigma \lambda_k Q_k^2 \tag{2-2}$$

In other words, the potential energy in terms of the normal coordinates involves no cross products but only squares of Q's, while the kinetic energy retains its original form. When Eq.2-2 is combined with Newton's Eq.1-7, the equations of motion become as follows, and

$$\partial/\partial t \partial T/\partial \dot{Q}_k + \partial V/\partial Q_k = \ddot{Q}_k + \lambda_k Q_k = 0$$

$$k = 1, 2, \cdots, 3N \tag{2-3}$$

the solutions of which are given in Eq.2-4,

$$Q_k = K_k \cos(\lambda_k^{1/2} t + \varepsilon_k) \quad k = 1, 2, \cdots, 3N \tag{2-4}$$

where K_k and ε_k are arbitrary constants.

II-B-3. Group Theoretical Treatment of Normal Coordinates.

The method of applying group theory to vibrational problems depends upon the fact that the normal coordinates and normal modes of vibration of symmetrical molecules have certain special symmetry properties. If the transformations which represent the effect of the symmetry operations upon the whole set of normal coordinates of the molecule are examined, it will be found that they form a representation of the symmetry group in the same sense that the transformations of the displacement coordinates ξ_i form a representation. This statement is true whether the normal coordinates of translation and rotation are included or not. In case a representation cannot be simplified any further, it is called an irreducible representation. When

the representation $\Gamma(R)$ occurs a_i times in the completely reduced form of the original representation, character of original (reduced) representation, $\chi(R)$, can be given for each operation R in the form of Eq.3-1, $\chi_i(R)$ being the

$$\chi(R) = a_1\chi_1(R) + a_2\chi_2(R) + \cdots = \Sigma a_i\chi_i(R) \quad (3\text{-}1)$$

character of the irreducible representation $\Gamma(R)$. It is possible to show a_i in relation to $\chi(R)$ and $\chi_i(R)$ as expessed in Eq.3-2,

$$a_i = 1/g\sum_R \chi(R)\chi_i(R) \quad (3\text{-}2)$$

where g is the number of operations in the symmetry group and the sum is over all the operations. This formula is written more conveniently as given in Eq.3-3.

$$a_i = 1/g\Sigma n\chi(R)\chi_i(R) \quad (3\text{-}3)$$

As has been stated before, g is the number of operations in the group, $\chi(R)$ refers to the reducible representation, $\chi_i(R)$ to the irreducible representation, and n is the number of times the irreducible representation $\Gamma(R)$ appears in the reduced representation. Thus a_i can be calculated on the basis of the group theoretical consideration.

II-B-4. Number of Normal Vibrations for Each Species.

It has already been stated how the number of normal modes of motion of each possible symmetry can be obtained. This section will treat the problem more thoroughly. The transformation of the displacement coordinates ξ_i of the atoms of the molecule form a reducible representation of the symmetry point group of the molecule. It follows directly

from this fact that the 3N normal coordinates (including translation and rotation) also form a basis of a representation of the group, since the normal coordinates Q_k are linear combinations of the displacement coordinates ξ_i. This normal coordinate representation is at least partially, and usually completely, reduced, in that the transformations do not mix normal coordinates corresponding to different frequencies. If it is desired to find the number of vibrational normal coordinates with each symmetry, the symmetry of the translational and rotational coordinates may be obtained and the proper numbers subtracted from the total values of a_i.

In general, if the symmetry operation R is applied to all the displacement coordinates, it can be written as

$$RX = UX \qquad (4\text{-}1)$$

where U is transformation matrix. The character of the matrix U is given by Eq.4-2,

$$\chi(R) = \pm N_R(1 + 2\cos\theta) \qquad (4\text{-}2)$$

where N_R is the number of nuclei unchanged by the symmetry operation R, θ is the rotational angle for the symmetry operation, and the + and - signs are for proper and improper rotations, respectively. Pure rotation and identity are called proper rotation. On the other hand, operation such as σ, i, and S_n are called improper rotation. The characters for the translational motion of the complex in the x, y, and z directions (denoted by T_x, T_y, and T_z) are as follows;

$$\chi_t(R) = \pm(1 + 2\cos\theta) \qquad (4\text{-}3)$$

where the + and - signs are for the proper and improper rotations, respectively. The characters for the rotations around the x, y, and z axes (denoted by R_x, R_y, and R_z) are given by

$$\chi_r(R) = +(1 + 2\cos\theta) \qquad (4\text{-}4)$$

for both proper and improper rotations.

To determine the number of normal vibrations belonging to each species, the characters corresponding to the translational ($\chi_t(R)$) and rotational ($\chi_r(R)$) motions of the complex must be substracted from $\chi(R)$. Therefore, the character for the vibration is obtained from Eq.4-5.

$$\chi_v(R) = \chi(R) - \chi_t(R) - \chi_r(R) \qquad (4\text{-}5)$$

II-B-5. Use of Internal Coordinates.

We have now no difficulty in carrying out such an analysis for any molecule using the methods described above. There is, however, an alternative approach with certain advantages. This approach uses internal coordinates, such as a suitable set of changes in bond lengths and bond angles, instead of cartesian displacement. Firstly, we assume that 3N-6 (3N-5 for linear cases) independent internal coordinates have been chosen. The transformations of these coordinates form a representation of the point group of the molecule, which is reducible, and can be reduced by the construction of suitable linear combinations of internal coordinates. Since for infinitesimal displacements the internal coordinates are linearly related

to the cartesian displacements and to the normal coordinates, and since they do not involve translation or rotation, the structure of the representation formed by the 3N-6 independent internal coordinates must be the same as that from the 3N-6 normal coordinates. The internal coordinates can therefore be used as the basis of an alternative method of finding the structure of the normal coordinate representation.

The procedure is, as before, to find the characters for the reducible representation and then to substitute them in the basic Eq.3-3 for a_i. It is immediately seen that the internal coordinates can be chosen so that they divide into a number of sets in such a way that the members of each set transform only among themselves. If a given internal coordinate S_t is transformed into some other member $S_{t'}, (t' \neq t)$ of the same set under an operation R, S_t will contribute nothing to the character χ_R, since R_{tt} is equal to zero. Only those coordinates which are transformed into themselves (sometimes with reversal of sign) will contribute. The process of determining the character thus consists, for each equivalent set of coordinates, of selecting one operation R from each class in the group, counting the number of internal coordinates of the set which are not permuted into others by R, and multiplying by -1 if R reverses the sign of these unpermuted coordinates. Each set of equivalent coordinates forms a representation which can be reduced separately, and the structure of the normal coordinate representation can be found by summing up the

contributions from the different sets.

One advantage of this approach arises from the fact that the normal frequencies are determined by the type of internal coordinate which is most strongly involved in the given mode. Another important advantage will appear when the factoring of the secular equation is treated.

II-B-6. Principle of GF Matrix Method.

GF matrix[1] makes the kinetic energy and the potential one express in the same internal coordinates. It has been shown that the kinetic energy of vibration can be written in terms of the internal coordinates in the form of Eq.6-1,

$$2T = \sum_{tt'} (G^{-1})_{tt'} S_t S_{t'} \qquad (6\text{-}1)$$

where G^{-1} is the matrix reciprocal to G, and G matrix depends on the geometry and masses of the molecule. If the potential energy is expressed in the same internal coordinates so that Eq.6-2 satisfies,

$$2V = \sum_{tt'} F_{tt'} S_t S_{t'} \qquad (6\text{-}2)$$

where $F_{tt'}$ is the force constants, the vibrational problem leads to a secular equation Eq.6-3.

$$\begin{vmatrix} F_{11}-(G^{-1})_{11}\lambda & F_{12}-(G^{-1})_{12}\lambda & \cdots & F_{1n}-(G^{-1})_{1n}\lambda \\ F_{21}-(G^{-1})_{21}\lambda & F_{22}-(G^{-1})_{22}\lambda & \cdots & F_{2n}-(G^{-1})_{2n}\lambda \\ \cdots & \cdots & \cdots & \cdots \\ F_{n1}-(G^{-1})_{n1}\lambda & F_{n2}-(G^{-1})_{n2}\lambda & \cdots & F_{nn}-(G^{-1})_{nn}\lambda \end{vmatrix} = 0 \qquad (6\text{-}3)$$

Here λ is equal to $4\pi^2\nu^2$ as usual and n is the number of internal coordinates, 3N-6 (or 3N-5 for the linear case). Symbolically it can also be written as Eq.6-4.

$$|F - G^{-1}\lambda| = 0 \qquad (6\text{-}4)$$

This form of the secular equation has the advantage of using the force constants F_{tt}, of direct physical significance (i.e., in terms of bond distances and angles, or interatomic distances). These force constants also appear directly in the elements of the equation and thus do not need any preliminary algebraic treatment before use. On the other hand, it is often inconvenient to have the unknown λ appear besides the principal diagonal (especially when numerical solution is employed) and the job of inverting the G matrix to get G^{-1} is somewhat tedious.

Another form of the secular equation can be obtained from the above by multiplying it through by the determinant of G

$$|G| = \begin{vmatrix} G_{11} & G_{12} & \cdots & G_{1n} \\ G_{21} & G_{22} & \cdots & G_{2n} \\ \cdots & \cdots & \cdots & \cdots \\ G_{n1} & G_{n2} & \cdots & G_{nn} \end{vmatrix} \qquad (6\text{-}5)$$

on the basis of the known rules for the multiplication of determinants. This yields the equation Eq.6-6,

$$\begin{vmatrix} \Sigma G_{1t}F_{t1}-\lambda & \Sigma G_{1t}F_{t2} & \cdots & \Sigma G_{1t}F_{tn} \\ \Sigma G_{2t}F_{t1} & \Sigma G_{2t}F_{t2}-\lambda & \cdots & \Sigma G_{2t}F_{tn} \\ \cdots & \cdots & \cdots & \cdots \\ \Sigma_{nt}F_{t1} & \Sigma G_{nt}F_{t2} & \cdots & \Sigma G_{nt}F_{tn}-\lambda \end{vmatrix} = 0 \qquad (6\text{-}6)$$

or symbolically, Eq.6-7

$$|GF - E\lambda| = 0 \qquad (6\text{-}7)$$

where E is the unit matrix.

In what follows frequent use will be made of the set of

quantities $G_{tt'}$, defined by Eq.6-8,

$$G_{tt'} = \sum_{i=1}^{3N} 1/m_i B_{ti} B_{t'i} \quad t, t' = 1, 2, \cdots, 3N-6 \qquad (6\text{-}8)$$

where m_i is the mass of the atom to which the subscript i refers. The coefficients B_{ti} is defined as Eq.6-9,

$$S_t = \sum_{i=1}^{3N} B_{ti} \xi_i \quad t = 1, 2, \cdots, 3N-6 \qquad (6\text{-}9)$$

where S_t and ξ_i are column matrix whose components are the internal and cartesian displacement coordinates, respectively.

If the molecule has some symmetry property, the orders of the G and F matrices are reduced by a proper similarity transformation. This results in reduction of the order of the secular equation to be solved. The symmetry coordinates, S_k, are employed for this purpose. Let the symmetry coordinates be given by Eq.6-10.

$$S_k = \Sigma U_{kt} S_t \qquad (6\text{-}10)$$

A proper U_{kt} matrix can be constructed from symmetry consideration.

$$| G_{kk'} F_{kk'} - E\lambda | = | GF - E\lambda | \qquad (6\text{-}11)$$

Here, $G_{kk'} = \sum_{tt'} U_{kt} U^*_{k't'} G_{tt'}$ and $F_{kk'} = \sum_{tt'} U_{kt} U^*_{k't'} F_{tt'}$.

II-B-7. Potential Fields and Force Constants.

The potential energy can be written in the form of Eq.7-1.

$$\begin{aligned} 2V = {} & \Sigma f_{r_i} (\Delta r_i)^2 + \Sigma f_{\alpha_{jk}} r_j r_k (\Delta \alpha_{jk})^2 + \\ & \Sigma f_{r_i r_j} (\Delta r_i \Delta r_j) + \Sigma f_{\alpha_{jk} \alpha_{lm}} \sqrt{r_j r_k r_l r_m} \cdot \\ & (\Delta \alpha_{jk} \Delta \alpha_{lm}) + \Sigma f_{r_i \alpha_{jk}} \sqrt{r_j r_k} (\Delta r_i \Delta \alpha_{jk}) \end{aligned} \qquad (7\text{-}1)$$

This type of potential field is called a generalized valence force field (GVFF). It consists of stretching and bending force constants, as well as the interaction force constants between them. The symbols Δr_i and $\Delta \alpha_{jk}$ are the change in the bond lengths and in the bond angles, respectively. Furthermore, r is the value of the interatomic distance at the equilibrium position and is inserted to make the force constants dimensionally similar. This method is satisfactory, however, only for simple molecules (e.g., high symmetrical metal complex). In order to reduce the number of interaction force constants, a potential field, in which some of the interaction force constants are neglected or the values of the analogous force constants are set to equal, is sometimes useful. A potential field consisting of stretching and bending force constants only is called a simple valence force field (SVFF).

In another approach, Shimanouchi[2] introduced the Urey-Bradley force field (UBFF), which consists of stretching and bending force constants, as well as repulsive force constants between nonbonded atoms. The general form of the potential field is given by Eq.7-2.

$$2V = \Sigma K_i(\Delta r_i)^2 + \Sigma H_{jk} r_j r_k (\Delta \alpha_{jk})^2 + \Sigma F_{jk}(\Delta q_{jk})^2 + \text{linear term} \qquad (7\text{-}2)$$

Here Δr_i, $\Delta \alpha_{jk}$, and Δq_{jk} are the changes in the bond lengths, bond angles, and distances between nonbonded atoms; the symbols K_i, H_{jk}, and F_{jk} represent the stretching, bending, and repulsive force constants, respectively.

Furthermore, r is the values of the distances at the equilibrium position. The number of force constants in the UBFF is, in general, much smaller than that in the GVFF. In addition, the UBFF has the advantages that (1) the force constants have clearer physical meanings than those of the GVFF, and (2) they are often transferable from molecule to molecule. However, the UBFF sometimes can not give a satisfactory agreement between the observed and the calculated frequencies because of the ignorance of the interactions between non-neighboring stretching vibrations and between bending vibrations. It is possible to improve the results by introducing more force constants (a modified Urey-Bradley force field: MUBFF), but an increase of the number of the force constants reduces the advantage of this field. Therefore, this field seems generally not to suitable for the normal coordinate analysis of metal complexes.

The normal vibrations of the $[Co(NH_3)_6]^{3+}$ complex will be taken as an example. Since the ligand and skeletal vibrations are very weakly coupled, one may consider the NH_3 ligands as point masses.[3] Shimanouchi, Nakagawa,[2] and Yeranos[4] have calculated the UBFF force constants for the CoX_6 skeleton of $[Co(NH_3)_6]^{3+}$, making this assumption and using only IR vibrational frequencies. The skeletal vibrations are classified according to the species:

$$\Gamma(O_h) = A_{1g}(R) + E_g(R) + 2T_{1u}(ir) + T_{2g}(R) + T_{2u}(-)$$

Since the Raman active frequencies calculated from the above-mentioned UBFF do not agree well with the measured

values, some of the force constants may be unreliable.

On the other hand, Schmidt and Müller have carried out the normal coordinate analysis of $[Co(NH_3)_6]^{3+}$ by using both the IR and Raman spectral data on the basis of GVFF and they have obtained the values of force conatants which can be assumed to be more reliable than previously reported values, which have obtained on the basis of UBFF.[2,5]

$$F_{11}(A_{1g}) = f_r + 4f_{rr} + f'_{rr} = 2.45$$
$$F_{22}(E_g) = f_r - 2f_{rr} + f'_{rr} = 1.96$$
$$F_{33}(T_{1u}) = f_r - f'_{rr} = 1.78$$
$$F_{34}(T_{1u}) = 2rf_{r\alpha} = 0.55$$
$$F_{44}(T_{1u}) = r^2(f_\alpha + 2f_{\alpha\alpha}) = 0.43$$
$$F_{55}(T_{2g}) = r^2(f_\alpha - 2f'_{\alpha\alpha}) = 0.26$$
$$f_r = 1.95 \quad f_{rr'} = 0.17 \quad f_{rr} = 0.08$$
$$f_{r\alpha} = 0.28 \quad f_\alpha = 0.35 \quad f_{\alpha\alpha} = f'_{\alpha\alpha} = 0.04$$

Here, the unit is 10^2 Nm^{-1}; the values of $f_\alpha = f_{\alpha\alpha}$ was evaluated by assuming $f_{\alpha\alpha} = f'_{\alpha\alpha}$.

By the use of this result, three very weak bands at 498, 477, and 449 cm^{-1} in the IR spectrum of $[Co(NH_3)_6]^{3+}$ have been considered split of band due to the IR active T_{1u} Co-N stretching mode because of lowering of symmetry in the crystalline state. Accordingly, we will use the GVFF which is simplified by some adequate assumptions on the interaction force constants (Chapter VI).

II-B-8. Depolarization of Raman Bands.

Experimentally, polarization of Raman bands provides

valuable information about the symmetry of normal vibrations. Here, we consider the polarization properties of Raman bands in liquids and solutions in which molecules or ions take completely random orientations.

Suppose that we irradiate plane polarized light (e.g., laser beam), with its electric vector in the z direction, from the positive y direction on a molecule fixed at the origin of a space-fixed coordinate system and observe the Raman scattering in the x direction as shown in Fig. 12. One component E_z gives induced dipole moments, P_x, P_y, and P_z. However, only P_y and P_z contribute to the scattering along the x axis, since an oscillating dipole cannot radiate in its own direction.

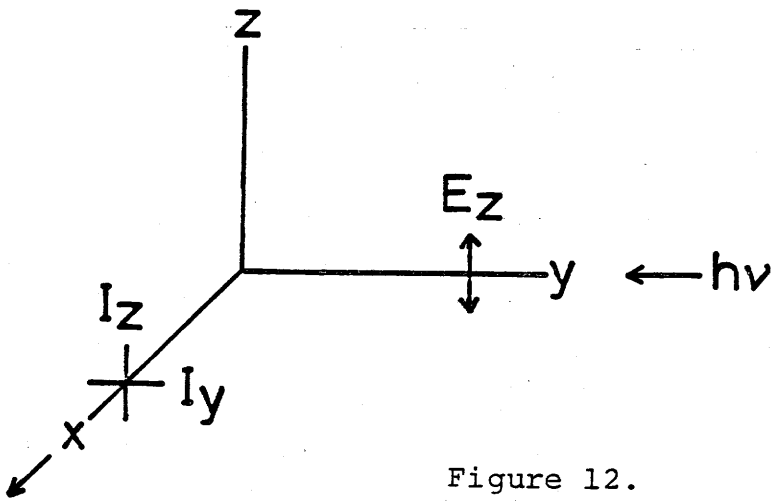

Figure 12.

Then, from the relation, $P = \alpha E$ (α is called the polarizability), we have Eqs.8-1 and 8-2.

$$P_y = \alpha_{yz} E_z \qquad (8\text{-}1)$$

$$P_z = \alpha_{zz} E_z \qquad (8\text{-}2)$$

The intensity of the scattered light is proportional to the sum of squares of the individual $\alpha_{ij}E_j$ terms. Thus, the ratio of the intensities in the y and z directions, I_y and

I_z, is given by Eq.8-3,

$$\rho_l = I_y/I_z = \alpha_{yz}^2 E_z^2 / \alpha_{zz}^2 E_z^2 \qquad (8\text{-}3)$$

where ρ_l is called the depolarization ratio for the polarized light. In solution, the complexes are randomly oriented, and we must consider the polarizability components averaged over all orientations. The results are expressed in terms of two quantities: $\bar{\alpha}$ (mean value) and γ (anisotropy):

$$\bar{\alpha} = 1/3(\alpha_{xx} + \alpha_{yy} + \alpha_{zz}) \qquad (8\text{-}4)$$

$$\gamma^2 = 1/2[(\alpha_{xx} - \alpha_{yy})^2 + (\alpha_{yy} - \alpha_{zz})^2 + (\alpha_{zz} - \alpha_{xx})^2 + 6(\alpha_{xy}^2 + \alpha_{yz}^2 + \alpha_{zx}^2)] \qquad (8\text{-}5)$$

These two quantities are invariant to any coordinate transformation. It can be shown that the average values of the squares of α_{ij} are given in Eqs.8-6 and 8-7.

$$\overline{(\alpha_{xx})^2} = \overline{(\alpha_{yy})^2} = \overline{(\alpha_{zz})^2} = 1/45[45(\bar{\alpha})^2 + 4\gamma^2] \qquad (8\text{-}6)$$

$$\overline{(\alpha_{xy})^2} = \overline{(\alpha_{yz})^2} = \overline{(\alpha_{zx})^2} = 1/15\gamma^2 \qquad (8\text{-}7)$$

Equation 8-3 can be written as Eq.8-8.

$$\rho_l = I_y/I_z = 3\gamma^2/(45(\bar{\alpha})^2 + 4\gamma^2) \qquad (8\text{-}8)$$

The total intensity, I_l, is given by Eq.8-9.

$$I_l = I_y + I_z = \text{const}[1/45\{45(\bar{\alpha})^2 + 7\gamma^2\}]E^2 \qquad (8\text{-}9)$$

The symmetry property of the normal vibration can be determined by measuring the depolarization ratio. From an inspection of character tables, it is obvious that $\bar{\alpha}$ is nonzero only for the totally symmetric vibrations. Then Eq. 8-8 gives $0 \leqq \rho_l < 3/4$, and the Raman bands are said to be polarized. For all the nontotally symmetric vibrations, $\bar{\alpha}$ is zero, and $\rho_l = 3/4$. Then the Raman bands are said to be

depolarized.

For example, consider the $[MX_6]$-type (O_h) and cis-$[MX_4Y_2]$-type (C_{2v}) complexes. The only vibration mode belonging to A_{1g} species for the $[MX_6]$-type complex plays the totally symmetric vibration. Accordingly, the depolarization ratio, ρ_1, of the vibration of A_{1g} species will show $0 \leqq \rho_1 < 3/4$. On the contrary, the depolarization ratio, ρ_1, of another vibrations (E_g and T_{2g}) will show $\rho_1 = 3/4$. The vibrations belonging to A_1 species for the cis-$[MX_4Y_2]$-type complex play the totally symmetric vibrations. Accordingly, the depolarization ratio, ρ_1, of the vibrations of A_1 species will show $0 \leqq \rho_1 < 3/4$. On the contrary, the depolarization ratio, ρ_1, of other vibrations (A_2, B_1, and B_2) will show $\rho_1 = 3/4$. We can consider the depolarization ratio, ρ_1, of other complexes like these examples.

Chapter III. Experimental

III-A. Preparation of Complexes.

III-A-1. Tris(bidentate)cobalt(III) Complexes with Six- and/or Five-Membered Chelate Rings.

(1) Bis(1,2-ethanediamine)(1,3-propanediamine)cobalt(III) Bromide: $[Co(en)_2(tn)]Br_3$ and (1,2-Ethanediamine)bis(1,3-propanediamine)cobalt(III) Bromide: $[Co(en)(tn)_2]Br_3$.

These Complexes were prepared by the method of H. Ogino and J. Fujita.[6] A mixture of $[Co(en)_2(tn)]Br_3$ and $[Co(en)(tn)_2]Br_3$ was prepared by the direct synthesis method using cobalt(II) chloride hexahydrate, 1,2-ethanediamine, and 1,3-propanediamine and the desired complexes were obtained by the fractional crystallization.

(2) Tris(1,3-propanediamine)cobalt(III) Chloride: $[Co(tn)_3]Cl_3$.

This complex was prepared by the direct synthesis method using cobalt(II) chloride hexahydrate, 1,3-propanediamine, and 1,3-propanediamine dihydrochloride by air oxidation.[7]

(3) (Glycinato)bis(1,3-propanediamine)cobalt(III) Iodide: $[Co(gly)(tn)_2]I_2$.

This complex was prepared by derivation from trans-$[CoCl_2(tn)_2]Cl$ and glycine.[8]

(4) (β-Alaninato)bis(1,2-ethanediamine)cobalt(III) Chloride: $[Co(\beta\text{-ala})(en)_2]Cl_2$ and Trans(O)-bis(β-alaninato)(1,2-ethanediamine)cobalt(III) Chloride:

trans(O)-[Co(β-ala)$_2$(en)]Cl.

These complexes were prepared by the method of M. Ogawa et. al.[9] with slight modifications as described below. The filtrate, which was obtained from trans-[CoCl$_2$(en)$_2$]Cl and β-alanine, was poured onto a column of SP-Sephadex C-25 (Na^+ form) and the adsorbed band was eluted with a 0.05 mol dm^{-3} aqueous NaCl solution. The fastest moving band contained trans(O)-[Co(β-ala)$_2$(en)]Cl and the sixth moving orange band contained [Co(β-ala)(en)$_2$]Cl$_2$.

(5) Bis(β-alaninato)(1,3-propanediamine)cobalt(III) Chloride: [Co(β-ala)$_2$(tn)]Cl.

This complex was prepared by a procedure similar to that used for [Co(gly)$_2$(en)]Cl.[10] A solution containing 1.7 cm^3 of 1,3-propanediamine and 3.6 g of β-alanine in 15 cm^3 of water was added to a solution containing 5 g of cobalt(II) chloride hexahydrate in 10 cm^3 of water. The solution was oxidized over a steam bath by gradually adding 10 g of lead dioxide for 1 h. After it had been cooled to room temperature, the mixture was filtered. The fitrate was poured onto a column of SP-Sephadex C-25 (Na^+ form, 3.5 cm x 60 cm). After the column had been swept with water, the adsorbed band was eluted with a 0.05 mol dm^{-3} aqueous NaCl solution. Three colored bands, violet(A-1), pink(A-2), and red-violet(A-3), were eluted in this order; they were present in a ratio of about 1.6 : 1.4 : 3.5 (A-1 : A-2 : A-3). Each eluate was concentrated to a small volume by the use of a rotary evaporator below 30 ℃, and the deposited

NaCl was filtered off. The filtrate was passed through a column of Sephadex G-10 (3 cm x 50 cm) to remove remaining NaCl by means of elution with water. A small amount of ethanol was added to the eluate after its concentration. The precipitate which appeared was collected by filtration.

(6) Fac(N)-tris(β-alaninato)cobalt(III): fac(N)-[Co(β-ala)$_3$].

This complex was prepared by a modified method of M. B. Ćelap et. al.[11] To a solution containing 4.6 g of $[Co(NH_3)_6]Cl_3$ in 17 cm^3 of water was added 4.6 g of β-alanine in 3 mol dm^{-3} aqueous KCl solution. The mixture was heated on a steam bath for 9 h. The solution was poured onto a column of Dowex 50W-X8 (Na^+ form) and the adsorbed band was eluted with water. The fourth purple band contained the desired complex.

(7) Mer(N)-tris(β-alaninato)cobalt(III): mer(N)-[Co(β-ala)$_3$].

This complex was prepared by the derivation from $Na_3[Co(CO_3)_3]$ and β-alanine.[11]

III-A-2. Cobalt(III) Complexes with Linear Terdentate Ligands Containing N and O Donor Atoms.

(8) Bis(3-azapentane-1,5-diamine)cobalt(III) Bromide: $[Co(dien)_2]Br_3$.

This complex was prepared by the direct synthesis method using cobalt(II) chloride hexahydrate, 3-azapentane-1,5-diamine, and 3-azapentane-1,5-diamine trihydrochloride by air oxidation[12,13] or derivation from $[CoCl(NH_3)_5]Cl_2$[12]

or $[Co(CO_3)_3]^{3+}$ and 3-azapentane-1,5-diamine. This procedure was based on the so-called tris(carbonato)cobaltate(III) method.[13]

(9) (3-Azapentane-1,5-diamine)(ethylenediamine-N-acetato)cobalt(III) Chloride: $[Co(edma)(dien)]Cl_2$.

This complex was prepared by the lead dioxide oxidation method using ethylenediamine-N-acetic acid dihydrochloride dihydrate and 3-azapentane-1,5-diamine.[14]

(10) (3-Azapentane-1,5-diamine)(iminodiacetato)cobalt(III) Perchlorate: $[Co(ida)(dien)]ClO_4$.

This complex was synthesized from $[Co(H_2O)_3(dien)]^{3+}$ and iminodiacetic acid, the former of which was obtained from $[CoCl_3(dien)]$.[15]

(11) Bis(ethylenediamine-N-acetato)cobalt(III) Ion: $[Co(edma)_2]^+$.

This complex was prepared by the direct synthesis method using cobalt(II) chloride hexahydrate and ethylenediamine-N-acetic acid dihydrochloride dihydrate.[16] Sym-fac-trans(N_t), unsym-fac-cis(N_t)trans(O), unsym-fac-cis(N_t)cis(O), and unsym-fac-trans(N_t) isomers were obtained as chloride and sym-fac-cis(N_t) and mer isomers as bromide.

(12) (Ethylenediamine-N-acetato)(iminodiacetato)cobalt(III): $[Co(ida)(edma)]$.

This complex was obtained by the lead dioxide oxidation method using iminodiacetic acid and ethylenediamine-N-acetic acid dihydrochloride dihydrate.[17]

(13) Potassium Bis(iminodiacetato)cobaltate(III): $K[Co(ida)_2]$

This complex was prepared by the method of J. Hidaka et. al.[18]

(14) Triammine(3-azapentane-1,5-diamine)cobalt(III) Chloride: $[Co(NH_3)_3(dien)]Cl_3$.

Two grams of $[CoCl_3(dien)]$ were dissolved in 50 cm^3 of 28 % aqueous ammonia, and the solution was evaporated to dryness on a steam bath. The precipitate was then dissolved in a small amount of water and poured onto a column (4 cm x 60 cm) containing strong acid cation exchange resin (SP-Sephadex, C-25, Na^+ form). Having been swept with water, the band adsorbed on the column was eluted with a 0.3 mol dm^{-3} aqueous NaCl solution. A yellow band of the desired complex was then eluted and fractionated. It was found, from the absorption spectra of the fractions, that the middle eluate contained $[Co(NH_3)_3(dien)]^{3+}$. Then the middle fractions were combined and concentrated to a small volume. The concentrated solution was purified by using a Sephadex G-10 column. To the solution was added a small amount of ethanol and the resulting solution was kept in a refrigerator for several days. The crystals were collected by filtration. However, they could not be recrystallized further because of their low yield.

(15) Cis(O)-triammine(iminodiacetato)cobalt(III) Perchlorate: cis(O)-$[Co(ida)(NH_3)_3]ClO_4$.

This complex was prepared by the method of K. Okamoto et. al.[19]

III-A-3. Cobalt(III) Complexes with Terdentate Ligands

Containing N-Methyl Group.

(16) (Ethylenediamine-N-acetato)(3-methyl-3-azapentane-1,5-diamine)cobalt(III) Ion: $[Co(edma)(mdien)]^{2+}$.

This complex was prepared by the direct synthesis method using cobalt(II) chloride hexahydrate, ethylenediamine-N-acetic acid dihydrochloride dihydrate and 3-methyl-3-azapentane-1,5-diamine trihydrochloride by lead dioxide oxidation.[14] Sym-fac, unsym-fac-mer(N_t), and mer isomers were obtained as sulfate and unsym-fac-fac(N_t) as bromide.

(17) (Iminodiacetato)(3-methyl-3-azapentane-1,5-diamine)cobalt(III) Chloride: [Co(ida)(mdien)]Cl.

This complex was prepared by the direct synthesis method using cobalt(II) sulfate hexahydrate, iminodiacetic acid, and 3-methyl-3-azapentane-1,5-diamine trihydrochloride.[20]

(18) (Ethylenediamine-N-acetato)(N-methyliminodiacetato)cobalt(III): [Co(mida)(edma)].

This complex was prepared by the lead dioxide oxidation method using cobalt(II) chloride hexahydrate, N-methyliminodiacetic acid, and ethylenediamne-N-acetic acid dihydrochloride dihydrate.[21]

(19) Sodium Sym-fac-(iminodiacetato)(N-methyliminodiacetato)cobaltate(III): sym-fac-Na[Co(ida)(mida)].

This complex was obtained by the isomerization reaction of unsym-fac isomer.[22]

(20) Potassium Unsym-fac-(iminodiacetato)(N-methyliminodiacetato)cobaltate(III): unsym-fac-K[Co(ida)(mida)].

This complex was prepared by the method of T. Yasui et.al.[22)]

(21) Potassium Mer-(iminodiacetato)(N-methyliminodiacetato)cobaltate(III): mer-K[Co(ida)(mida)].

This complex was obtained by the isomerization of unsym-fac-$[Co(ida)(mida)]^-$ in weakly basic aqueous solution.[23)]

(22) (3-Methyl-3-azapentane-1,5-diamine)(N-methyliminodiacetato)cobalt(III) Chloride: [Co(mida)(mdien)]Cl.

This complex was prepared by the direct synthesis method using cobalt(II) sulfate hexahydrate, N-methyliminodiacetic acid, and 3-methyl-3-azapentane-1,5-diamine trihydrochloride by lead dioxide oxidation.[20)]

(23) Potassium Bis(N-methyliminodiacetato)cobaltate(III): $K[Co(mida)_2]$.

This complex was prepared by using the procedure given by T. Ama et. al.[24)]

III-A-4. Cobalt(III) Complexes with Quadridentate Ligands.

(24) Cis-α-(1,2-ethanediamine)(3,6-diazapentane-1,8-diamine)cobalt(III) Iodide: cis-α-$[Co(en)(trien)]I_3$.

This complex was prepared by derivation from cis-α-$[CoCl_2(trien)]Cl$ and 1,2-ethanediamine.[25)]

(25) Cis-β-(1,2-ethanediamine)(3,6-diazapentane-1,8-

diamine)cobalt(III) Chloride: cis-β-[Co(en)(trien)]Cl_3.

This complex was separated from cis-α isomer using SP-Sephadex column chromatography.[25,26]

(26) (Oxalato)(3,6-diazapentane-1,8-diamine)cobalt(III) Chloride: [Co(ox)(trien)]Cl.

Cis-α- and cis-β-[Co(ox)(trien)]I, which were prepared in the same way as has been reported,[27] were converted to the chloride by passing the solution through a column of Dowex 1-X8 anion exchange resin in the chloride form.

(27) (1,2-Ethanediamine)(tris(2-aminoethyl)amine)cobalt(III) Chloride: [Co(en)(tren)]Cl_3.

This complex was prepared by a procedure alternative to that used in the literatures.[28] To a solution of [$CoCl_2$(tren)]Cl (3.3 g) in 20 cm^3 of water on a steam bath was added 1,2-ethanediamine (0.6 g). Heating was continued for 30 min. After cooling, [Co(en)(tren)]Cl_3 was isolated by the column chromatographic method using SP-Sephadex C-25 (Na^+ form, 4 cm x 20 cm) and 0.2 mol dm^{-3} aqueous NaCl solution as an eluting solvent.

(28) (Oxalato)(tris(2-aminoethyl)amine)cobalt(III) Chloride: [Co(ox)(tren)]Cl.

This complex was prepared by a procedure similar to that used for $[Co(ox)(trien)]^+$. A solution containing [$CoCl_2$(tren)]Cl (0.5 g) and oxalic acid (0.4 g) in 10 cm^3 of water was warmed on a steam bath for 30 min. After cooling,

the resulting red solution was passed through a column of SP-Sephadex C-25 (Na^+ form, 3 cm x 40 cm) with 0.05 mol dm^{-3} aqueous NaCl solution for elution. The red eluate was concentrated and then cooled in an ice bath in order to obtain [Co(ox)(tren)]Cl.

(29) (1,2-Ethanediamine)(ethylenediamine-N,N'-diacetato)cobalt(III) Perchlorate: $[Co(edda)(en)]ClO_4$.

This complex was prepared by the direct synthesis method using cobalt(II) carbonate, ethylenediamine-N,N'-diacetic acid, and 1,2-ethanediamine.[29)]

(30) (Ethylenediamine-N,N'-diacetato)(1,3-propanediamine)cobalt(III) Perchlorate: $[Co(edda)(tn)]ClO_4$.

The preparation procedure was identical with that of $[Co(edda)(en)]^+$, except that 1,3-propanediamine was used instead of 1,2-ethanediamine. A reaction mixture was poured onto a column of Dowex 50W-X8 (200 - 400 mesh, Na^+ form, 3 cm x 60 cm) and three main red bands were eluted. It was found that the second eluate was cis-α-$[Co(edda)(tn)]^+$ and the third one was cis-β-$[Co(edda)(tn)]^+$.

(31) Cis-α-diammine(ethylenediamine-N,N'-diacetato)cobalt(III) Nitrate: cis-α-$[Co(edda)(NH_3)_2]NO_3$.

This complex was prepared by the direct synthesis method using cobalt(II) carbonate, ethylenediamine-N,N'-diacetic acid, and ammonia water.[29)]

(32) Cis-α-(ethylenediamine-N,N'-diacetato)(glycinato)cobalt(III): cis-α-

[Co(edda)(gly)].

This complex was prepared by using the procedure given by J. I. Legg et. al.[30]

(33) Cis-α-(β-alaninato)(ethylenediamine-N,N'-diacetato)cobalt(III): cis-α-[Co(edda)(β-ala)].

This complex has been prepared by H. Nakazawa et. al.,[31] but the synthesis in the present work was carried out according to the procedure of the complex with the glycinate ligand,[30] except that it was carried out using β-alanine in place of glycine.

(34) Sodium (Ethylenediamine-N,N'-acetato)(oxalato)cobaltate(III): Na[Co(edda)(ox)].

This complex was prepared by using the procedure given by P. F. Coleman.[32]

(35) (N-(2-Aminoethyl)iminodiacetato)(1,2-ethanediamine)cobalt(III) Chloride: [Co(aeida)(en)]Cl.

This complex was prepared by derivation from $Na[Co(aeida)(NO_2)_2]$ and 1,2-ethanediamine. Two isomers were separated by an SP-Sephadex C-25 column chromatography using an aqueous NaCl solution in place of that of $NaClO_4$ as an eluent given in the literature.[33]

III-A-5. Cobalt(III) Complexes with Sulfur-containing Ligands.

(36) (2-Aminoethanethiolato)bis(1,2-ethanediamine)cobalt(III) Nitrate: $[Co(aet)(en)_2](NO_3)_2$.

This complex was prepared from $Co(NO_3)_2 \cdot 6H_2O$ and $(NH_2CH_2CH_2S-)_2 \cdot 2HCl$.[34,35]

(37) (2-Mercaptoacetato)bis(1,2-ethanediamine)cobalt(III) Iodide: $[Co(SCH_2COO)(en)_2]I$.

This complex was prepared by derivation from trans-$[CoCl_2(en)_2]Cl$ and 2-mercaptoacetic acid.[36]

(38) (2-Aminoethanesulfenato)bis(1,2-ethanediamine)cobalt(III) Nitrate: $[Co(aese)(en)_2](NO_3)_2$.

This complex was prepared from the oxidation of $[Co(aet)(en)_2]^{2+}$ by addition of a calculated amount of 1 % aqueous H_2O_2.[34,37]

(39) (2-Aminoethanesulfinato)bis(1,2-ethanediamine)cobalt(III) Nitrate: $[Co(aesi)(en)_2](NO_3)_2$.

This complex was prepared by addition of aqueous H_2O_2 to the aqueous solution of $[Co(aet)(en)_2]^{2+}$.[34,38]

(40) (2-Methylthioethylamine)bis(1,2-ethanediamine)cobalt(III) Nitrate: $[Co(mea)(en)_2](NO_3)_3$.

This complex was prepared by addition of dimethyl sulfate to the aqueous solution of $[Co(aet)(en)_2]^{2+}$.[34,39]

III-A-6. Cobalt(III) Complexes with Branched Terdentate Ligands.

(41) (DL-Aspartato)(3-azapentane-1,5-diamine)cobalt(III) Chloride: $[Co(DL\text{-}asp)(dien)]Cl$.

This complex was prepared by derivation from $[CoCl_3(dien)]$ and DL-aspartic acid.[40]

(42) Sodium Bis(DL-aspartato)cobalt(III): $Na[Co(DL\text{-}asp)_2]$.

This complex was prepared by a procedure similar to that used for $Na[Co(L\text{-}asp)_2]$,[41], using DL-aspartic acid instead of L-aspartic acid.

(43) Bis(S-methyl-L-cysteinato)cobalt(III) Chloride: $[Co(L\text{-}smc)_2]Cl$.

Three isomers were prepared from cobalt(II) chloride hexahydrate and S-methyl-L-cysteine and separated by a Dowex 50W-X8 column chromatography using an aqueous NaCl solution in place of that of $NaClO_4$ as an eluent in the literature.[42]

(44) Bis(L-methioninato)cobalt(III) Bromide: $[Co(L\text{-}met)_2]Br$.

This complex was prepared by the direct synthesis method using cobalt(II) chloride hexahydrate and L-methionine by lead dioxide oxidation.[43]

III-B. Measurements.

Raman spectra were recorded on a JASCO Laser Raman spectrometer equipped with a data processor, model DP-500. This spectrometer was specially designed and was arranged by the Japan Spectroscopic Co., Ltd., Tokyo, for the measurements of the Raman spectra of the complexes in aqueous solution; it consists of grating double monochromator, model CT-25ND (f: 250 mm, F/4.3). The resolving power is comparatively high and its maximal value is 1 cm^{-1} at 632.8 nm. The photomultiplier, model HTV R-475

of Hamamatsu Photonics K.K., Ltd., was used for the detection of the Raman bands. The source of excitation radiation was an NEC He-Ne laser, model GLG-8500 (> 50 mW), at 632.8 nm.

The Raman spectra of the complexes were measured at room temperature in 0.3 cm^3 cylindrical quartz cell in aqueous solution. All the sample solutions were prepared in ca. 0.001 - 0.05 mol dm^{-3} to avoid the self-absorption. The solution was filtered through a micropore filter to remove any insoluble substances, which are liable to cause unfavorable elastic scattering. The Raman spectral signals were repeatly accumulated on the data processor in order to improve the S/N ratio of the spectra. After the Raman spectral measurements, the absorption spectra were recorded for the solution in order to confirm no decomposition of the complexes by the excitation radiation. The observed frequencies were calibrated by the 533.8 cm^{-1} band of indene. The depolarization degree, ρ_l, was calculated as the ratio of the depolarization intensities ($I_\perp / I_{//}$) by using a polarization attachment. The Raman spectra of the N-deuterated complexes were also measured in order to make assignments of the Raman bands. N-deuterated complexes were prepared by dissolving the complex in 99.8 % D_2O and standing for 0.5 - 24 h at room temperature.

Electronic absorption spectra were measured with a JASCO UVIDEC-1 and -610 spectrophotometers.

^1H and ^{13}C NMR spectra were recorded in deuterium oxide on a JEOL JNM-FX-100 NMR spectrometer at the probe

temperature.

III-C. Calculation.

Numerical calculations for the normal coordinate analysis were carried out using the computer system FACOM 230-45S of Toyama University, by means of a computer program (BGLZ and LSMB) reported by Shimanouchi.[44)]

III-D. Elemental Analytical Data.

Elemental analytical data of the complexes are summarized in Table 1. The complexes, which are not given in Table 1, were characterized according to the absorption spectra and/or the ^{1}H and ^{13}C NMR spectra.

III-E. Absorption Spectra.

Table 2 shows the absorption data of the cobalt(III) complexes which were prepared for the first time.

Table 2. Absorption Data of the Cobalt(III) Complexes

Complex	First band	Second band
C_1-cis(O)-[Co(β-ala)$_2$(tn)]$^+$	19.3 (2.17)	27.4 (1.99)
C_2-cis(O)-[Co(β-ala)$_2$(tn)]$^+$	19.9 (2.07)	27.6 (1.95)
trans(O)-[Co(β-ala)$_2$(tn)]$^+$	18.1 (2.17) 21.5 (1.88sh)	27.3 (2.12)
[Co(ox)(tren)]$^+$	20.12(2.13)	28.17(2.16)
cis-α-[Co(edda)(tn)]$^+$	18.59(2.00) 21.69(1.73sh)	27.55(2.18)
cis-β-[Co(edda)(tn)]$^+$	19.92(2.14)	27.86(2.23)

Table 1. Elemental Analytical Data

Complex	Found (%)			Calcd (%)		
	C	H	N	C	H	N
$[Co(en)_2(tn)]Br_3 \cdot 1/2H_2O$	16.85	5.66	16.60	16.75	5.42	16.74
$[Co(tn)_3]Cl_3 \cdot H_2O \cdot 5/4HCl$	23.94	7.58	18.64	23.96	7.43	18.62
$[Co(gly)(tn)_2]I_2$	17.93	4.66	12.91	17.96	4.52	13.09
trans(O)-$[Co(\beta\text{-ala})_2(en)]Cl \cdot H_2O \cdot 1/5NaCl$	26.75	6.21	15.41	26.66	6.15	15.55
C_1-cis(O)-$[Co(\beta\text{-ala})_2(tn)]Cl \cdot 1/2H_2O \cdot 1/4NaCl$	29.18	6.45	15.22	29.35	6.30	15.21
C_2-cis(O)-$[Co(\beta\text{-ala})_2(tn)]Cl \cdot 3/2H_2O \cdot 5/8NaCl$	26.24	6.17	13.57	26.48	6.17	13.72
trans(O)-$[Co(\beta\text{-ala})_2(tn)]Cl \cdot 5/4H_2O \cdot 1/7NaCl$	28.76	6.51	14.89	28.78	6.58	14.92
fac(N)-$[Co(\beta\text{-ala})_3] \cdot 5/2H_2O$	29.33	6.03	11.44	29.36	6.30	11.41
mer(N)-$[Co(\beta\text{-ala})_3] \cdot 1/2H_2O$	32.87	5.72	12.63	32.53	5.78	12.73
sym-fac-$[Co(dien)_2]Br_3$	19.01	5.20	16.80	19.03	5.20	16.65
sym-fac-$[Co(edma)(dien)]Cl_2 \cdot 1/2H_2O$	27.03	6.36	19.34	26.75	6.46	19.50
unsym-fac-fac(N_t)-$[Co(edma)(dien)]Cl_2 \cdot 3/2H_2O$	25.70	6.67	18.69	25.48	6.68	18.57
unsym-fac-mer(N_t)-$[Co(edma)(dien)]Cl_2 \cdot 3/2H_2O$	25.44	6.58	18.54	25.48	6.68	18.57
mer-$[Co(edma)(dien)]Cl_2 \cdot 2H_2O$	24.96	6.78	17.85	24.88	6.79	18.14

Table 1. Continued

Complex	Found (%)			Calcd (%)		
	C	H	N	C	H	N
sym-fac-[Co(ida)(dien)]ClO_4	24.37	4.60	14.23	24.47	4.62	14.27
unsym-fac-[Co(ida)(dien)]ClO_4	24.47	4.65	14.13	24.47	4.62	14.27
sym-fac-trans(N_t)-[Co(edma)$_2$]Cl $\cdot$ $2H_2O$	26.14	6.04	15.34	26.35	6.08	15.36
sym-fac-cis(N_t)-[Co(edma)$_2$]Br $\cdot$ H_2O	24.27	5.03	14.03	24.57	5.15	14.33
unsym-fac-cis(N_t)trans(O)-[Co(edma)$_2$]Cl $\cdot$ $2H_2O$	26.31	6.05	15.35	26.35	6.08	15.36
unsym-fac-cis(N_t)cis(O)-[Co(edma)$_2$]Cl $\cdot$ $2H_2O$	25.59	5.98	15.27	26.35	6.08	15.35
unsym-fac-trans(N_t)-[Co(edma)$_2$]Cl $\cdot$ H_2O	27.70	5.74	16.17	27.72	5.82	16.16
mer-[Co(edma)$_2$]Br	25.54	4.88	14.80	25.75	4.86	15.01
sym-fac-[Co(ida)(edma)]	30.86	4.76	13.53	31.28	4.59	13.68
unsym-fac-mer(N)-[Co(ida)(edma)] $\cdot$ H_2O	29.24	5.14	12.74	29.55	4.96	12.92
sym-fac-K[Co(ida)$_2$] $\cdot$ $2H_2O$	24.31	3.53	7.21	24.25	3.57	7.07
unsym-fac-K[Co(ida)$_2$] $\cdot$ $5/2H_2O$	23.65	3.61	7.03	23.71	3.74	6.91
cis(O)-[Co(ida)(NH_3)$_3$]ClO_4 $\cdot$ $2H_2O$	12.75	4.75	14.89	12.76	4.83	14.88
sym-fac-[Co(edma)(mdien)]SO_4 $\cdot$ $2H_2O$	25.51	6.45	16.42	25.41	6.64	16.47

Table 1. Continued

Complex	Found (%)			Calcd (%)		
	C	H	N	C	H	N
unsym-fac-fac(N_t)-[Co(edma)(mdien)]$Br_2 \cdot 1/2H_2O$	23.60	5.42	14.97	23.39	5.45	15.16
unsym-fac-mer(N_t)-[Co(edma)(mdien)]$SO_4 \cdot 3/2H_2O$	26.19	6.76	16.53	25.96	6.54	16.82
mer-[Co(edma)(mdien)]$SO_4 \cdot 5/2H_2O$	24.96	6.50	16.15	24.89	6.73	16.12
sym-fac-[Co(mida)(edma)]$\cdot H_2O$	31.79	5.51	12.39	31.87	5.35	12.39
unsym-fac-fac(N)-[Co(mida)(edma)]$\cdot 2H_2O$	30.22	5.70	11.77	30.26	5.64	11.76
sym-fac-Na[Co(ida)(mida)]$\cdot H_2O$	28.60	3.74	7.60	28.74	3.75	7.45
unsym-fac-K[Co(ida)(mida)]$\cdot 2H_2O$	26.39	3.86	7.06	26.35	3.93	6.83
mer-K[Co(ida)(mida)]$\cdot 1/2H_2O$	28.18	3.82	7.27	28.21	3.42	7.31
unsym-fac-K[Co(mida)$_2$]$\cdot 3/2H_2O$	29.06	4.08	6.76	28.92	4.13	6.75
cis-α-[Co(en)(trien)]I_3	14.76	4.18	13.04	14.88	4.06	13.01
cis-β-[Co(en)(trien)]$Cl_3 \cdot H_2O \cdot 13/10NaCl$	20.59	6.08	18.02	20.64	6.06	18.05
cis-α-[Co(ox)(trien)]$Cl \cdot 1/2H_2O$	28.27	5.63	16.47	28.46	5.67	16.59
cis-β-[Co(ox)(trien)]$Cl \cdot 9/4H_2O$	25.98	5.92	15.18	26.03	6.14	15.18
[Co(en)(tren)]$Cl_3 \cdot 2H_2O$	23.47	7.48	20.50	23.57	7.42	20.62

Table 1. Continued

Complex	Found (%)			Calcd (%)		
	C	H	N	C	H	N
[Co(ox)(tren)]Cl·H_2O	27.69	5.88	16.23	27.72	5.82	16.16
cis-α-[Co(edda)(en)]ClO_4	24.31	4.69	14.22	24.47	4.62	14.27
cis-β-[Co(edda)(en)]ClO_4·H_2O	23.23	4.94	13.52	23.40	4.91	13.64
cis-α-[Co(edda)(tn)]ClO_4	26.48	4.87	13.61	26.58	4.96	13.78
cis-β-[Co(edda)(tn)]ClO_4·H_2O	25.43	5.18	13.00	25.45	5.22	13.19
cis-α-[Co(edda)$(NH_3)_2$]NO_3·1/3H_2O·7/8NH_4NO_3	17.78	4.93	23.13	17.79	5.02	23.33
cis-α-[Co(edda)(gly)]·2H_2O	28.04	5.21	12.17	28.00	5.29	12.24
cis-α-[Co(edda)(β-ala)]·3/4H_2O	32.02	5.24	12.67	32.30	5.27	12.56
cis-α-Na[Co(edda)(ox)]·2H_2O	25.38	3.65	7.53	25.28	3.71	7.37
cis-β-Na[Co(edda)(ox)]·5/2H_2O	24.56	3.90	7.26	24.69	3.89	7.20
trans(O)-[Co(aeida)(en)]Cl·3H_2O	25.00	6.27	14.70	25.11	6.32	14.64
cis(O)-[Co(aeida)(en)]Cl·2H_2O	26.27	5.19	15.27	26.35	6.08	15.36
[Co(SCH_2COO)$(en)_2$]I	17.94	4.60	14.01	18.19	4.58	14.14
s-[Co(DL-asp)(dien)]Cl·3/2H_2O·1/3NaCl	25.65	5.60	14.99	25.61	5.64	14.94

Table 1. Continued

Complex	Found (%)			Calcd (%)		
	C	H	N	C	H	N
u[1]-[Co(DL-asp)(dien)]Cl·5/4H_2O·1/5C_2H_5OH·1/6NaCl	27.30	5.91	15.14	27.36	5.91	15.14
u[2]-[Co(DL-asp)(dien)]Cl·1/2H_2O·1/5NaCl	27.51	5.50	16.18	27.51	5.48	16.04
trans(N)-Na[Co(DL-asp)$_2$]·9/4H_2O·1/2NaCl	23.01	3.51	6.72	23.22	3.53	6.77
trans(O_5)-Na[Co(DL-asp)$_2$]·3H_2O·2/5NaCl	22.75	3.89	6.75	22.80	3.83	6.65
trans(O_6)-Na[Co(DL-asp)$_2$]·3/2H_2O	25.68	3.54	7.50	25.89	3.53	7.55
trans(N)-[Co(L-smc)$_2$]Cl·2H_2O·3/5NaCl	22.18	4.68	6.51	22.15	4.65	6.46
trans(O)-[Co(L-smc)$_2$]Cl·H_2O·1/3NaCl	24.06	4.55	7.09	24.01	4.53	7.00
trans(S)-[Co(L-smc)$_2$]Cl·2H_2O·9/5NaCl	19.19	4.09	5.56	19.07	4.00	5.56
trans(N)-[Co(L-met)$_2$]Br	27.57	4.59	6.47	27.60	4.63	6.44
trans(O)-[Co(L-met)$_2$]Br	27.51	4.64	6.52	27.60	4.63	6.44
trans(S)-[Co(L-met)$_2$]Br	27.38	4.66	6.43	27.60	4.63	6.44

Chapter VI. Normal Coordinate Analysis of $[Co(en)_3]^{3+}$ and $[Co(tn)_3]^{3+}$

VI-A. Introduction.

The assignment of the normal vibrations of metal complexes have been mainly made on the basis of the infrared (IR) spectra. However, there are the continuing controversy over the assignment of the IR-active metal-ligand vibrations. Therefore, in order to discuss the vibrational spectra in detail, the Raman spectra of several complexes have been measured in recent years and the assignment of the IR bands of the complexes have been reexamined on the basis of the Raman spectra.

A large amount of data have also been collected on the vibrational spectra of metal chelate complexes of en and tn. Especially, vibrational spectra of bis(ethylenediamine)-type metal complexes have been discussed by several authors.[45] Moreover, for the tris(ethylenediamine)-type metal complexes, the IR and Raman spectra have already been reported. However, interpretation of these results is still very unsatisfactory and band assignments and interpretations have almost been made without any assistance from the normal coordinate calculations except for some examples.[46] Accordingly, the main purpose of this chapter is to make sure the assignments of the skeletal vibrations of $[Co(en)_3]^{3+}$ and $[Co(tn)_3]^{3+}$ which are the fundamental and the representative examples of the cobalt(III) complexes. Attempts to give detailed assignments of the IR and Raman

spectra based upon the complete normal coordinate calculation will be presented in this chapter.

VI-B. Results

VI-B-1. Normal Coordinate Analysis of $[Co(en)_3]^{3+}$

Treatment of a framework of $[Co(en)_3]^{3+}$ under the point group D_3 reduces the 33 normal modes of vibration to the irreducible representation

$$\Gamma = 6A_1(R) + 5A_2(IR) + 11E(R,IR)$$

where (R) and (IR) indicate the Raman and infrared active modes, respectively.

The normal coordinate analysis was performed as a 13-body problem using the Wilson's GF matrix method (Chapter II). The potential function employed here was of the generalized valence force field (GVFF) type. The internal coordinates are given in Figs. 13 and 14. The symmetry coordinates listed in Table 3 were derived making use of the D_3 symmetry of the complex. The force constants in terms of the GVFF are selected as given in Table 4 and are based on values for trans-$[Co(CN)_2(en)_2]^+$ [47] (Table 5). The values used for the interatomic distances and bond angles are as follows; r(Co-N) = 1.978 Å, r(C-N) = 1.478 Å, r(C-C) = 1.520 Å, N-Co-N = 90.0° , Co-N-C = 99.6° , and C-C-N = 103.4° . A calculation procedure is schematically shown as follows:

$$S_t = \sum_{i=1}^{3N} B_{ti}\,\xi_i \quad (t = 1,2,\cdots,3N-6)\text{(Chapter II, Eq. 6-8)}$$

$$\downarrow$$

$$B_{ti}$$

$$|$$

$G = BM^{-1}\tilde{B}$ (M^{-1} is a diagonal matrix whose components are μ_i, where μ_i is the reciprocal of the mass of the i-th atom.)

↓ G

$G_S = UG\tilde{U}$

↓ G_S

$|GF-E\lambda| = |G_SF_S-E\lambda| = 0$ (Chapter II, Eq. 6-10)

↓ λ

$\tilde{\nu} = 1302.83\sqrt{\lambda}$

↓ $\tilde{\nu}$

The calculated frequencies are given in Table 6, which also includes an approximate description of the vibrational modes based upon the PED (potential energy distribution) of each vibration among the symmetry coordinates.

IV-B-2. Normal Coordinate Analysis of $[Co(tn)_3]^{3+}$

Irreducible representation of $[Co(tn)_3]^{3+}$ based on the point group D_3 is

$$\Gamma = 7A_1(R) + 7A_2(IR) + 14E(R,IR)$$

where (R) and (IR) indicate the Raman and infrared active modes, respectively. The calculation method is the same as that of $[Co(en)_3]^{3+}$. The values used for the interatomic distances and bond angles are as follows; r(Co-N) = 1.985 Å, r(C-N) = 1.498 Å, r(C-C) = 1.468 Å, N-Co-N = 90.0° , Co-N-C = 120.6° , C-C-N = 113.9° , and C-C-C = 93.7° . Tables 7 and 8 show the calculated values of force constants and the frequencies, respectively.

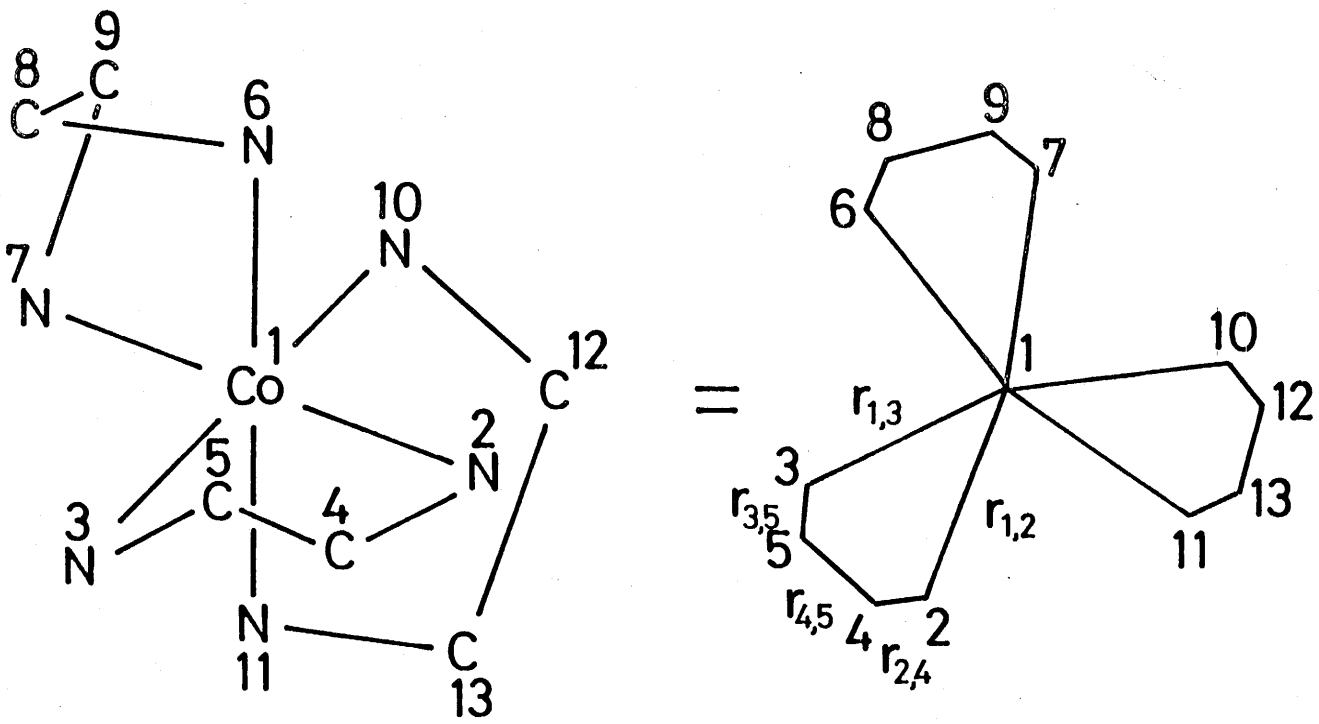

Figure 13. The internal bond stretching coordinates.

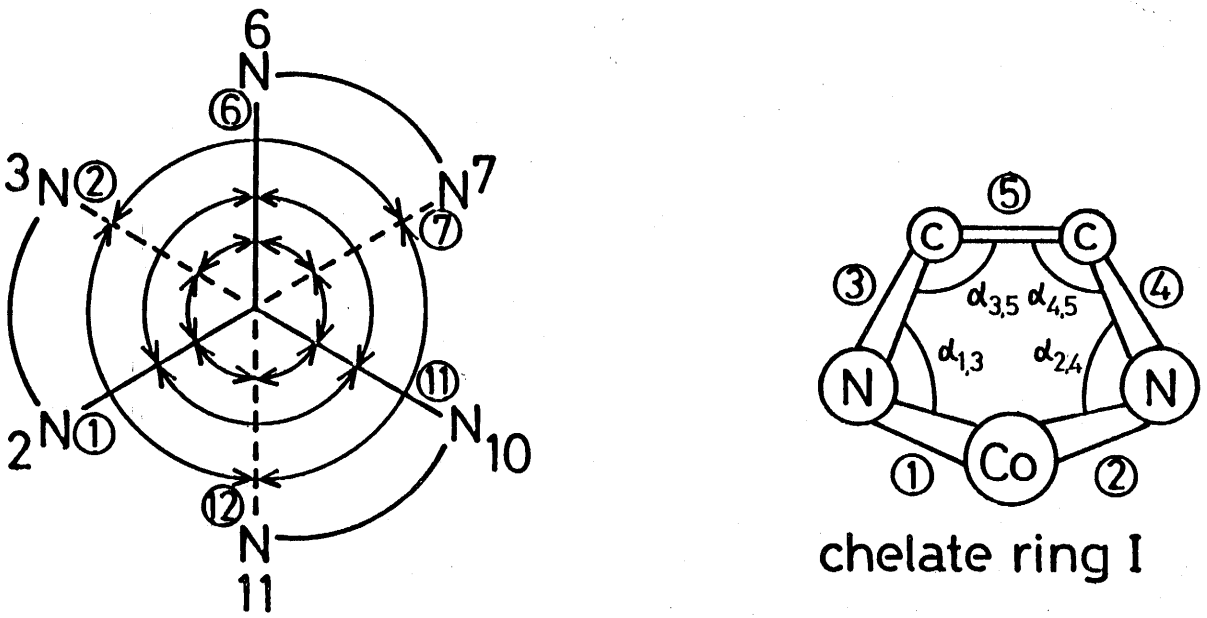

Figure 14. The internal angle deformation coordinates.

Table 3. Symmetry Coordinates for $[Co(en)_3]^{3+}$

Species A_1

$$S_1 = 1/\sqrt{6}(r_{1,2} + r_{1,3} + r_{1,6} + r_{1,7} + r_{1,10} + r_{1,11})$$

$$S_2 = 1/\sqrt{6}(r_{2,4} + r_{3,5} + r_{6,8} + r_{7,9} + r_{10,12} + r_{11,13})$$

$$S_3 = 1/\sqrt{3}(r_{4,5} + r_{8,9} + r_{12,13})$$

$$S_4 = 1/\sqrt{6}(\alpha_{1,3} + \alpha_{2,4} + \alpha_{6,8} + \alpha_{7,9} + \alpha_{11,13} + \alpha_{12,14})$$

$$S_5 = 1/\sqrt{6}(\alpha_{3,5} + \alpha_{4,5} + \alpha_{8,10} + \alpha_{9,10} + \alpha_{13,15} + \alpha_{14,15})$$

$$S_6 = 1/\sqrt{6}(\alpha_{1,2} + \alpha_{6,7} + \alpha_{11,12} + \alpha_{7,11} + \alpha_{1,12} + \alpha_{2,6})$$

$$S_7 = 1/\sqrt{6}(\alpha_{1,2} + \alpha_{6,7} + \alpha_{11,12} - \alpha_{7,11} - \alpha_{1,12} - \alpha_{2,6})$$

$$S_8 = 1/\sqrt{6}(\alpha_{1,6} + \alpha_{2,7} + \alpha_{6,11} + \alpha_{7,12} + \alpha_{1,11} + \alpha_{2,12})$$

Species A_2

$$S_1 = 1/\sqrt{6}(r_{1,2} - r_{1,3} + r_{1,6} - r_{1,7} + r_{1,10} - r_{1,11})$$

$$S_2 = 1/\sqrt{6}(r_{2,4} - r_{3,5} + r_{6,8} - r_{7,9} + r_{10,12} - r_{11,13})$$

$$S_3 = 1/\sqrt{6}(\alpha_{1,3} - \alpha_{2,4} + \alpha_{6,8} - \alpha_{7,9} + \alpha_{11,13} - \alpha_{12,14})$$

$$S_4 = 1/\sqrt{6}(\alpha_{3,5} - \alpha_{4,5} + \alpha_{8,10} - \alpha_{9,10} + \alpha_{13,15} - \alpha_{14,15})$$

$$S_5 = 1/\sqrt{6}(\alpha_{1,6} - \alpha_{2,7} + \alpha_{6,11} - \alpha_{7,12} + \alpha_{1,11} - \alpha_{2,12})$$

Species E

$$S_1 = 1/\sqrt{12}(2r_{1,2} + 2r_{1,3} - r_{1,6} - r_{1,7} - r_{1,10} - r_{1,11})$$

$$s_2 = 1/\sqrt{12}(2r_{2,4} + 2r_{3,5} - r_{6,8} - r_{7,9} - r_{10,12} - r_{11,13})$$

$$s_3 = 1/\sqrt{6}(2r_{4,5} - r_{8,9} - r_{12,13})$$

$$s_4 = 1/\sqrt{12}(2\alpha_{1,3} + 2\alpha_{2,4} - \alpha_{6,8} - \alpha_{7,9} - \alpha_{11,13} - \alpha_{12,14})$$

$$s_5 = 1/\sqrt{12}(2\alpha_{3,5} + 2\alpha_{4,5} - \alpha_{8,10} - \alpha_{9,10} - \alpha_{13,15} - \alpha_{14,15})$$

$$s_6 = 1/\sqrt{12}(2\alpha_{1,2} - \alpha_{6,7} - \alpha_{11,12} + 2\alpha_{7,11} - \alpha_{1,12} - \alpha_{2,6})$$

$$s_7 = 1/\sqrt{12}(-\alpha_{1,6} + 2\alpha_{2,7} - \alpha_{6,11} - \alpha_{7,12} + 2\alpha_{1,11} - \alpha_{2,12})$$

Table 4. Force Constants $F_{kk'}$ for $[Co(en)_3]^{3+}$

A_1 Species

$$F_{11} = f(\underset{1}{Co\text{-}N}) + 4f(\underset{2}{Co\text{-}N, Co\text{-}N}) + f(\underset{3}{Co\text{-}N, Co\text{-}N'})$$

$$F_{22} = f(\underset{4}{C\text{-}N})$$

$$F_{33} = f(\underset{5}{C\text{-}C})$$

$$F_{44} = r_{Co\text{-}N} r_{C\text{-}N} f(\underset{6}{Co\text{-}N\text{-}C})$$

$$F_{55} = r_{C\text{-}N} r_{C\text{-}C} f(\underset{7}{C\text{-}C\text{-}N})$$

$$F_{66} = 1/2 r^2_{Co\text{-}N} f(\underset{8}{N\text{-}Co\text{-}N}) + 1/2 r^2_{Co\text{-}N} f(\underset{8}{N\text{-}Co\text{-}N}) + 2r^2_{Co\text{-}N} f(\underset{9}{N\text{-}Co\text{-}N, N\text{-}Co\text{-}N'})$$

$$F_{77} = 1/2 r^2_{Co\text{-}N} f(\underset{8}{N\text{-}Co\text{-}N}) + 1/2 r^2_{Co\text{-}N} f(\underset{8}{N\text{-}Co\text{-}N}) - 2r^2_{Co\text{-}N} f(\underset{9}{N\text{-}Co\text{-}N, N\text{-}Co\text{-}N'})$$

$$F_{88} = r^2_{Co\text{-}N} f(\underset{8}{N\text{-}Co\text{-}N}) + 2r^2_{Co\text{-}N} f(\underset{9}{N\text{-}Co\text{-}N, N\text{-}Co\text{-}N'})$$

$$F_{12} = f(\underset{10}{Co\text{-}N, C\text{-}N})$$

$$F_{14} = \sqrt{r_{Co\text{-}N} r_{C\text{-}N}} f(\underset{11}{Co\text{-}N, Co\text{-}N\text{-}C})$$

$$F_{16} = r_{Co\text{-}N} f(\underset{12}{Co\text{-}N, N\text{-}Co\text{-}N}) + r_{Co\text{-}N} f(\underset{12}{Co\text{-}N, N\text{-}Co\text{-}N})$$

$$F_{17} = r_{Co\text{-}N} f(\underset{12}{Co\text{-}N, N\text{-}Co\text{-}N}) - r_{Co\text{-}N} f(\underset{12}{Co\text{-}N, N\text{-}Co\text{-}N})$$

$$F_{18} = 2r_{Co\text{-}N} f(\underset{12}{Co\text{-}N, N\text{-}Co\text{-}N})$$

$$F_{23} = \sqrt{2} f(\underset{13}{C\text{-}N, C\text{-}C})$$

$$F_{24} = \sqrt{r_{Co\text{-}N} r_{C\text{-}N}} f(\underset{14}{C\text{-}N, Co\text{-}N\text{-}C})$$

$$F_{25} = \sqrt{r_{C-N} r_{C-C}}\, f(C-N,C-C-N)_{15}$$

$$F_{35} = \sqrt{r_{C-N} r_{C-C}}\, f(C-C,C-C-N)_{16}$$

$$F_{68} = r^2_{Co-N} f(N-Co-N,N-Co-N')_{9} + r^2_{Co-N} f(N-Co-N,N-Co-N')_{17} + r^2_{Co-N} f(N-Co-N,N-Co-N')_{9} + r^2_{Co-N} f(N-Co-N,N-Co-N')_{17}$$

A_2 Species

$$F_{11} = f(Co-N)_{1} - f(Co-N,Co-N')_{3}$$

$$F_{22} = f(C-N)_{4}$$

$$F_{33} = r_{Co-N} r_{C-N} f(Co-N-C)_{6}$$

$$F_{44} = r_{C-N} r_{C-C} f(C-C-N)_{7}$$

$$F_{55} = r^2_{Co-N} f(N-Co-N)_{8} + 2r^2_{Co-N} f(N-Co-N,N-Co-N')_{9}$$

$$F_{12} = f(Co-N,C-N)_{10}$$

$$F_{13} = \sqrt{r_{Co-N} r_{C-N}}\, f(Co-N,Co-N-C)_{11}$$

$$F_{15} = 2r_{Co-N} f(Co-N,N-Co-N)_{12}$$

$$F_{23} = \sqrt{r_{Co-N} r_{C-N}}\, f(C-N,Co-N-C)_{14}$$

$$F_{24} = \sqrt{r_{C-N} r_{C-C}}\, f(C-N,C-C-N)_{15}$$

E Species

$$F_{11} = f(Co-N)_{1} - 1/2f(Co-N,Co-N)_{2} - 1/2f(Co-N,Co-N')_{3}$$

$$F_{22} = f(C-N)_{4}$$

$$F_{33} = f(C-C)_{5}$$

$$F_{44} = r_{Co-N} r_{C-N} f_{6}(Co-N-C)$$

$$F_{55} = r_{C-N} r_{C-C} f_{7}(C-C-N)$$

$$F_{66} = 1/2 r^2_{Co-N} f_{8}(N-Co-N) + 1/2 r^2_{Co-N} f_{8}(N-Co-N) - r^2_{Co-N} f_{9}(N-Co-N,N-Co-N')$$

$$F_{77} = r^2_{Co-N} f_{8}(N-Co-N) - r^2_{Co-N} f_{9}(N-Co-N,N-Co-N')$$

$$F_{12} = f_{10}(Co-N,C-N)$$

$$F_{14} = \sqrt{r_{Co-N} r_{C-N}} f_{11}(Co-N,Co-N-C)$$

$$F_{16} = r_{Co-N} f_{12}(Co-N,N-Co-N) - 1/2 r_{Co-N} f_{12}(Co-N,N-Co-N)$$

$$F_{17} = 1/2 r_{Co-N} f_{12}(Co-N,N-Co-N)$$

$$F_{23} = \sqrt{2} f_{13}(C-N,C-C)$$

$$F_{24} = \sqrt{r_{Co-N} r_{C-N}} f_{14}(C-N,Co-N-C)$$

$$F_{25} = \sqrt{r_{C-N} r_{C-C}} f_{15}(C-N,C-C-N)$$

$$F_{35} = \sqrt{r_{C-N} r_{C-C}} f_{16}(C-C,C-C-N)$$

$$F_{67} = r^2_{Co-N} f_{17}(N-Co-N,N-Co-N') - r_{Co-N} f_{9}(N-Co-N,N-Co-N') + r^2_{Co-N} f_{17}(N-Co-N,N-Co-N') - r_{Co-N} f_{9}(N-Co-N,N-Co-N')$$

Table 5. Valence Force Constants for $[Co(en)_3]^{3+}$

Force Type		Atoms Involved	Value Final	Value Initial[a)]
Stretch	1	Co-N	2.0338	1.593
	4	C-N	4.6664	3.385
	5	C-C	3.8919	2.802
Stretch-stretch	2	Co-N,Co-N	0.2500	-
	3	Co-N,Co-N'	-0.0870	0.054
	10	Co-N,C-N	0.0000	0.059
	13	C-N,C-C	0.0815	0.117
Bend	6	Co-N-C	0.0985	0.383
	7	C-C-N	0.2213	0.989
	8	N-Co-N	0.5125	1.531
Stretch-bend	11	Co-N,Co-N-C	0.1831	0.093
	12	Co-N,N-Co-N	-0.1620	0.110
	14	C-N,Co-N-C	0.0410	0.086
	15	C-N,C-C-N	0.1670	0.257
	16	C-C,C-C-N	0.1670	0.259
Bend-bend	9	N-Co-N,N-Co-N'	-0.0150	-
	17	N-Co-N,N-Co-N'	0.1328	-

a) Ref. 47. Force constants in units of $mdyn \cdot Å^{-1}$ (stretch, stretch-stretch), $mdyn \cdot Å \cdot rad^{-2}$ (bend, bend-bend), and $mdyn \cdot rad^{-1}$ (stretch-bend).

Table 6. Calculated (ν_{calc}, cm^{-1}) and Observed (ν_{obs}, cm^{-1}) Frequencies and Main Potential Energy Distribution (PED, %) for $[Co(en)_3]^{3+}$ from a 17-Parameter GVFF Based Upon the Spectra of $[Co(en)_3]^{3+}$

Species	ν_{calc}	ν_{obs} [a]	PED
A_1	1091	1066	ν(CN)(73), ν(CC)(26)
	894	897	ν(CC)(79), ν(CN)(23)
	535	525	ν(MN)(72)
	366	338	δ(NMN)(80), δ(CCN)(22)
	263	283	δ(NMN)(156)
	168	207	δ(CCN)(49)
A_2	1013	1009	ν(CN)(97)
	576	580	δ(NMN)(88)
	449	442	ν(MN)(79)
	209	200	δ(MNC)(77)
E	1100	1127	ν(CN)(74)
	900	897	ν(CC)(83), ν(CN)(19)
	427	440	ν(MN)(109)
	367	378	δ(NMN)(48)
	229	200	δ(NMN)(143)
	158	163	δ(NMN)(59)

a) Freshly measured solvent and solid data and data of refs. 49 and 50 were used.

Table 7. Valence Force Constants for $[Co(tn)_3]^{3+}$

Force Type	Atoms Involved	Value Final[a)]
Stretch	Co-N	1.7246
	C-N	4.6660
	C-C	3.8920
Stretch-stretch	Co-N,Co-N	0.2500
	Co-N,Co-N'	-0.0870
	Co-N,C-N	0.0000
	C-N,C-C	0.0820
	C-C,C-C	0.0820
Bend	Co-N-C	0.1529
	C-C-N	0.2666
	N-Co-N	0.5441
	C-C-C	0.0992
Stretch-bend	Co-N,Co-N-C	0.0828
	Co-N,N-Co-N	-0.1620
	C-N,Co-N-C	0.0410
	C-N,C-C-N	0.1670
	C-C,C-C-N	0.1670
	C-C,C-C-C	0.1670
Bend-bend	N-Co-N,N-Co-N'	-0.0150
	N-Co-N,N-Co-N'	0.1680

a) The values of $[Co(en)_3]^{3+}$ were used as initial values. Force constants in units of mdyn $\cdot$ Å^{-1} (stretch, stretch-stretch), mdyn $\cdot$ Å $\cdot$ rad^{-2} (bend, bend-bend), mdyn $\cdot$ rad^{-1} (stretch-bend).

Table 8. Calculated (ν_{calc}, cm^{-1}) and Observed (ν_{obs}, cm^{-1}) Frequencies and Main Potential Energy Distribution (PED, %) for $[Co(tn)_3]^{3+}$ from a 20-Parameter GVFF Based Upon the Spectra of $[Co(tn)_3]^{3+}$

Species	ν_{calc}	ν_{obs} [a]	PED
A_1	1087	1072	ν(CN)(83), ν(CC)(15)
	794	818	ν(CC)(91), ν(CN)(11)
	521	530	ν(MN)(39)
	441	451	δ(CCN)(58), ν(MN)(13)
	317	304	δ(NMN)(142)
	259	250	δ(NMN)(80)
	216	213	δ(NMN)(109)
	201	168	δ(MNC)(40), δ(CCN)(26), δ(NMN)(32)
	80	100 [b]	δ(MNC)(37), δ(NMN)(35)
A_2	814	819	ν(CN)(60), δ(NMN)(40)
	759	763	δ(NMN)(56), ν(CN)(26)
	420	422	ν(MN)(61), δ(CCN)(30)
	334	360	ν(CC)(67), δ(MNC)(15)
	123	111	δ(MNC)(37)
	56	50 [b]	δ(CCN)(49), δ(MNC)(41)
E	1042	1033	ν(CC)(51), ν(CN)(46)
	511	490	δ(CCN)(42)
	470	472	ν(CC)(28), ν(CN)(23)
	359	352	ν(MN)(80)
	257	258	δ(CCN)(41), δ(NMN)(29)
	215	216	δ(NMN)(243)
	81	84	δ(MNC)(45)

78	$70^{b)}$	δ(MNC)(33)	

a) Freshly measured solvent and solid data and data of ref. 50 were used.

b) Arbitrary values.

VI-C. Discussion

It is obvious from Tables 6 and 8 that the calculated frequencies (ν_{calc}) give the fit with the observed frequencies (ν_{obs}). The value of the Co-N stretching force constant was found to decrease from 2.0338 mdyn/Å in $[Co(en)_3]^{3+}$ to 1.7246 mdyn/Å in $[Co(tn)_3]^{3+}$. This trend reflects a weaker bond strength (Co-N) in the latter complex as compared with the former one and may also be correlated to the absorption spectra of the $^1T_{1g} \leftarrow {}^1A_{1g}$ (O_h) electronic transition energy; 21.30×10^3 cm^{-1} $[Co(en)_3]^{3+}$ > 20.49×10^3 cm^{-1} $[Co(tn)_3]^{3+}$.

The Raman bands at 525, 440, and 378 cm^{-1} of $[Co(en)_3]^{3+}$ in aqueous solution have been assigned to the totally symmetric stretching vibration, ν_{ts}(Co-N), the non-totally symmetric stretching vibration, ν(Co-N), and the bending deformation, δ(N-Co-N), respectively (V-B-1). This calculation confirms the assignment of these Raman bands; ν(MN)(72) for the band at 525 cm^{-1}, ν(MN)(109) for that at 440 cm^{-1}, and δ(NMN)(48) for that at 378 cm^{-1}. The Raman band at 283 cm^{-1} has been assigned to the chelate ring deformation,[48] but this calculation indicates that the Raman band at 283 cm^{-1} consist mainly of N-Co-N deformation characteristic, δ(NMN)(156). Accordingly, the band at 283 cm^{-1} may be considered to the chelate ring deformation which is mainly influenced by the N-Co-N deformation.

From PED of $[Co(tn)_3]^{3+}$, the Raman band at 530 cm^{-1} of $[Co(tn)_3]^{3+}$ can be assigned to ν_{ts}(Co-N) (Table 8) and this result is consistent with the assignment based on the Raman

spectra of $[Co(en)_n(tn)_{3-n}]$-type complexes (V-B-1). However, the Raman bands at 352 and 451 cm^{-1} can be assigned to ν(Co-N) and δ(CCN) + ν(Co-N), respectively, by the normal coordinate analysis and these assignments disagree with those given in V-B-1. In view of the degree of confidence of PED and the Raman spectra of $[Co(en)_n(tn)_{3-n}]$-type complexes, the Raman bands at 352 and 451 cm^{-1} may be attributed to N-Co-N deformation and Co-N stretching, respectively.

Chapter V. Raman Spectral Characteristics of Cobalt(III) Complexes

V-A. Introduction.

It has generally been accepted that vibrational spectra are one of the most useful means for examination on the configurations of transition metal complexes. Especially, the skeletal vibrations of the complexes, which appear in lower frequency region, reflect well their structural characteristics.

Differentiation between the geometrical isomers of the cobalt(III) complexes has mainly been made by the electronic absorption, the nuclear magnetic resonance, and the circular dichroism spectral and the X-ray structure analysis methods. The X-ray structural method is one of the most definite method for the differentiation among the geometrical isomers but this technique is generally applied to crystal structure which is strictly different from the structure in solution. Moreover, a method using radial distribution function for the structure in solution is difficult to refer to as the direct method. The NMR spectral method is too complicated for the cobalt(III) complexes. The usefulness of the electronic absorption spectral method is limited to those cases where the ligand field strengths of the ligands are different each other, being enough to cause a splitting in the first d-d absorption band.

The Raman spectral criteria[51] in the skeletal vibration region have recently been established for differentiating the geometrical isomers of the several

cobalt(III) complexes; the Raman spectra in the skeletal vibration region of $[Co(a)(b)(en)_2]$,[52] $[Co(a)(b)(NH_3)_4]$,[53] $[Co(a)(b)(tn)_2]$,[54] $[Co(a)_2(NH_3)_2(en)]$,[55] and $[Co(CN)_2(L\text{-}ala)_2]$,[56] where a and b stand for unidentate ligands, have been measured in order to find the vibrational criteria. Furthermore, the nitro-ammine series of the cobalt(III) complexes have been studied in order to establish the assignments of the Raman bands[57] and the solution structure of the Cr(III)-edta complex as a function of pH have also been studied by the Raman spectroscopy.[58]

The purpose of the investigations in this chapter is to deduce general Raman spectral characteristics of several cobalt(III) complexes and to obtain the definite criteria for differentiating their geometrical isomers.

V-B. Results and Discussion.

V-B-1. Raman Spectra of Cobalt(III) Complexes with Bidentate Ligands Containing N and/or O Donor Atoms.

Raman spectral data of the $[Co(gly)_x(ox)_y(en)_z]^{(3-x-2y)+}$ complexes are summarized in Table 9.[59] $[Co(en)_3]^{3+}$ and $[Co(ox)_3]^{3-}$ give the same spectral characteristics; a polarized band in the 520 - 610 cm^{-1} region (depolarization ratio: ca. 0), two depolarized bands in the 400 - 520 cm^{-1} and 300 - 400 cm^{-1} regions, and a polarized one in the 200 - 300 cm^{-1} region (depolarized ratio: 0.12 - 0.16). Both $[Co(en)_3]^{3+}$ and $[Co(ox)_3]^{3-}$ have the same effective symmetry (vide infra) of O_h. Furthermore, it is clear that the Raman

bands of $[Co(en)_3]^{3+}$ can well be correlated to those of $[Co(NH_3)_6]^{3+}$ having an O_h symmetry, except the polarized one in the 200 - 300 cm^{-1} region, which relates to the en chelate ring[59] (Fig. 15). Hence it may be expected that, so far as the skeletal vibrations of the octahedral tris(bidentate)cobalt(III) complexes with five-membered chelate rings are concerned, the Raman spectra are treated in terms of the effective symmetry,[59] which is mainly specified by arrangement of coordinated atoms around the central metal atom. This simplified treatment can also be supported by the Raman spectra of trans(O)-$[Co(gly)_2(en)]^+$ and trans(N)-$[Co(gly)_2(ox)]^-$ having the effective symmetry of D_{4h} (Fig. 15). Accordingly, by analogy to $[Co(NH_3)_6]^{3+}$,[59] the polarized bands in the 520 - 610 cm^{-1} region, the depolarized bands in the 400 - 520 cm^{-1} region, the depolarized bands in the 300 - 400 cm^{-1} region, and the polarized bands in the 200 - 300 cm^{-1} region can be assigned to a totally symmetric stretching vibration mode, a stretching vibration mode excluding the totally symmetric one (i.e., non-totally symmetric one), a skeletal bending deformation mode, and a chelate ring deformation mode,[59] respectively.

It is interesting to note that the coordinated gly, ox, and en ligands have characteristic bands in the regions 584 - 608, 564 - 570, and 521 - 542 cm^{-1}, respectively. These results demonstrate that the coordinated bidentate ligands behave as a unit owing to restrictions by the chelate rings (Table 9). Furthermore, it can be seen from Table 9 that

Table 9. Raman Spectral Data of $[Co(gly)_x(ox)_y(en)_z]$-Type Complexes.

No.	Complexes	Raman frequency / cm^{-1} a)						
1	$[Co(NH_3)_6]^{3+}$			495 s(p)		440 m(dp)	320 w(dp)	
				495 [67]		440 [67]		
				490 [68]		440 [68]	317 [68]	
				494 [69]		442 [69]	322 [69]	
2	$[Co(en)_3]^{3+}$			525 s(p)		440 w(dp)	378 w(dp)	283 s(p)
				526 [48]		444 [48]	376 [48]	280 [48]
3	$[Co(gly)(en)_2]^{2+}$	584 w(p)		521 s(p)	471 vw(dp)	447 w(dp)	374 w(dp)	279 s(p)
4	$[Co(ox)(en)_2]^{+}$		565 m(p)	528 s(p)	480 vw(dp)	456 w(dp)	374 w(dp) 358 vw(dp)	278 s(p)
5	C_1-cis(O)-$[Co(gly)_2(en)]^{+}$	593 m(p)		526 m(p)	494 w(dp) 469 w(dp)	430 vw(dp) 422 vw(dp)	358 w(dp)	276 s(p)
6	C_2-cis(O)-$[Co(gly)_2(en)]^{+}$	598 m(p)		538 s(p)	486 w(dp)	433 w(dp)	360 w(dp)	276 s(p)
7	trans(O)-$[Co(gly)_2(en)]^{+}$	596 m(p)		523 m(p)	504 sh(dp)	458 w(dp)	368 w(dp)	275 s(p)
8	mer(N)-$[Co(gly)(ox)(en)]$	602 w(p)	567 m(p)	532 m(p)	498 vw(dp) 476 w(dp)	436 vw(dp)	362 w(dp)	275 s(p)
9	mer(N)-$[Co(gly)_3]$	602 s(p)			540 vw(dp) 496 w(dp)	440 vw(dp)	356 w(dp)	272 s(p)
10	fac(N)-$[Co(gly)_3]$	603 s(p)			487 w(dp)	438 w(dp)	364 w(dp)	270 s(p)
11	fac(N)-$[Co(gly)(ox)(en)]$	603 m(p)	566 m(p)	531 s(p)	488 w(dp)	426 w(dp)	358 w(dp)	270 s(p)
12	trans(N)-$[Co(gly)_2(ox)]^{-}$	608 vw(p)	565 vw(p)		494 w(dp)	440 w(dp)	348 w(dp)	260 w(p)
13	C_2-cis(N)-$[Co(gly)_2(ox)]^{-}$	602 m(p)	564 m(p)		510 w(dp)	432 w(dp)	348 w(dp)	260 s(p)

14	C_1-cis(N)-$[Co(gly)_2(ox)]^-$	604 m(p)	564 m(p)		512 w(dp) 504 w(dp)	432 w(dp) 419 w(dp)	342 w(dp)	262 s(p)
15	$[Co(ox)_2(en)]^-$		567 s(p)	542 m(p)	492 w(dp)	432 w(dp)	354 w(dp) 340 vw(dp)	268 s(p)
16	$[Co(gly)(ox)_2]^{2-}$	605 w(p)	567 w(p)		505 w(dp)	446 w(dp)	340 w(dp)	260 w(p)
17	$[Co(ox)_3]^{3-}$		570 w(p)		506 w(dp)		335 w(dp)	257 w(p)

Assignment [a]	ν_{ts}(Co-L) for gly	ν_{ts}(Co-L) for ox	ν_{ts}(Co-L) for en	ν(Co-O)	ν(Co-N)	δ_{sbd}(L-Co-L)	$\delta_{crd}(Co\overset{L}{\prec}_{L})$

a) The following abbreviations are used: s, strong; m, medium; w, weak; vw, very weak; sh, shoulder; p, polarized; dp, depolarized; ν_{ts}, totally symmetric stretching vibration mode; ν, stretching vibration mode excluding the totally symmetric stretching character; δ_{sbd}, skeletal bending deformation mode; δ_{crd}, chelate ring deformation mode; and L, donor atom (N and/or O). The Raman band intensities (s, m, w, vw, and sh) are classified by a comparison of all the Raman bands among all the complexes.

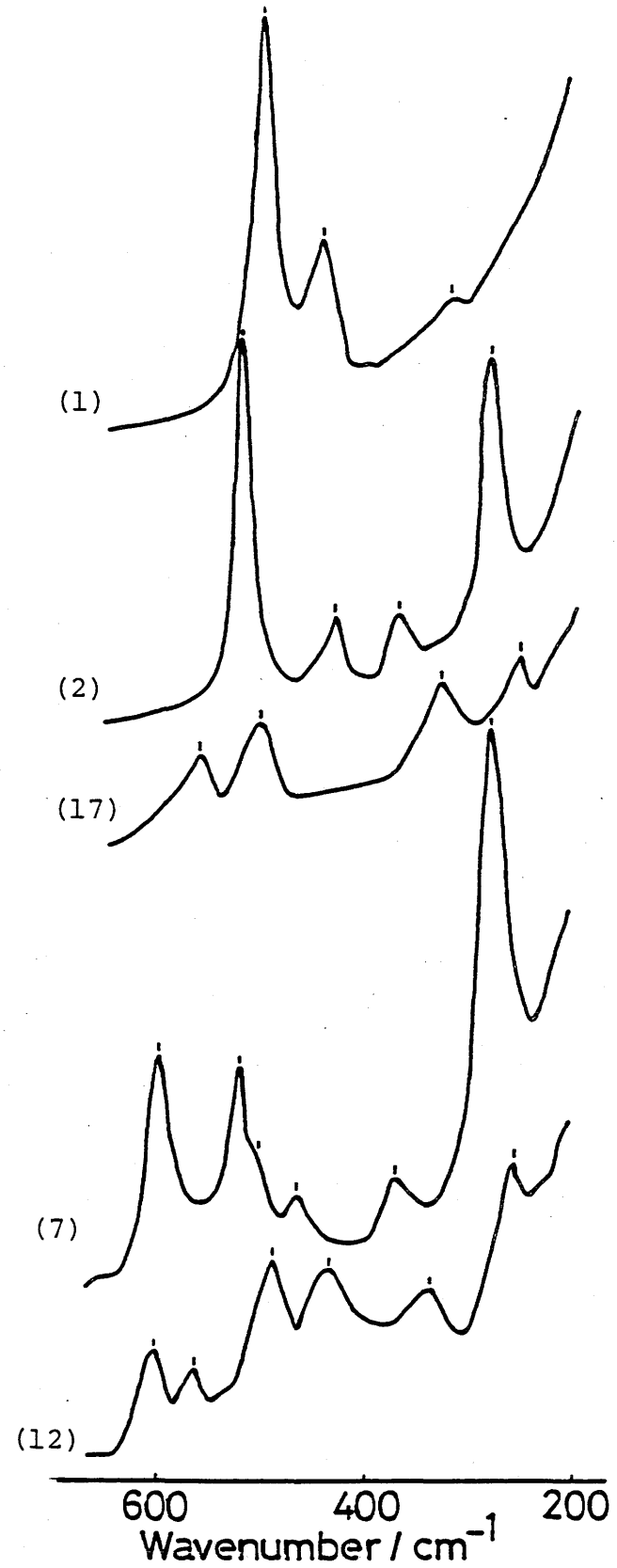

Figure 15. Raman spectra of $[Co(NH_3)_6]^{3+}$, $[Co(en)_3]^{3+}$, $[Co(ox)_3]^{3-}$, trans(O)-$[Co(gly)_2(en)]^+$, and trans(N)-$[Co(gly)_2(ox)]^-$. Numbers in parentheses correspond to those in Table 9.

the Raman bands in the stretching vibration mode excluding the totally symmetric one show some unique aspects. The Co-N stretching mode lies as a general rule in the region below 460 cm^{-1} and the Co-O stretching mode above 470 cm^{-1}.

The Raman spectral data in the skeletal vibration region of the tris(bidentate)cobalt(III) complexes containing the six-membered tn and/or β-ala chelate ring are summarized in Table 10. There is a significant distinction in the Raman spectral characteristics; on going from the cobalt(III) complexes with five-membered chelate rings to those containing six-membered ones, the number of the Raman bands is increased, and the bands are shifted to lower frequencies. For instance, the Raman spectrum of $[Co(en)_3]^{3+}$ exhibits four major low frequency lines, which were assigned to the stretching and bending deformation modes ($A_{1g} + E_g + T_{2g}$ with the effective symmetry of O_h) and to the chelate ring deformation mode on the basis of a comparison with the skeletal vibrations of $[Co(NH_3)_6]^{3+}$,[48,59] whereas the spectrum of $[Co(tn)_3]^{3+}$ exhibits eight Raman bands. The increase in the number of Raman bands reflects the difference between tn and en chelate rings, and it is expected that the Raman bands of $[Co(tn)_3]^{3+}$ can be treated in terms of a molecular symmetry slightly lower than the true one, $D_3(3A_1 + 5E)$, which is determined by the configuration of the chelate rings. Above all, the 451 cm^{-1} band (strong and polarized) and the 431 cm^{-1} band (shoulder and depolarized) can be assigned to A_1

(totally symmetric stretching mode) and E (stretching vibration mode excluding the totally symmetric one), respectively. An X-ray structure analysis and model consideration of $[Co(tn)_3]^{3+}$ show that the six-membered rings are more flexible than the five-membered ones and that the distortion of the octahedral coordination[60] make the former more conformationally labile than the latter. In fact, the CD spectrum of Δ-$(+)_{589}$-$[Co(tn)_3]^{3+}$ indicates a conformational equilibrium in solution between the tris skew-boat and tris chair forms.[61] Accordingly, it may be inferred that the Raman spectrum of $[Co(tn)_3]^{3+}$ reflects the conformational complexity of the six-membered chelate ring. Here, we should refer to the Raman spectra of the $[Co(a)(b)(tn)_2]$-type complexes, where a and b denote unidentate ligands, exhibiting also some Raman bands in the region of 400 - 550 cm^{-1}.[54] The very strong band at ca. 450 cm^{-1} and the bands in the region of 480 - 550 cm^{-1} have been assigned[54] to the Co-N(tn) stretching mode, ν(Co-N(tn)), and the deformation vibration of the chelate ring, δ(CCN), respectively, by considering the Raman spectra of the $[Co(a)(b)(en)_2]$-type complexes and the $[M(en)_2]^{2+}$ (M = Cu, Pd, and Pt) complexes based on the normal coordinate analysis. However, in the case of the $[Co(tn)_3]^{3+}$ complex, it seems reasonable to consider that the bands in the region of 450 - 530 cm^{-1} can be assigned to the totally symmetric stretching vibration mode, because the bands at 451 and 530 cm^{-1} of $[Co(tn)_3]^{3+}$ are shifted to lower frequencies (ca. 15 cm^{-1}) upon a deuteration of the amino protons of the 1,3-

propanediamine ligand, as is to be expected for the bands due to the Co-N stretching vibration. The difference in the region of each vibration mode between the cobalt(III) complexes containing the six-membered chelate rings and those with five-membered rings is not so much, as is shown in Tables 9 and 10, and it should be noted that the Raman spectra of cobalt(III) complexes with bidentate ligands can be generally treated in terms of the effective symmetry, irrespective of the chelate ring size (five- and six-membered ones). Accordingly, the Raman spectra of the cobalt(III) complexes containing the six-membered chelate ring can also be classified into four vibration modes, like those with the five-membered chelate rings: The totally symmetric stretching vibration mode (440 - 640 cm^{-1}), the stretching vibration mode excluding the totally symmetric one (i.e., non-totally symmetric one) (380 - 480 cm^{-1}), the skeletal bending deformation mode (260 - 400 cm^{-1}), and the chelate ring deformation mode (220 - 290 cm^{-1}) from the higher frequency region.

A comparison of the Raman spectra in the skeletal vibration region of the four $[Co(en)_n(tn)_{3-n}]^{3+}$ (n = 0 - 3) complexes (Fig. 16 and Table 10) clearly demonstrates that the number of the Raman bands increase with the substitution of the en ligand by the tn one and that the Raman bands of the chelate ring deformation mode are shifted to lower frequencies. Furthermore, $[Co(en)_2(tn)]^{3+}$ and $[Co(en)(tn)_2]^{3+}$ exhibit equally the bands due to the Co-

N(en) and Co-N(tn) totally symmetric stretching vibration mode; the bands due to ν_{ts}(Co-N(en)) and ν_{ts}(Co-N(tn)) are observed in the region above 500 cm^{-1} and ca. 450 cm^{-1}, respectively. The shift of the Raman bands due to ν_{ts}(Co-N(en)), 525, 517, and 506 cm^{-1} for the $[Co(en)_n(tn)_{3-n}]$-type complexes may be attributed to the increased relaxation of the Co-N(en) bonds by stepwise substitution of the tn ligand for the en one. That is, there is no appreciable vibration coupling between ν_{ts}(Co-N(tn)) and ν_{ts}(Co-N(en)). In addition, the intensities of the bands, ν_{ts}(Co-N(tn)) and ν_{ts}(Co-N(en)), of the mixed ligand complexes are proportional to the number of the en ligand and the tn one. Here, it is worthy to note that the ν_{ts}(Co-N) Raman shifts of $[Co(NH_3)_6]^{3+}$, $[Co(en)_3]^{3+}$, and $[Co(tn)_3]^{3+}$ decrease in the following order; ν_{ts}(Co-N(en)) > ν_{ts}(Co-N(NH_3)) > ν_{ts}(Co-N(tn)). This decreasing order is in line with that for the $^1T_{1g} \leftarrow {}^1A_{1g}(O_h)$ electronic transition energy of the $[Co(N)_6]$ chromophore; 21.30 x 10^3 cm^{-1} ($[Co(en)_3]^{3+}$)[62] > 20.96 x 10^3 cm^{-1} ($[Co(NH_3)_6]^{3+}$)[63] > 20.49 x 10^3 cm^{-1} ($[Co(tn)_3]^{3+}$).[7] The spectral behavior caused by the substitution of the en ligand by the tn one is also observed for the $[Co(gly)(en)_2]^{2+}$ and $[Co(gly)(tn)_2]^{2+}$ complexes. That is, $[Co(gly)(tn)_2]^{2+}$ shows more Raman bands than does $[Co(gly)(en)_2]^{2+}$, as is to be expected from the results for the $[Co(en)_n(tn)_{3-n}]$-type complexes (Fig. 17). The Raman band due to the chelate ring deformation mode of $[Co(gly)(tn)_2]^{2+}$ is also shifted to a lower frequency. Furthermore, a comparison of the Raman bands in the totally

symmetric stretching vibration region of $[Co(tn)_3]^{3+}$ (Fig. 16) and $[Co(gly)(tn)_2]^{2+}$ suggests that the band at 482 cm^{-1} of $[Co(gly)(tn)_2]^{2+}$ is the characteristic band of the coordinated gly ligand, similar to the spectral relation between $[Co(en)_3]^{3+}$ and $[Co(gly)(en)_2]^{2+}$.[59]

The Raman spectra of $[Co(\beta\text{-ala})(en)_2]^{2+}$ and $[Co(en)_3]^{3+}$ reveal that the replacement of the en ligand in $[Co(en)_3]^{3+}$ by the β-ala one causes no changes in the intrisic spectral features; the four bands of $[Co(\beta\text{-ala})(en)_2]^{2+}$ can be correlated to those of $[Co(en)_3]^{3+}$ (Fig. 18). This spectral behavior is in quite contrast to that resulting from the replacement of the en ligand by the gly one.[59] The good correlation of the Raman spectral features between $[Co(\beta\text{-ala})(en)_2]^{2+}$ and $[Co(en)_3]^{3+}$ may result from the fact that the skeletal vibration behavior of the former is determined by the two en chelate rings because of the conformational restriction due to the five-membered chelate ring and because of the proximity of the reduced mass of the donor atoms. The Raman spectra of $[Co(\beta\text{-ala})(en)_2]^{2+}$ and trans(O)-$[Co(\beta\text{-ala})_2(en)]^{+}$ show that the Raman spectral features are no longer retained upon a structural change from the former to the latter (Fig. 18), whereas a comparison of the spectra of $[Co(gly)(en)_2]^{2+}$ and trans(O)-$[(gly)_2(en)]^{+}$ reveals that the spectral features are well retained even after the structural change.[59] This Raman spectral evidence clearly demonstrates that the six-membered β-ala chelate ring is more flexible than the five-membered

gly chelate ring, as in the case of the tn and en chelate rings (vide supra).

Finally, it should be pointed out that the characteristic feature of the Raman spectrum of C_1-cis(O)-$[Co(\beta\text{-ala})_2(tn)]^+$ is considered to be an overlapping one with those of fac(N)-$[Co(\beta\text{-ala})_3]$ and $[Co(tn)_3]^{3+}$ as is shown in Fig. 19. That is, we can state that the strong and polarized band at 454 cm^{-1} of C_1-cis(O)-$[Co(\beta\text{-ala})_2(tn)]^+$ corresponds to the totally symmetric stretching vibration mode, ν_{ts}(Co-N(tn)), and also that the polarized bands in the region above 490 cm^{-1} are principally related to the β-ala ligand. This feature corresponds to the results that Raman bands in the totally symmetric stretching vibration mode of the $[Co(gly)_x(ox)_y(en)_z]$-type complexes can be separated into three groups according to the coordinated en, ox, and gly ligands.[59] Incidentally, the complexes containing more than one β-ala ligand exhibit their highest frequency polarized bands around 630 cm^{-1}, somewhat higher than those for the complexes containing the gly ligand. It is not certain at present what has brought about this interesting feature, but we can infer that it reflects the skeletal vibrational characteristics of the cobalt(III) complexes with six-membered aminocarboxylate chelate rings.

V-B-2. Raman Spectral Characteristics of the Geometrical Isomers of Cobalt(III) Complexes with Five- and Six-membered Chelate Rings.

The numbers of the Raman bands in the stretching

Table 10. Raman Spectral Data of Tris(bidentate)cobalt(III) Complexes with Six-Membered Chelate Rings

No.	Complexes	Raman frequency / cm^{-1} a)			
18	$[Co(en)_2(tn)]^{3+}$	517 s(p) 502 sh(-) 449 m(p)	423 m(dp)	364 m(dp)	254 m(p)
19	$[Co(en)(tn)_2]^{3+}$	534 vw(-) 506 s(p) 449 s(p)	423 sh(dp)	355 w(dp) 271 vw(dp)	226 w(p)
20	$[Co(tn)_3]^{3+}$	530 w(p) 502 vw(-) 451 s(p)	431 sh(dp)	352 m(dp) 307 vw(-) 269 vw(dp)	222 m(p)
21	$[Co(gly)(tn)_2]^{2+}$	590 w(-) 534 vw(-) 482 m(p) 450 s(p)	380 m(dp)	342 w(dp)	221 w(p)
22	$[Co(\beta\text{-ala})(en)_2]^{2+}$	523 m(p)	439 vw(-)	440 vw(dp)	256 w(p)
23	trans(O)-$[Co(\beta\text{-ala})_2(en)]^{+}$	624 w(p) 510 m(p) 493 sh(-)	421 vw(dp)	382 w(p)	
24	C_1-cis(O)-$[Co(\beta\text{-ala})_2(tn)]^{+}$	628 vw(p) 534 w(p) 498 m(p) 454 s(p)	402 vw(-)	350 vw(dp)	
25	C_2-cis(O)-$[Co(\beta\text{-ala})_2(tn)]^{+}$	633 w(p) 534 vw(p) 486 s(p)	466 sh(dp) 407 m(p)	371 w(dp) 362 w(dp)	

26	trans(O)-[Co(β-ala)$_2$(tn)]$^+$	634 w(p) 507 m(p) 465 s(p)	479 sh(dp)		
27	fac(N)-[Co(β-ala)$_3$]	616 vw(p) 531 m(p) 503 w(p)	405 w(p)	378 w(p)	288 vw(-)
28	mer(N)-[Co(β-ala)$_3$]	632 vw(-) 534 w(-) 509 w(-) 485 w(-)	409 vw(-)	381 vw(-)	

Assignment [a]	ν_{ts}(Co-L)	ν(Co-L)	δ_{sbd}(L-Co-L)	δ_{crd}(Co$\langle^{L}_{L}$)

a) The following abbreviations are used: s, strong; m, medium; w, weak; vw, very weak; sh, shoulder; p, polarized; dp, depolarized; ν_{ts}, totally symmetric stretching vibration mode; ν, stretching vibration mode excluding the totally symmetric stretching character; δ_{sbd}, skeletal bending deformation mode; δ_{crd}, chelate ring deformation mode. The Raman band intensities (s, m, w, vw, and sh) are classified by a comparison of all the Raman bands among all the complexes.

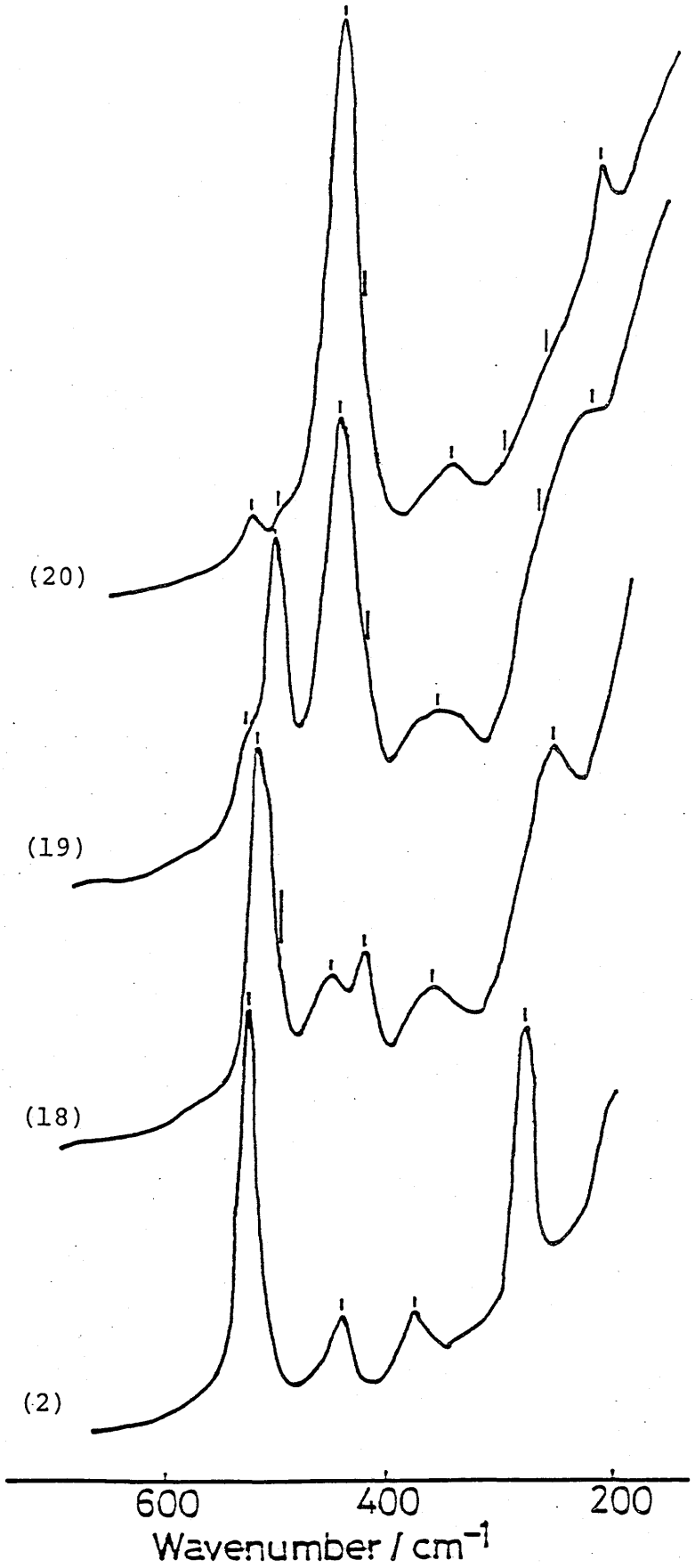

Figure 16. Raman spectra of $[Co(en)_n(tn)_{3-n}]^{3+}$ (n = 0, 1, 2, and 3). Numbers in parentheses correspond to those in Tables 9 and 10.

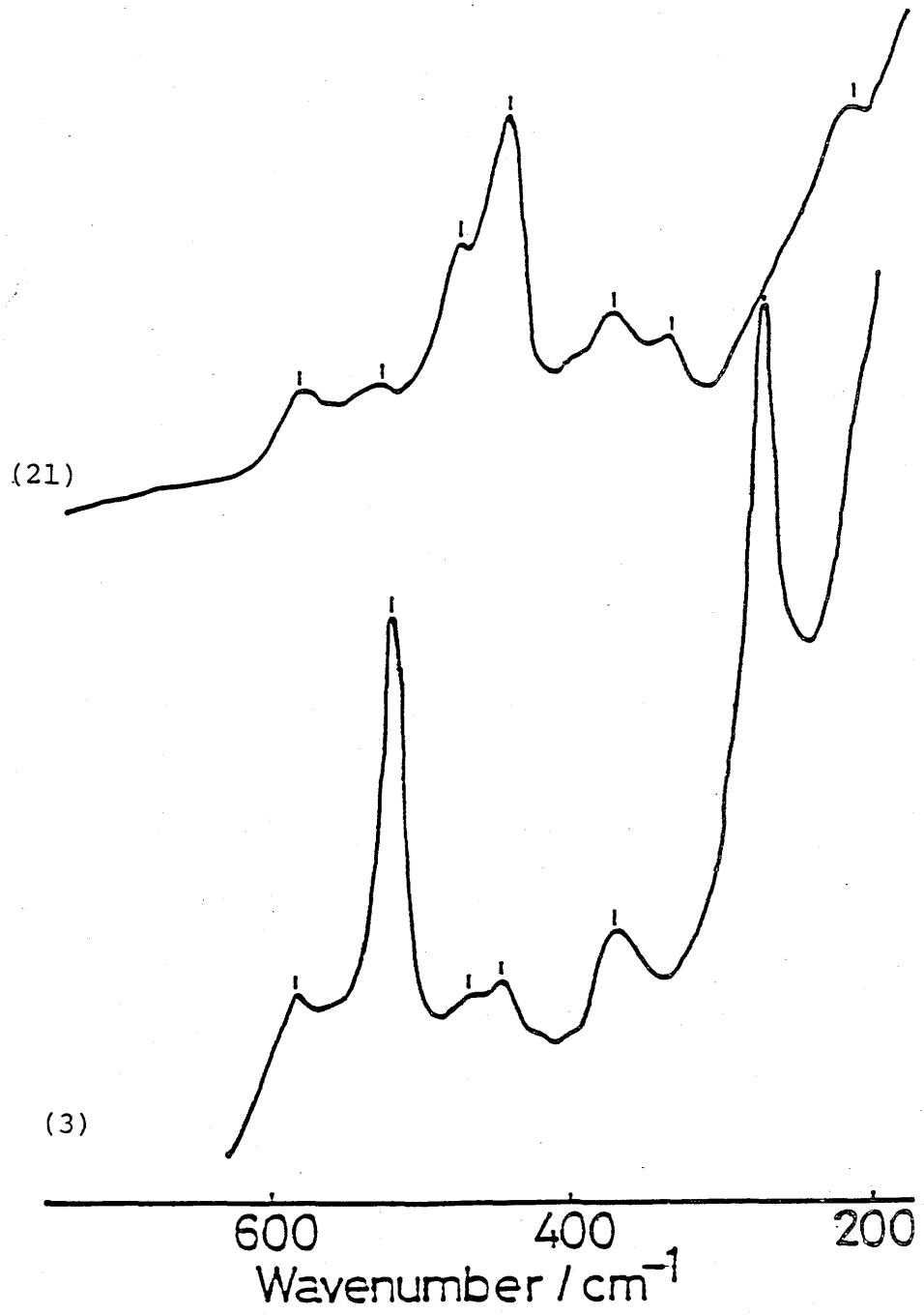

Figure 17. Raman spectra of $[Co(gly)(tn)_2]^{2+}$ and $[Co(gly)(en)_2]^{2+}$. Numbers in parentheses correspond to those in Tables 9 and 10.

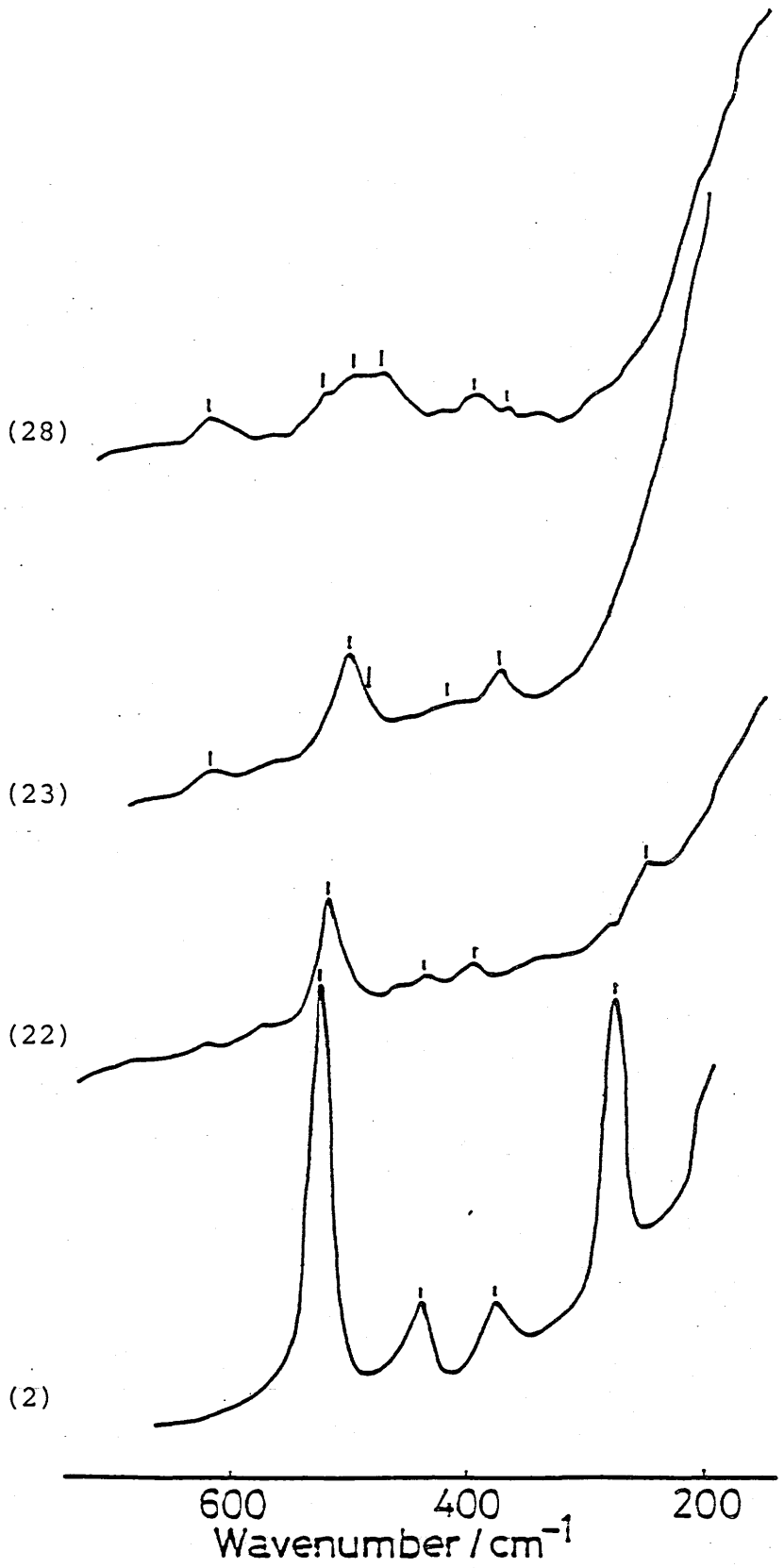

Figure 18. Raman spectra of mer(N)-$[Co(\beta\text{-ala})_3]$, trans(O)-$[Co(\beta\text{-ala})_2(en)]^+$, $[Co(\beta\text{-ala})(en)_2]^{2+}$, and $[Co(en)_3]^{3+}$. Numbers in parentheses correspond to those in Tables 9 and 10.

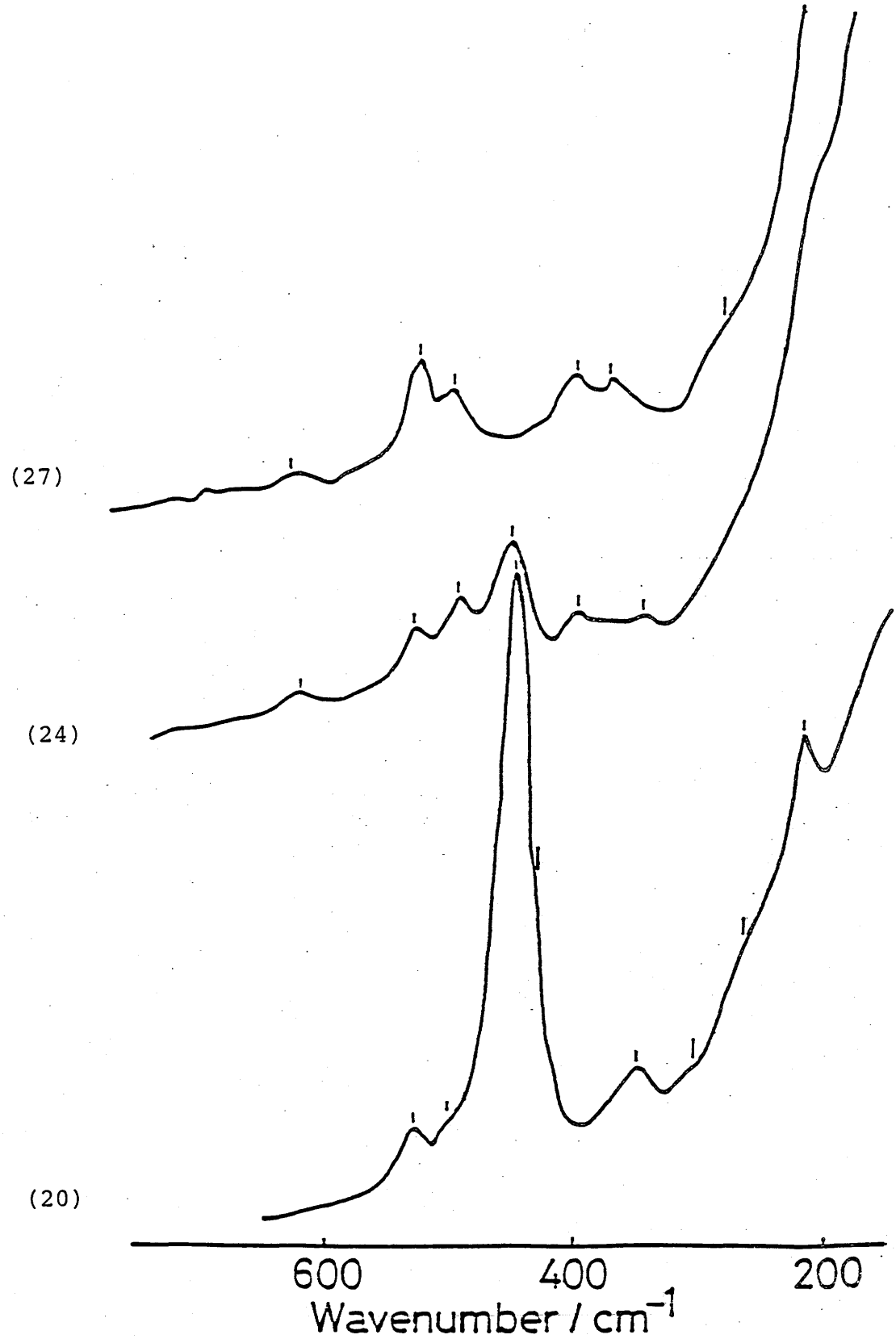

Figure 19. Raman spectra of fac(N)-[Co(β-ala)$_3$], C_1-cis(O)-[Co(β-ala)$_2$(tn)]$^+$, and [Co(tn)$_3$]$^{3+}$. Numbers in parentheses correspond to those in Table 10.

vibration mode excluding the totally symmetric one (i. e., the non-totally symmetric one) are characteristic of the geometry of the $[Co(N)_4(O)_2]$-, $[Co(N)_2(O)_4]$-, and $[Co(N)_3(O)_3]$-type complexes with five-membered chelate rings; C_2-cis(O) and C_2-cis(N) isomers of $[Co(gly)_2(en)]^+$ and $[Co(gly)_2(ox)]^-$ give doublets while C_1-cis(O) and C_1-cis(N) isomers quartets. The fac isomers of $[Co(gly)_3]$ and [Co(gly)(ox)(en)] with the higher effective symmetry, C_{3v}, give doublets while the mer isomers with the lower one, C_{2v}, triplets. These features can be used for the differentiation of the fac and mer isomers of the latter and of the C_2-cis and C_1-cis isomers of former.[59] Especially, the differentiation of the C_2-cis and C_1-cis isomers is considered to be of practical importance because it is hard to distinguish between these isomers by absorption spectroscopy owing to cis-$[Co(N)_4(O)_2]$ chromophore or cis-$[Co(N)_2(O)_4]$ one.

The Raman spectral differences among the geometrical isomers of the cobalt(III) complexes with five-membered chelate rings are noticed in the stretching vibration mode excluding the totally symmetric stretching one while those of the complexes with the six-membered chelate rings appear in the totally symmetric stretching vibration mode. For example, as is shown in Fig. 20, a conspicuous difference between fac(N)- and mer(N)-$[Co(\beta\text{-ala})_3]$ is found in the totally symmetric stretching vibration mode; the mer(N) isomer exhibits a more complicated Raman spectrum than does

the fac(N) one.

The Raman spectral features of the three geometrical isomers, trans(O)-, C_2-cis(O)-, and C_1-cis(O)-$[Co(\beta\text{-ala})_2(tn)]^+$ are, in a first approximation, similar to each other, as in the case of the geometrical isomers, trans(O)-, C_2-cis(O)- and C_1-cis(O)-$[Co(gly)_2(en)]^+$ [59] (Fig. 21). On a closer inspection, however, we can find some differences among the Raman spectral features of the three geometrical isomers of $[Co(\beta\text{-ala})_2(tn)]^+$. Firstly, the difference between the trans(O) isomer and the two cis(O) ones can be observed in the skeletal bending deformation region; the trans(O) isomer has no Raman band, but the cis(O) isomers have a few Raman bands. Incidentally, the trans(O) isomer exhibits the strong and polarized band (465 cm^{-1}) at a slightly lower frequency than the depolarized one (479 cm^{-1}). Secondly, a difference between the two cis(O) isomers of $[Co(\beta\text{-ala})_2(tn)]^+$ can be observed in the totally symmetric stretching vibration mode region in contrast to the stretching vibration mode region excluding the totally symmetric one for a difference between the two cis(O) isomers of $[Co(gly)_2(en)]^+$; the C_2-cis(O)-$[Co(\beta\text{-ala})_2(tn)]^+$ isomer with a higher symmetry exhibits three Raman bands, but the corresponding Raman bands of the C_1-cis(O)-$[Co(\beta\text{-ala})_2(tn)]^+$ isomer splits into a quartet in the totally symmetric stretching vibration mode region.

V-B-3. Raman Spectra of Cobalt(III) Complexes with Linear Terdentate Ligands Containing N and O Donor Atoms.

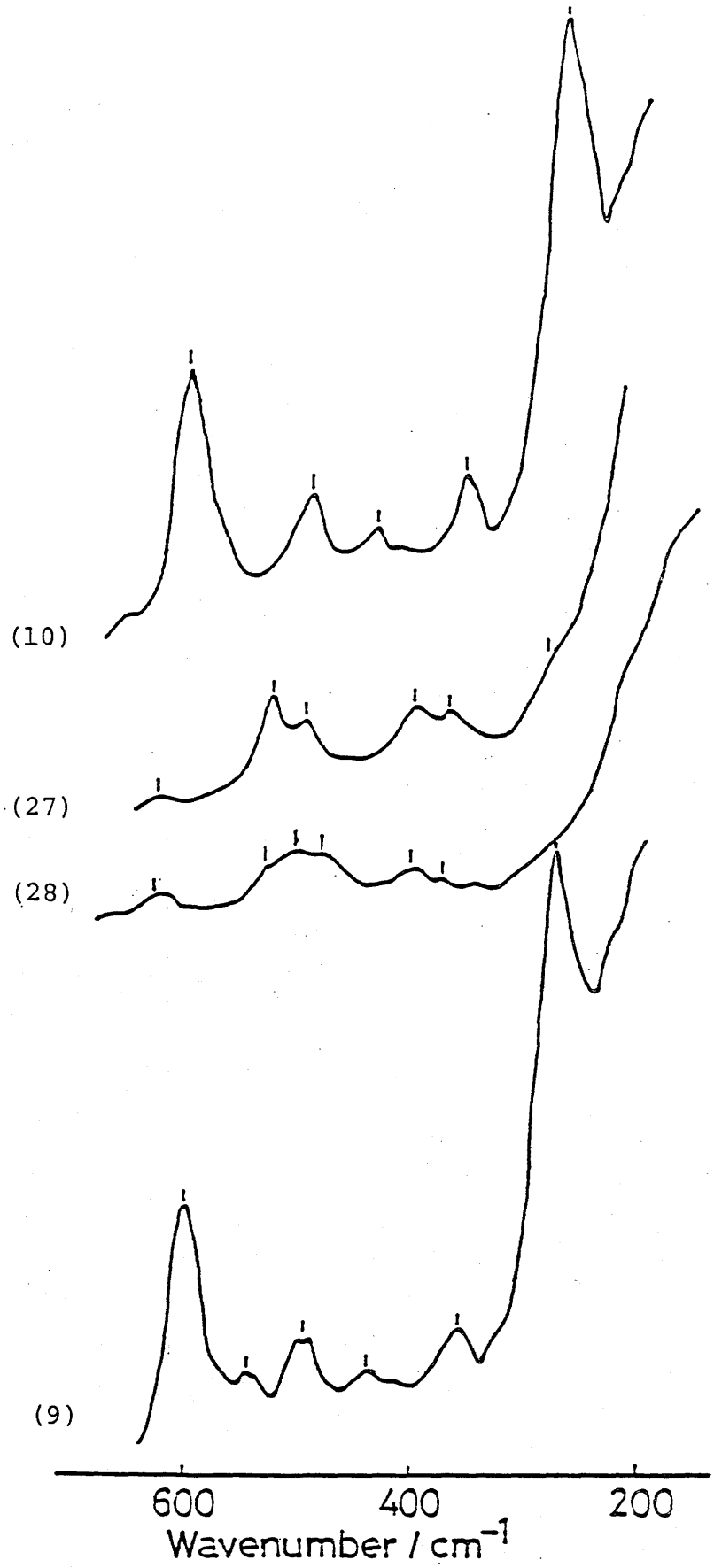

Figure 20. Raman spectra of mer(N) and fac(N) isomers of $[Co(gly)_3]$ and $[Co(\beta\text{-ala})_3]$. Numbers in parentheses correspond to those in Tables 9 and 10.

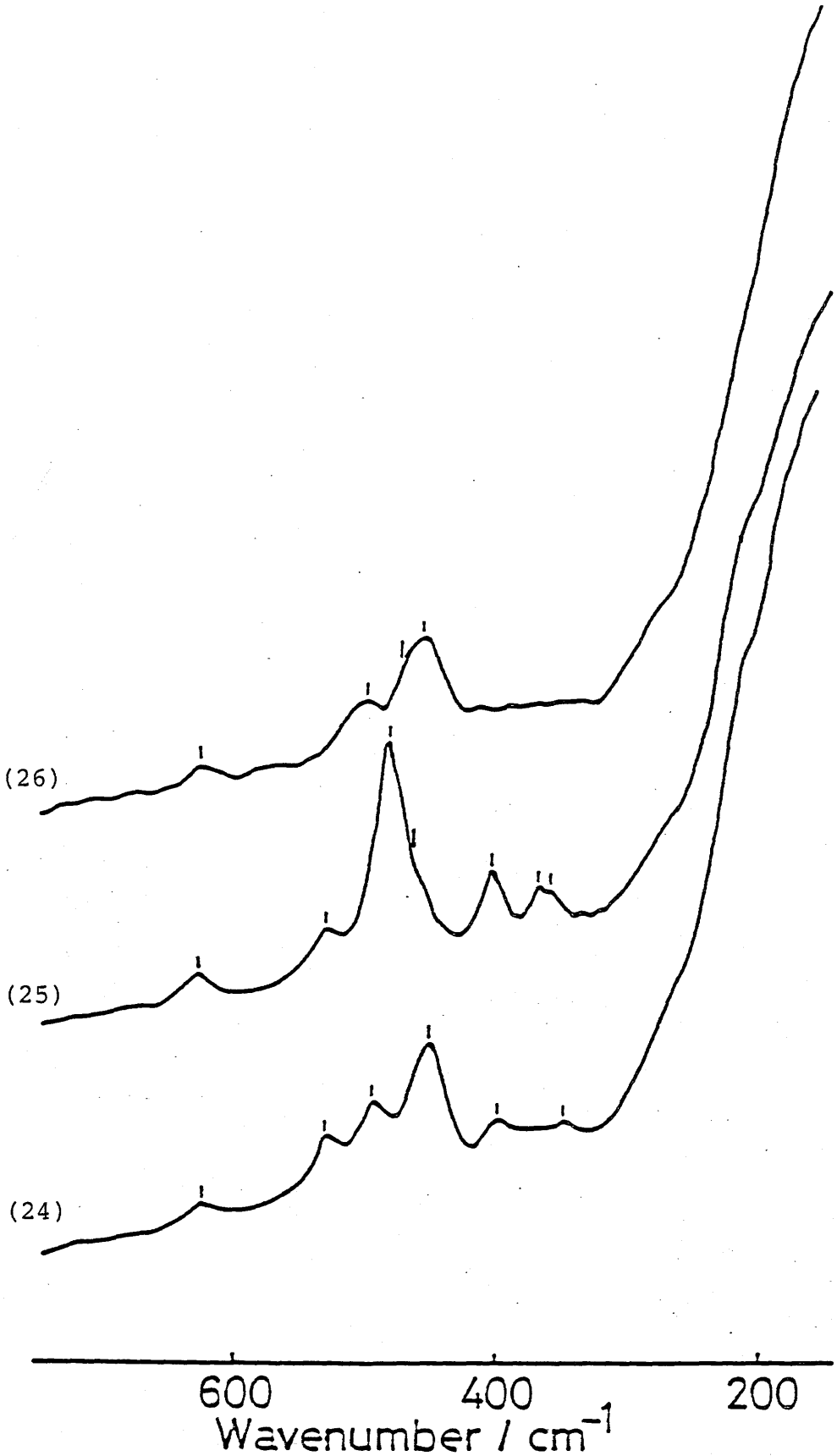

Figure 21. Raman spectra of three geometrical isomers of $[Co(\beta\text{-ala})_2(tn)]^+$. Numbers in parentheses correspond to those in Table 10.

General Aspects.

Raman spectral data of the cobalt(III) complexes with the linear terdentate ligands, dien, edma, and ida, are summarized in Table 11. Figure 22 shows the Raman spectra of unsym-fac-$[Co(dien)_2]^{3+}$, $[Co(en)_3]^{3+}$, and $[Co(NH_3)_6]^{3+}$ as representatives for the general spectral consideration. These three complexes have the same effective symmetry of O_h. Unsym-fac-$[Co(dien)_2]^{3+}$ shows the Raman spectral charactristics similar to $[Co(en)_3]^{3+}$ and $[Co(NH_3)_6]^{3+}$ except for a polarized band at 409 cm^{-1}. That is, the Raman bands at 546, 434 - 485, and 321 cm^{-1} of the unsym-fac isomer correspond to those at 525, 440, and 378 cm^{-1} of $[Co(en)_3]^{3+}$ and to those at 495, 440, and 320 cm^{-1} of $[Co(NH_3)_6]^{3+}$. Further, the Raman band at 255 cm^{-1} of the unsym-fac-$[Co(dien)_2]^{3+}$ corresponds to that at 283 cm^{-1} of $[Co(en)_3]^{3+}$. Similar spectral characteristics can also be observed for the cobalt(III) complexes with edma or ida ligand: The Raman spectra of unsym-fac-$[Co(ida)(dien)]^{+}$, unsym-fac-trans(N_t)-$[Co(edma)_2]^{+}$, and C_2-cis(O)-$[Co(gly)_2(en)]^{+}$, which belong to cis(O)-$[Co(N)_4(O)_2]$-type and have the same effective symmetry of C_{2v}, are given in Fig. 23. The Raman bands at 546 - 610, 453 - 504, 301, and 235 cm^{-1} of unsym-fac-$[Co(ida)(dien)]^{+}$ and those at 552 - 638, 470 - 526, 294, and 245 cm^{-1} of unsym-fac-trans(N_t)-$[Co(edma)_2]^{+}$ (even though the Raman band at 526 cm^{-1} of unsym-fac-trans(N_t)-$[Co(edma)_2]^{+}$ is polarized) correspond to those at 538 - 598, 433 - 486, 360 and 276 cm^{-1} of C_2-

cis(O)-$[Co(gly)_2(en)]^+$, respectively. Moreover, as shown in Fig. 24, a similar relation can also be found in the Raman spectra of unsym-fac-$[Co(ida)_2]^-$, C_2-cis(N)-$[Co(gly)_2(ox)]^-$, and $[Co(ox)_2(en)]^-$ which belong to cis(N)-$[Co(N)_2(O)_4]$-type and have the same effective symmetry of C_{2v}. Hence we may expect that the Raman spectra of the cobalt(III) complexes with linked five-membered chelate ligands can be treated as a first approximation on the basis of the effective symmetry, which mainly determined by the arrangement of the coordinated atoms around the central metal atom, as in the case of the tris(bidentate)cobalt(III) complexes with the five-membered chelate rings.

On the basis of the above discussion and the Raman spectral characteristics summarized in Table 11, the Raman spectra of the cobalt(III) complexes with the linear terdentate ligands containing N and O donor atoms can be classified into five categories; polarized bands in the 510 - 650 cm^{-1} region, depolarized ones in the 430 - 540 cm^{-1} region, polarized ones in the 370 - 490 cm^{-1} region, depolarized ones in the 290 - 420 cm^{-1} region, and polarized ones in the 220 - 270 cm^{-1}. Comparison with the assignments of the cobalt(III) complexes with bidentate ligands, these categories, except polarized bands in the 370 - 490 cm^{-1} region, can be assigned to the totally symmetric stretching vibration mode (510 - 650 cm^{-1}), the stretching vibration mode excluding the totally symmetric one (i.e., non-totally symmetric one)(430 - 540 cm^{-1}), the skeletal bending deformation mode (270 - 420 cm^{-1}), and the chelate ring

deformation mode (220 - 270 cm^{-1}). Furthermore, the polarized bands in the 370 - 490 cm^{-1} region can be regarded as the characteristic Raman bands of the cobalt(III) complexes with the linear terdentate ligands, because we could not find the corresponding bands in the Raman spectra of the $[Co(NO_2)_n(NH_3)_{6-n}]$-type,[57] and tris(bidentate)-type complexes. On the basis of the Raman frequency and polarization characteristics, these Raman bands are tentatively assigned to the breathing mode, which corresponds to the symmetric vibration of the overall structure of the complex, i.e., the coupled vibration of the totally symmetric metal-ligand stretching and the chelate ring deformation.

It is obvious that the Raman spectrum of $[Co(NH_3)_3(dien)]^{3+}$ can be better correlated to those of sym-fac- and unsym-fac-$[Co(dien)_2]^{3+}$ than to that of $[Co(NH_3)_6]^{3+}$ (Fig. 25 and Table 11). Further, Fig. 26 and Table 11 demonstrate that the Raman spectral characteristics of fac-$[Co(ida)(NH_3)_3]^{+}$ can be correlated to those of sym-fac- and unsym-fac-$[Co(ida)(dien)]^{+}$. That is, the character of the linked chelate rings appears similarly in the spectra of the mono(terdentate)cobalt(III)-type complexes. Consequently, the Raman bands at 547, 454 - 486, and 422 cm^{-1} of $[Co(NH_3)_3(dien)]^{3+}$ and at 514 - 614, 457 - 505, and 403 - 417 cm^{-1} of $[Co(ida)(NH_3)_3]^{+}$ can be assigned to the totally symmetric stretching vibration mode, the stretching vibration mode excluding the totally symmetric one, and the

skeletal breathing vibration mode, respectively, and the Raman band at 339 cm^{-1} of fac-$[Co(ida)(NH_3)_3]^+$ can be assigned to the skeletal bending deformation mode. However, both $[Co(NH_3)_3(dien)]^{3+}$ and fac-$[Co(ida)(NH_3)_3]^-$ have no Raman bands corresponding to the chelate ring deformation mode.

It is interesting to point out that the polarized bands in the chelate ring deformation mode region of the bis(terdentate)cobalt(III) complexes, except for unsym-fac-cis(N_t)trans(O)-$[Co(edma)_2]^+$, appear at a lower frequency than those of the tris(bidentate)cobalt(III) complexes (Tables 9 and 11).

Finally, it should be noted that sym-fac-$[Co(dien)_2]^{3+}$ has more Raman bands than those expected from C_{2h} symmetry ($4A_g + 2B_g$) because of the splitting of the chelate ring deformation mode. In crystalline state, sym-fac-$[Co(dien)_2]Br_3$ has been reported to have an "approximate" C_{2h} symmetry as a result of X-ray crystal structure analysis.[13,64] This Raman spectral evidence implies that the sym-fac isomer is somewhat distorted structurally from C_{2h} molecular symmetry in an aqueous solution so far as the skeletal vibration characteristics are concerned.

Raman Spectral Characteristics of the Geometrical Isomers of Cobalt(III) Complexes with Linear Terdentate Ligands.

The Raman spectra of the isomers of $[Co(dien)_2]^{3+}$, $[Co(edma)(dien)]^{2+}$, $[Co(ida)(dien)]^+$, $[Co(edma)_2]^+$,

Table 11. Raman Spectral Data of Cobalt(III) Complexes With Linear Terdentate Ligands Containing N and O Donor Atoms.

No.	Complexes	Raman frequency / cm^{-1} a)				
29	sym-fac-$[Co(dien)_2]^{3+}$	549 s(p)	478 m(dp) 448 vw(-) 437 m(dp)	401 m(p)		260 vw(-) 230 vw(-)
30	unsym-fac-$[Co(dien)_2]^{3+}$	546 s(p)	485 m(dp) 444 m(dp) 434 m(dp)	409 w(p)	321 m(dp)	255 vw(-)
31	mer-$[Co(dien)_2]^{3+}$	579 m(p) 546 vw(-) 514 s(p)		480 s(p) 442 s(p)	402 m(dp) 381 vw(dp) 323 m(dp)	222 m(p)
32	sym-fac-$[Co(edma)(dien)]^{2+}$	641 w(p) 553 s(p)	509 w(dp) 456 w(dp)	401 m(p)		235 w(p)
33	unsym-fac-fac(Nt)-$[Co(edma)(dien)]^{2+}$	642 w(p) 558 s(p)	506 w(-) 473 vw(-) 447 vw(-)	421 m(p)	307 vw(-)	
34	unsym-fac-mer(Nt)-$[Co(edma)(dien)]^{2+}$	635 w(p) 547 s(p)	514 w(-) 453 m(dp)	411 m(p)	306 vw(-)	247 w(-)
35	mer-$[Co(edma)(dien)]^{2+}$	577 vw(-) 538 w(p) 518 vw(-)		481 vw(-) 445 m(p)	414 w(dp)	
36	sym-fac-$[Co(ida)(dien)]^{+}$	609 m(p) 546 s(p)	510 w(dp) 472 w(dp) 461 sh(dp)	418 w(-) 387 s(p)		235 s(p)
37	unsym-fac-$[Co(ida)(dien)]^{+}$	610 m(p) 546 s(p)	504 m(dp) 470 vw(dp) 453 vw(dp)	410 m(p) 401 m(p)	301 w(dp)	235 w(p)

38	mer-[Co(ida)(dien)]$^{+}$	614 vw(p) 585 w(p) 524 s(p)		476 m(p) 451 s(p) 436 w(-) 390 s(p)	346 w(dp) 302 vw(dp)	
39	sym-fac-trans(Nt)-[Co(edma)$_2$]$^{+}$	635 m(p) 549 s(p) 523 s(p)	459 w(dp)	407 m(p) 381 sh(-)		233 m(p)
40	sym-fac-cis(Nt)-[Co(edma)$_2$]$^{+}$	639 m(p) 577 s(p) 529 m(p)	486 w(dp)	394 s(p)		240 vw(p)
41	unsym-fac-cis(Nt)trans(O)-[Co(edma)$_2$]$^{+}$	649 m(p) 570 s(p) 522 s(p)	467 w(dp)	417 m(p)	305 w(-)	261 vw(-)
42	unsym-fac-cis(Nt)cis(O)-[Co(edma)$_2$]$^{+}$	645 m(p) 569 s(p) 526 s(p)	485 w(dp)	419 m(p) 400 sh(-)	299 vw(-)	243 w(p)
43	unsym-fac-trans(Nt)-[Co(edma)$_2$]$^{+}$	638 m(p) 552 s(p) 526 s(p)	470 w(dp)	415 m(p)	294 vw(-)	245 w(p)
44	mer-[Co(edma)$_2$]$^{+}$	634 w(p) 544 m(p) 510 w(p)	470 vw(-)[b] 461 vw(-)[b]	421 s(p)	379 w(dp)	
45	sym-fac-[Co(ida)(edma)]	618 w(-) 573 m(p)	533 w(-) 497 vw(-)	390 m(p)		229 vw(-)
46	unsym-fac-mer(N)-[Co(ida)(edma)]	645 w(-) 565 m(p)	529 w(-)	409 m(p) 401 m(p)	290 vw(-)	
47	sym-fac-[Co(ida)$_2$]$^{-}$	610 s(p) 569 m(p)	522 vw(dp)	394 w(-) 372 m(p)		229 m(p)
48	unsym-fac-[Co(ida)$_2$]$^{-}$	621 s(p) 562 m(p)	446 vw(-)	398 m(p) 382 vw(-)	291 w(-)	

49 $[Co(NH_3)_3(dien)]^{3+}$	547 s(p)	486 m(dp) 469 m(dp) 454 w(dp)	422 s(p)		
50 fac-$[Co(ida)(NH_3)_3]^{+}$	614 w(p) 514 m(p)	505 sh(dp) 457 vw(dp)	417 m(p) 403 m(p)	339 vw(dp)	

Assignment [a]	ν_{ts}(Co-L)	ν(Co-L)	ν_{br}	δ_{sbd}(L-Co-L)	δ_{crd}(Co$\prec_{L}^{L}$))

a) The following abbreviations are used: s, strong; m, medium; w, weak; vw, very weak; sh, shoulder; p, polarized; dp, depolarized; ν_{ts}, totally symmetric stretching vibration mode; ν, stretching vibration mode excluding the totally symmetric stretching character; ν_{br}, skeletal breathing vibration mode; δ_{sbd}, skeletal bending deformation mode; δ_{crd}, chelate ring deformation mode. The Raman band intensities (s, m, w, vw, and sh) are classified by a comparison of all the Raman bands among all the complexes. b) Consult the text.

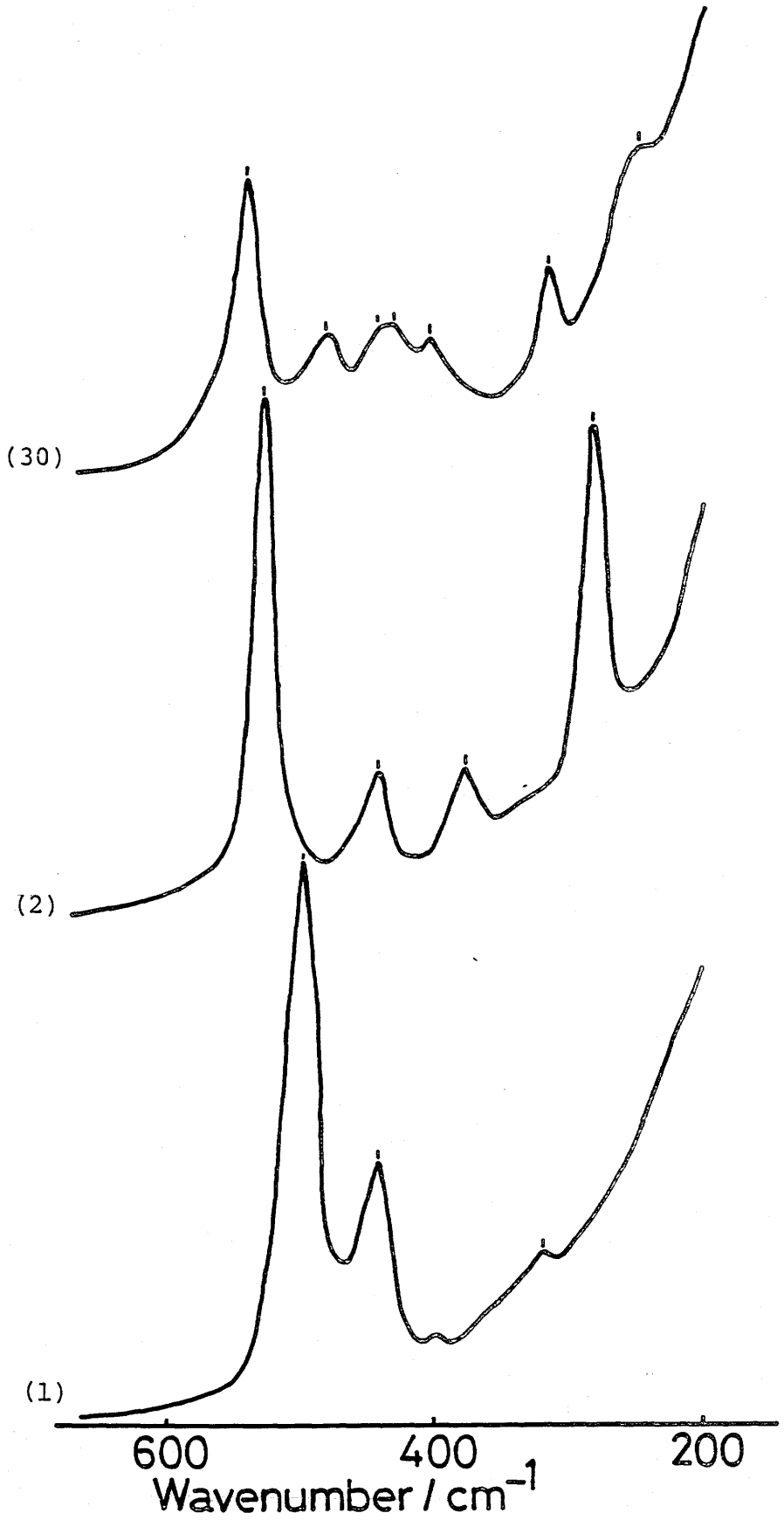

Figure 22. Raman spectra of unsym-fac-$[Co(dien)_2]^{3+}$, $[Co(en)_3]^{3+}$, and $[Co(NH_3)_6]^{3+}$. Numbers in parentheses correspond to those in Tables 9 and 11.

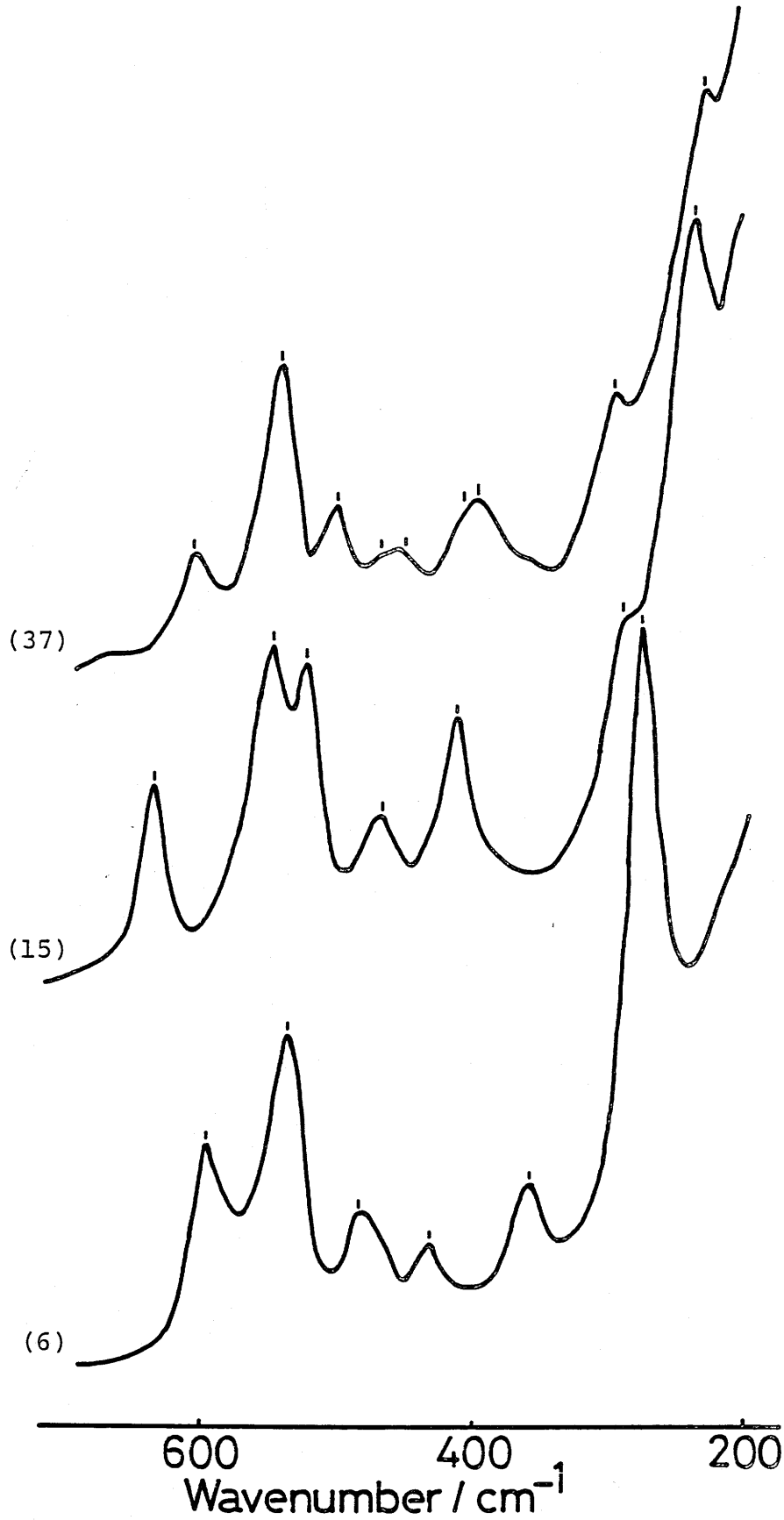

Figure 23. Raman spectra of unsym-fac-$[Co(ida)(dien)]^+$, unsym-fac-trans(N_t)-$[Co(edma)_2]^+$, and C_2-cis(O)-$[Co(gly)_2(en)]^+$. Numbers in parentheses correspond to those in Tables 9 and 11.

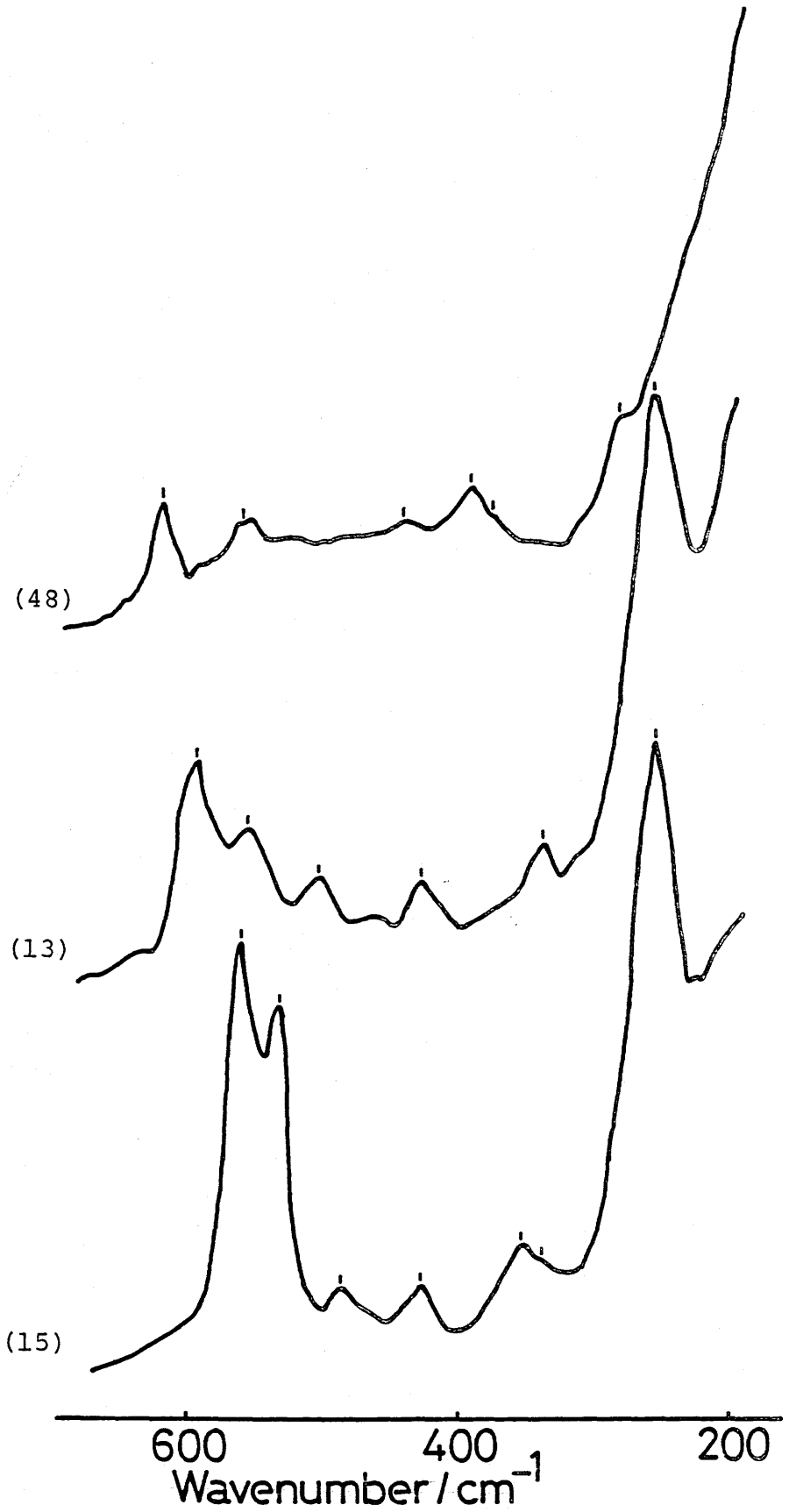

Figure 24. Raman spectra of unsym-fac-$[Co(ida)_2]^-$, C_2-cis(N)-$[Co(gly)_2(ox)]^-$, and $[Co(ox)_2(en)]^-$. Numbers in parentheses correspond to those in Tables 9 and 11.

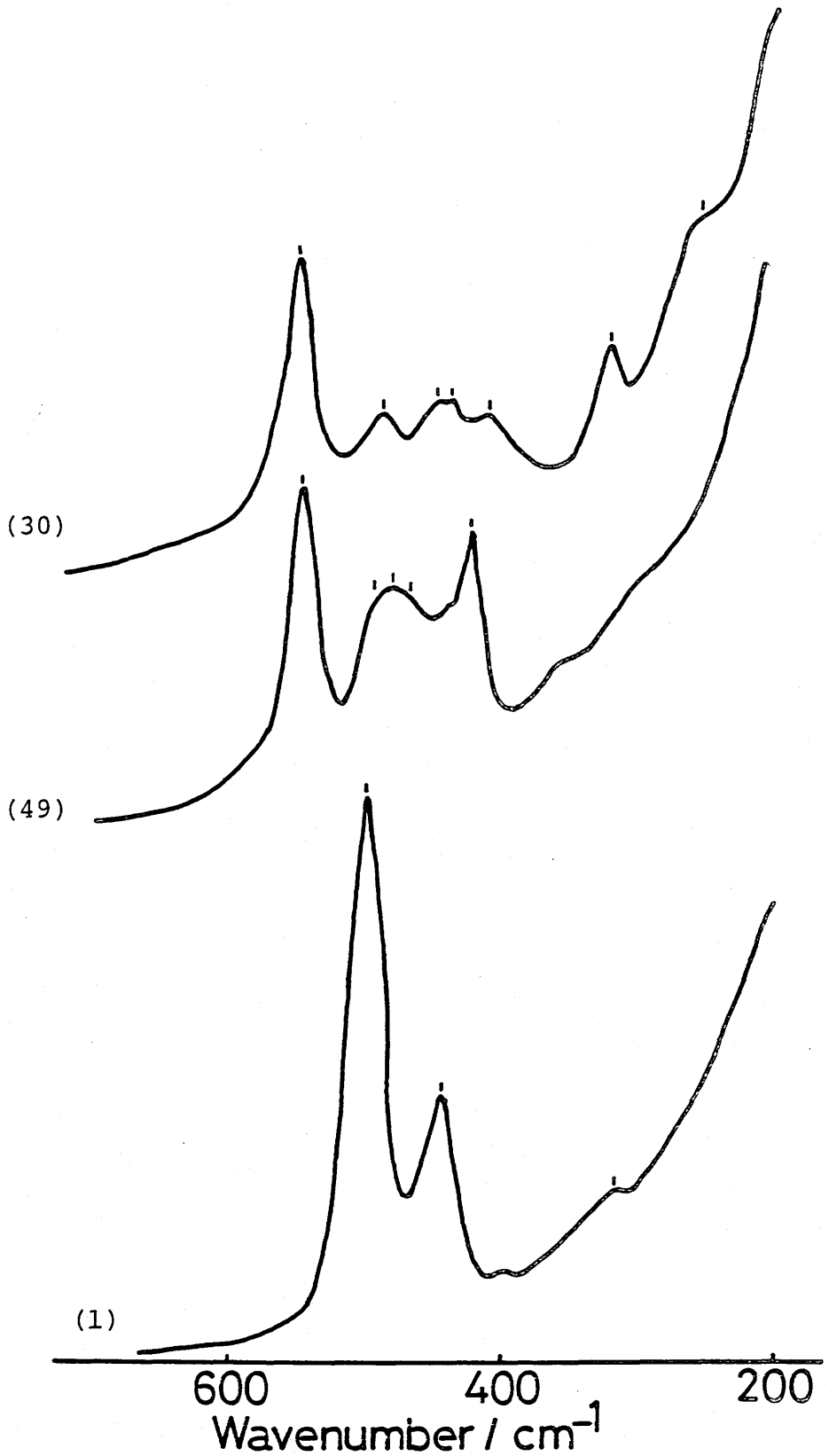

Figure 25. Raman spectra of unsym-fac-$[Co(dien)_2]^{3+}$, $[Co(NH_3)_3(dien)]^{3+}$, and $[Co(NH_3)_6]^{3+}$. Numbers in parentheses correspond to those in Tables 9 and 11.

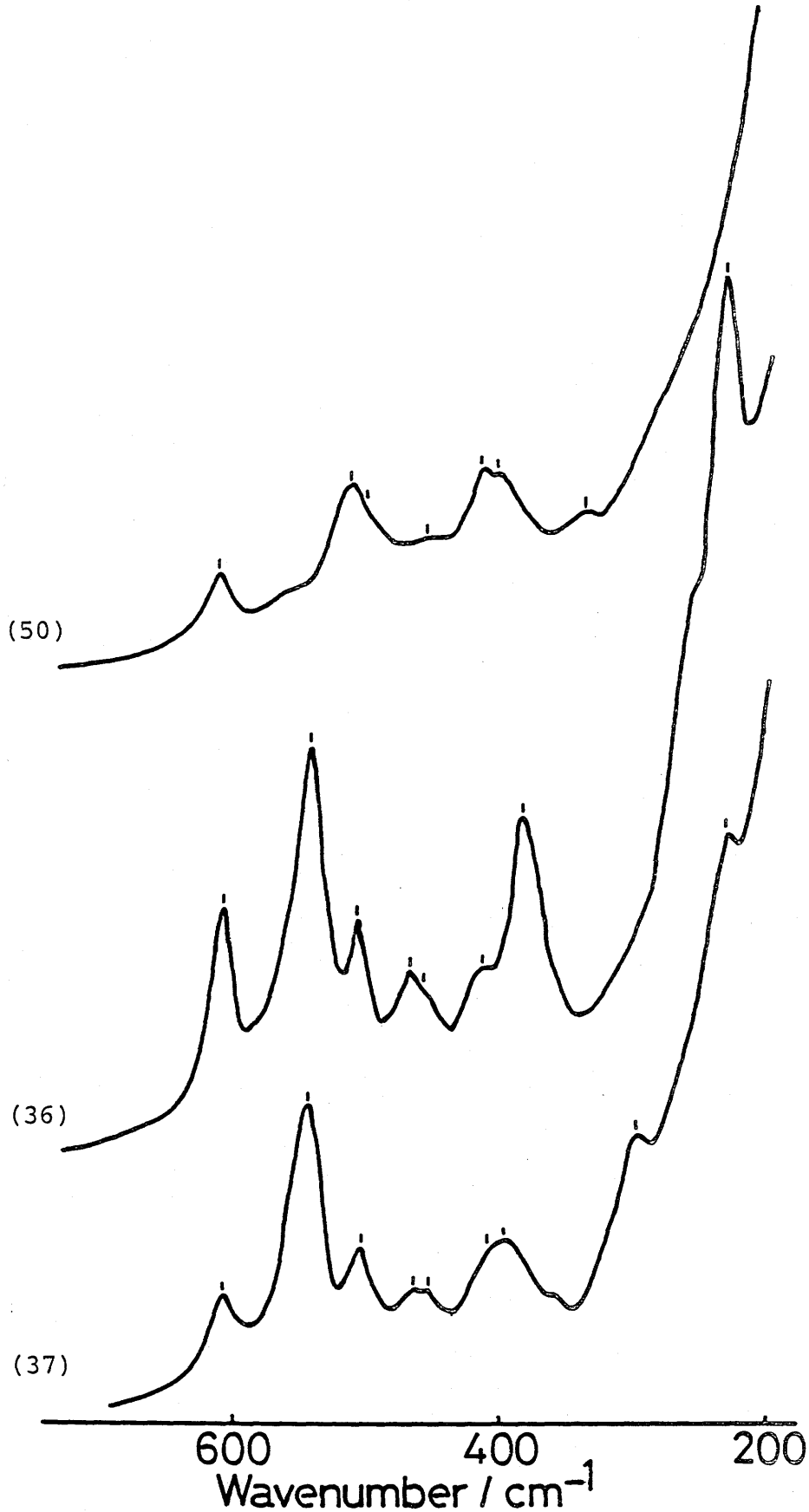

Figure 26. Raman spectra of fac-$[Co(ida)(NH_3)_3]^+$, sym-fac-$[Co(ida)(dien)]^+$, and unsym-fac-$[Co(ida)(dien)]^+$. Numbers in parentheses correspond to those in Table 11.

[Co(ida)(edma)], and $[Co(ida)_2]^-$ are shown in Figs. 27 - 32, respectively. It is obvious from Fig. 27 and Table 11 that the mer isomer of $[Co(dien)_2]^{3+}$ of the $[Co(N)_6]$-type shows Raman spectral characteristics quite different from those of the fac ones. Such striking difference in the fac and mer isomers for the chelate ring arrangement can also be observed in $[Co(edma)(dien)]^{2+}$ of the $[Co(N)_5(O)]$-type and $[Co(ida)(dien)]^+$ and $[Co(edma)_2]^+$ of the $[Co(N)_4(O)_2]$-type (Figs. 28 - 30). Furthermore, the Raman spectra of the mer isomers have many resemblances to each other and the similarity of the Raman spectra among the same isomers of $[Co(dien)_2]^{3+}$, $[Co(edma)(dien)]^{2+}$, $[Co(ida)(dien)]^+$, and $[Co(edma)_2]^+$ can also be observed in the Raman spectra of the fac isomers. That is, mer isomers, except mer-$[Co(edma)_2]^+$ (vide infra), exhibit several polarized bands, but no depolarized bands, in the 390 - 640 cm^{-1} region, while those of the fac isomers exhibit both polarized and depolarized bands in this region; in the skeletal breathing vibration mode, the mer isomers exhibit the sharp Raman bands at the higher frequency than the fac ones; the Raman bands due to the skeletal bending deformation of the mer isomers also appear at the higher frequency; and the mer isomers have no bands in the chelate ring deformation mode region except $[Co(dien)_2]^{3+}$. These features can be ascribed to the difference of the strain energy in vibrational motion between the ligand of the meridional arrangement and that of the facial one; in fact, the mer isomer of $[Co(dien)_2]^{3+}$ is

distorted from the regular octahedral structure, for the Co-N (imino nitrogen) bond in the mer isomer is appreciably stronger than the other.[13,65] Thus, the Raman spectral characteristics as described above can be used as the vibrational criteria for the differentiation of the fac and mer isomers. In view of the above discussion, the Raman spectral characteristics of $[Co(NH_3)_3(dien)]^{3+}$ can be correlated to those of the fac isomers of $[Co(dien)_2]^{3+}$ rather than to those of the mer isomer. Hence, we can expect that the dien in $[Co(NH_3)_3(dien)]^{3+}$ takes the facial coordination. On the other hand, close inspection of the Raman frequencies, intensities, and depolarization ratios of mer-$[Co(edma)_2]^+$ having two asymmetrical linear terdentate ligands reveal not the retention of the polarized character of the other mer isomers in the 390 - 640 cm^{-1} region any longer: Or more precisely, this polarized character is found to be obscured in mer-$[Co(edma)_2]^+$. Reliable estimation of the Raman bands at 470 and 461 cm^{-1} to the polarized ones was unsuccessful because they were too weak to measure their depolarization ratios precisely; rather, they were tentatively classified into the depolarized ones based on the profiles of the polarized and depolarized Raman spectra in this region. The obscurity of the polarized character in mer-$[Co(edma)_2]^+$ may in part be attributed to disturbance of overall harmonic stretching vibrational motion by different terminal donor atoms and force constants. However, as shown in Fig. 33, it is thought that the Raman bands at ca. 520 and ca. 440 cm^{-1} are

characteristic ones for the mer isomers.

The difference between the sym-fac and unsym-fac isomers for the chelate ring arrangement can be observed in the skeletal bending deformation mode (Figs. 27 - 32 and Table 11): Each unsym-fac isomer has a depolarized band while fac ones have none. The Raman spectra reflect the chelate ring structure and it can be said that the combination of the chelate rings changes the metal-ligand skeletal bending deformation characteristics. This result is quite unlike to that for the $[Co(gly)_x(ox)_y(en)_z]$-type complexes, each of which gives a Raman band, irrespective of the chelate ring structure, except for the $[Co(ox)_y(en)_z]$-type complexes, which have a major band accompanied by a very weak one. This fact indicates that the Raman bands in the skeletal bending deformation mode region can be used as one of the criteria for the differentiation of the sym-fac and unsym-fac isomers of the bis(terdentate)cobalt(III) complexes.

In the Raman spectra of the isomers of $[Co(edma)_2]^+$, sym-fac-trans(N_t) and unsym-fac-cis(N_t)cis(O) isomers having lower symmetries, C_i and C_1, respectively, give doublet in the skeletal breathing mode region, whereas sym-fac-cis(N_t), unsym-fac-cis(N_t)trans(O), and unsym-fac-trans(N_t) isomers having higher symmetry, C_2, give only one Raman band in this region. Furthermore, the Raman spectral difference between sym-fac-trans(N_t) and unsym-fac-cis(N_t)trans(O) isomers belonging to the trans(O)-$[Co(N)_4(O)_2]$-type and sym-fac-

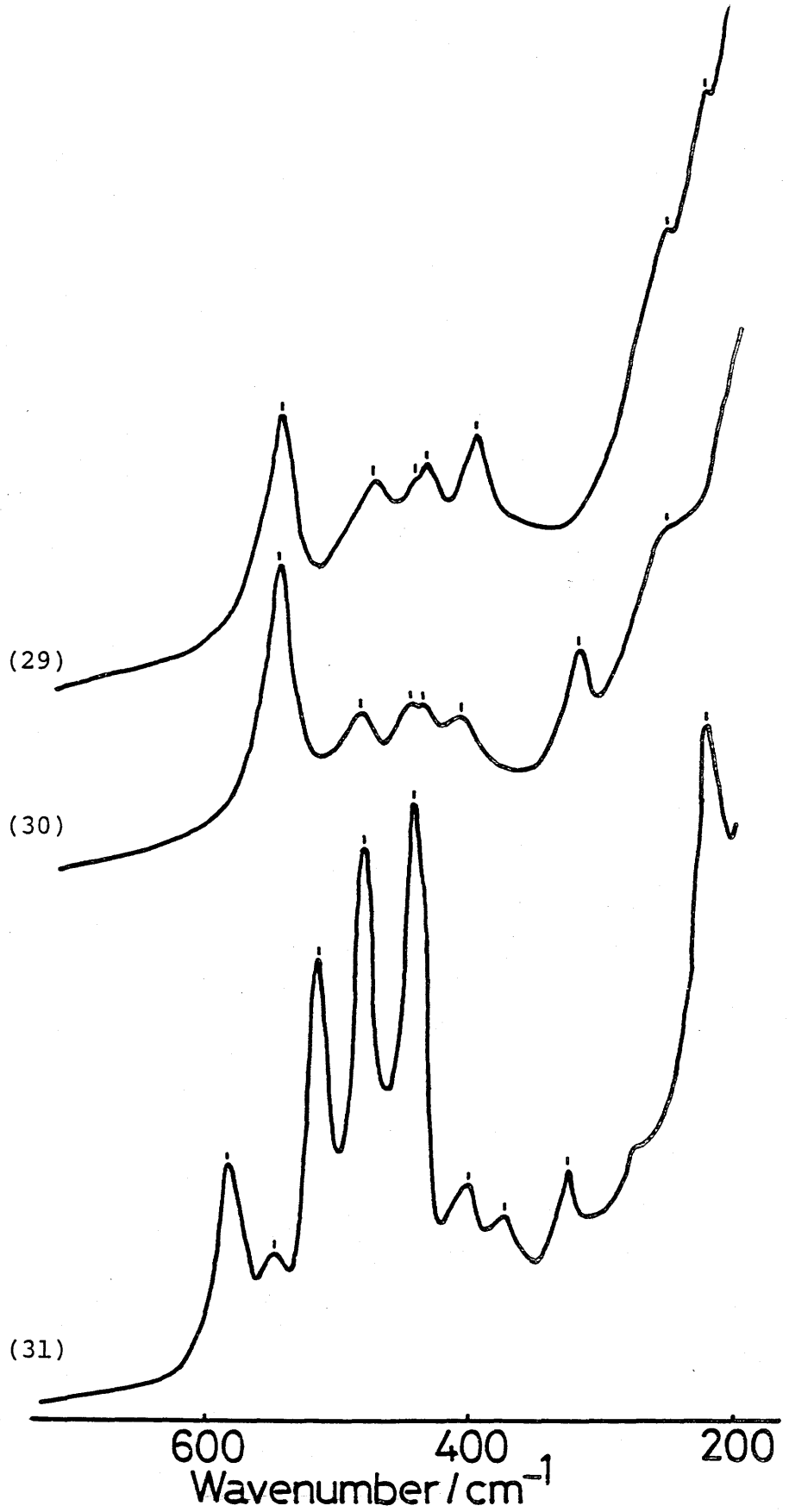

Figure 27. Raman spectra of three geometrical isomers of $[Co(dien)_2]^{3+}$. Numbers in parentheses correspond to those in Table 11.

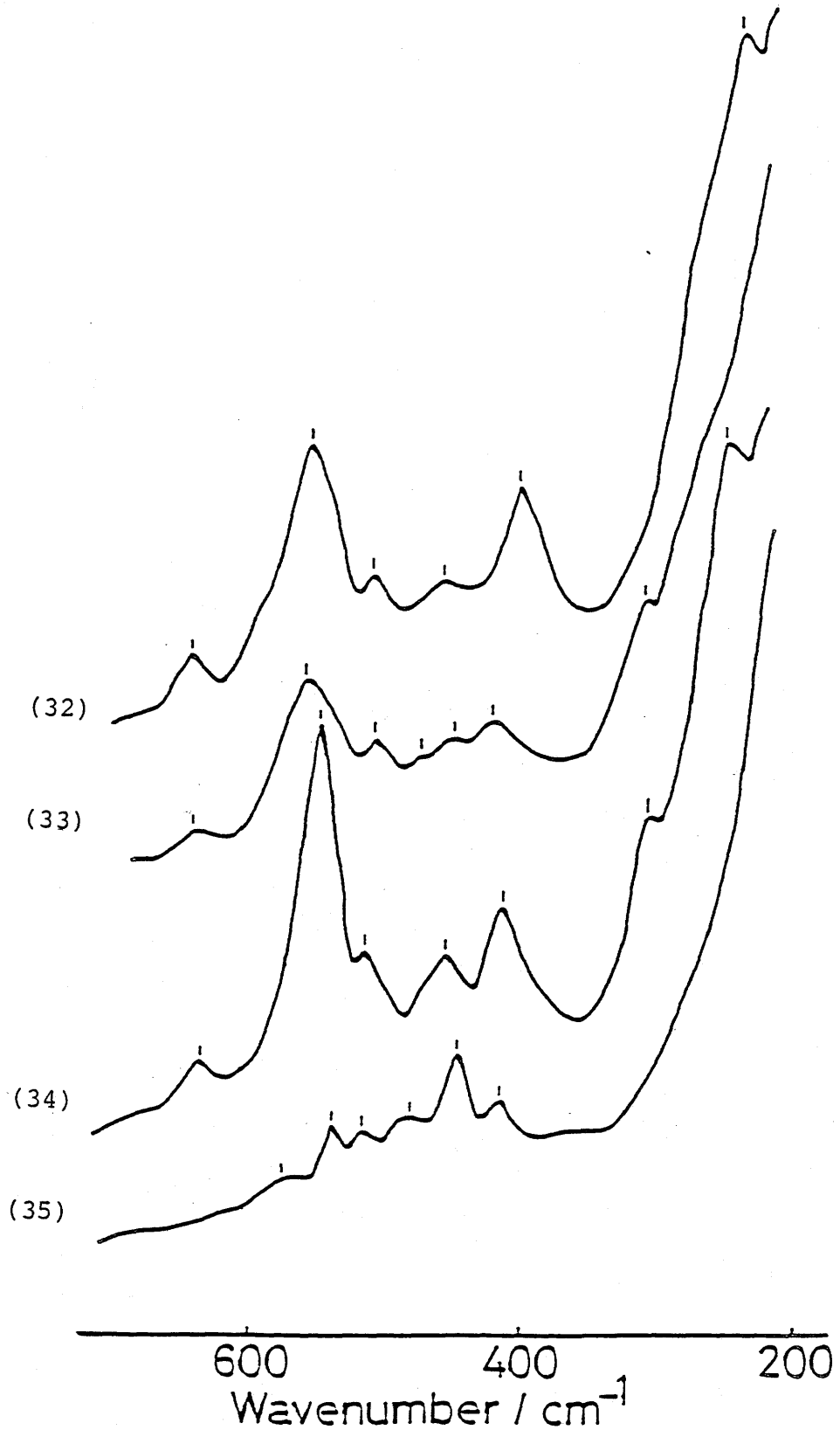

Figure 28. Raman spectra of four geometrical isomers of $[Co(edma)(dien)]^{2+}$. Numbers in parentheses correspond to those in Table 11.

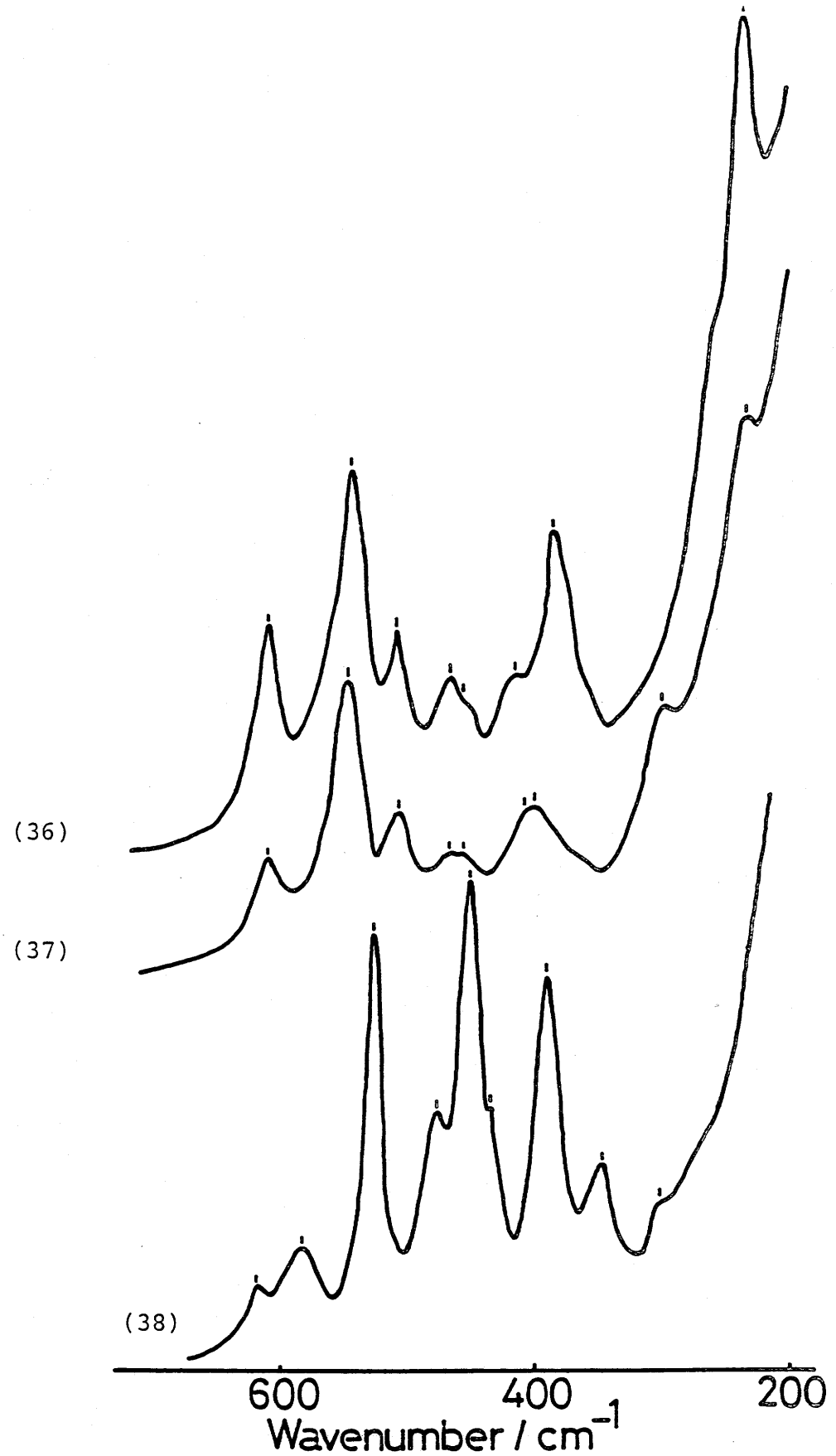

Figure 29. Raman spectra of three geometrical isomers of $[Co(ida)(dien)]^+$. Numbers in parentheses correspond to those in Table 11.

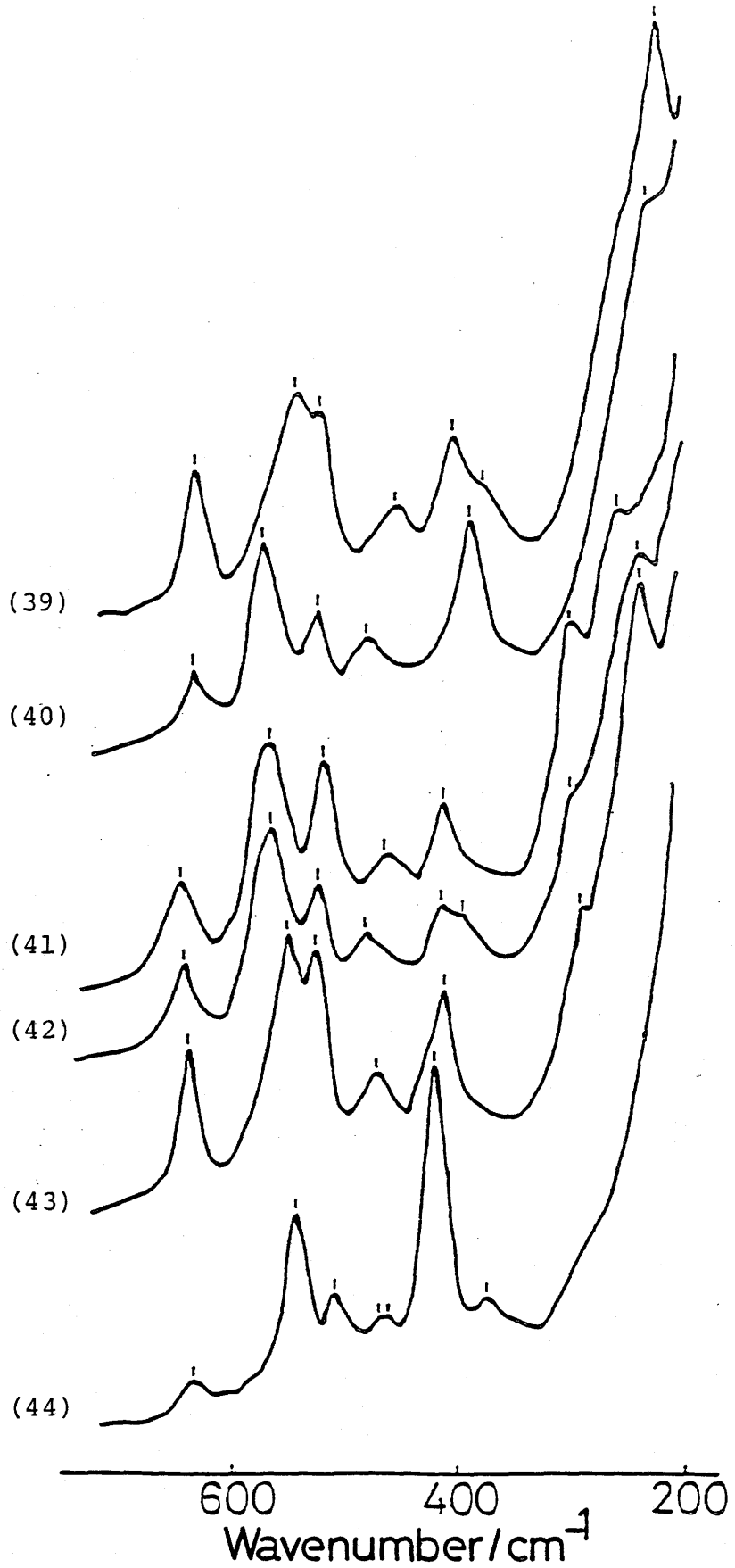

Figure 30. Raman spectra of six geometrical isomers of $[Co(edma)_2]^+$. Numbers in parentheses correspond to those in Table 11.

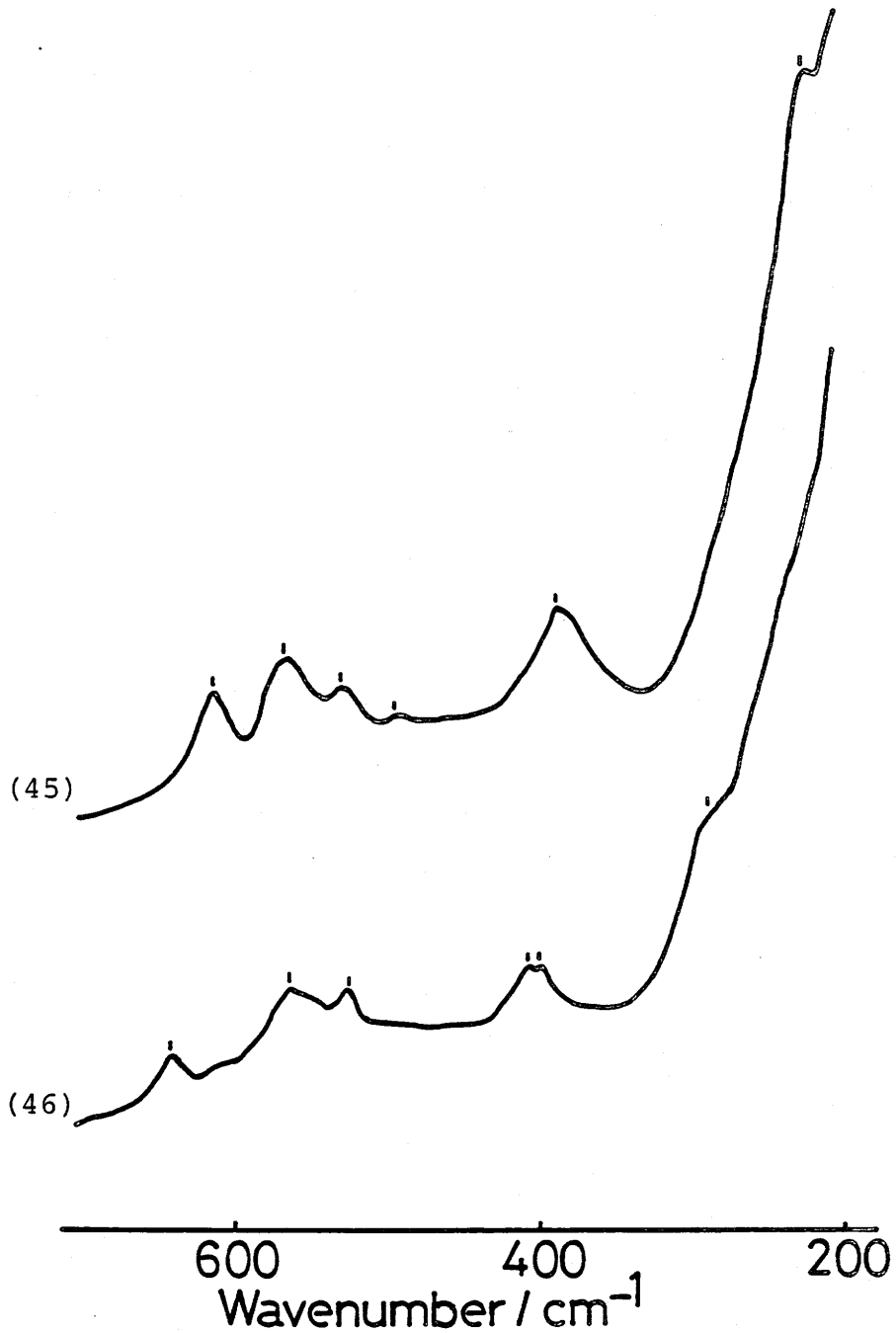

Figure 31. Raman spectra of two geometrical isomers of [Co(ida)(edma)]. Numbers in parentheses correspond to those in Table 11.

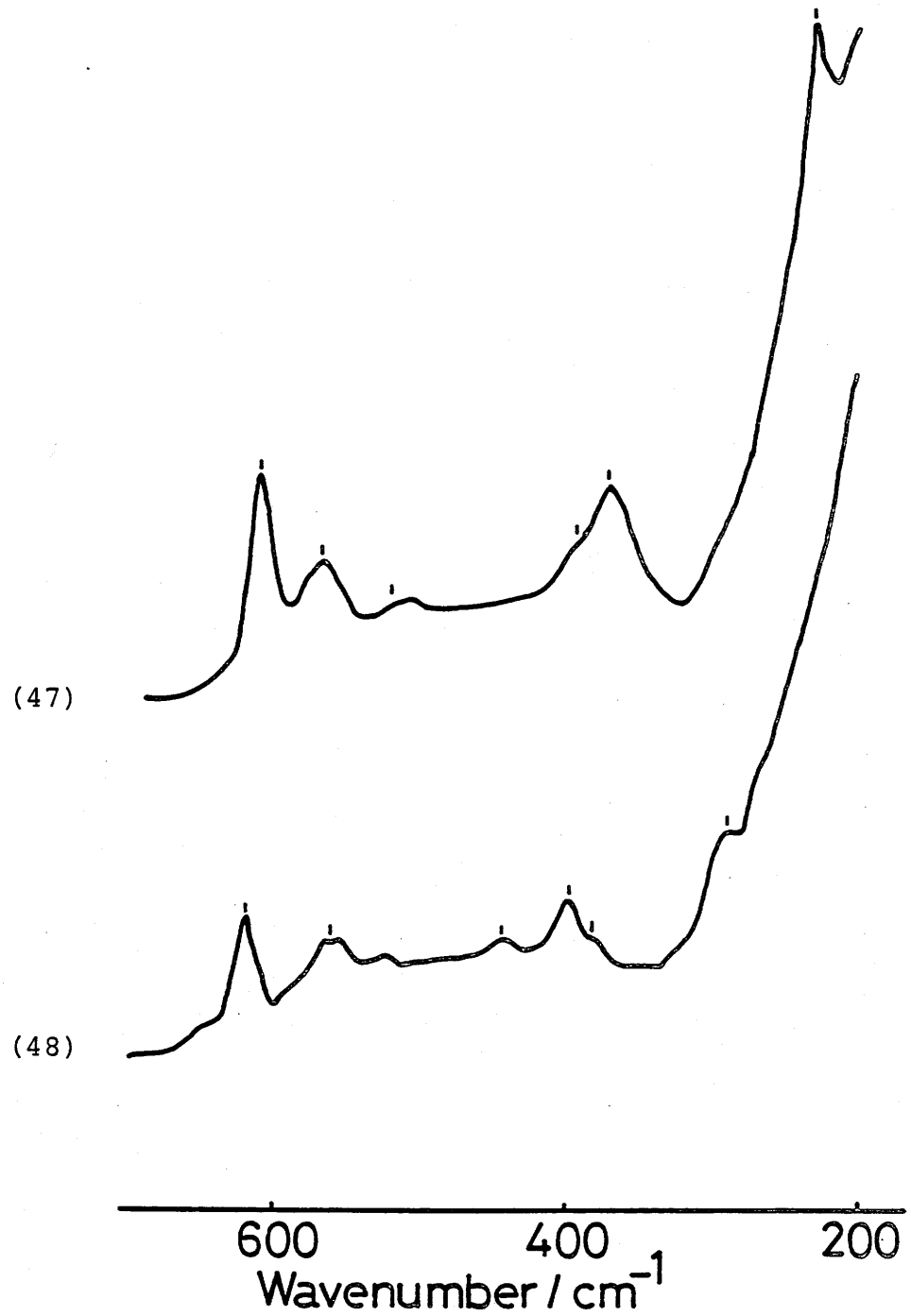

Figure 32. Raman spectra of two geometrical isomers of $[Co(ida)_2]^-$. Numbers in parentheses correspond to those in Table 11.

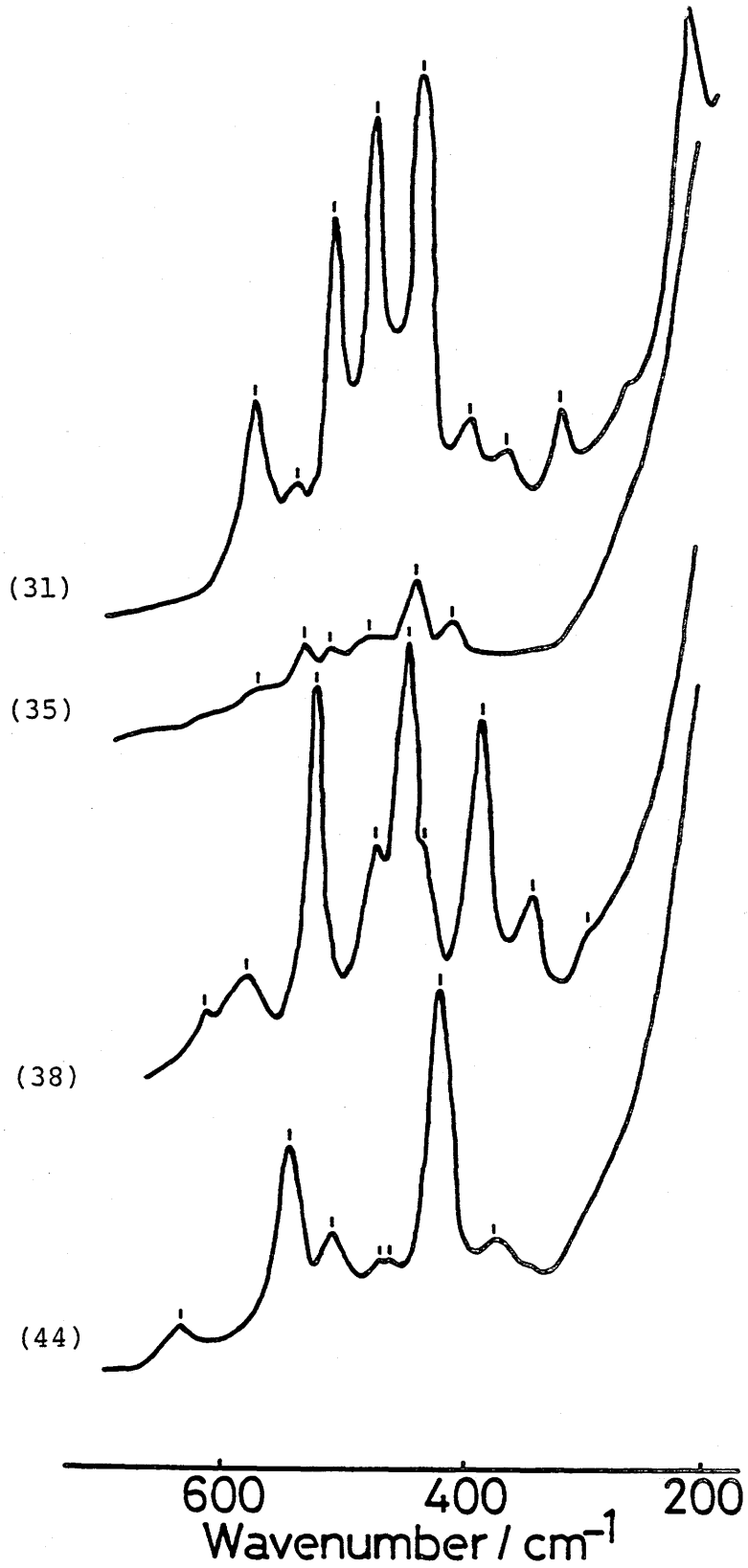

Figure 33. Raman spectra of mer isomers of $[Co(dien)_2]^{3+}$, $[Co(edma)(dien)]^{2+}$, $[Co(ida)(dien)]^{+}$, and $[Co(edma)_2]^{+}$. Numbers in parentheses correspond to those in Table 11.

cis(N_t), unsym-fac-cis(N_t)cis(O), and unsym-fac-trans(N_t) isomers belonging to the cis(O)-[Co$(N)_4(O)_2$]-type is of no intrinsic importance.

On the basis of the above discussion, so far as bis(terdentate)cobalt(III) complexes having the same numbers of the coordinated nitrogen and oxygen donor atoms are concerned, the Raman spectral characteristics depend mainly on the arrangement of the chelate ring around the central metal atom. Accordingly, Raman spectrosopy can be applied to the differentiation of the geometrical isomers of the cobalt(III) complexes with the linear terdentate ligands.

Influence of Coordinated Atoms and Ligands on Raman Spectral Characteristics of Cobalt(III) Complexes with Linear Terdentate Ligands.

Figures 34 and 35 show the Raman spectra of the sym-fac and unsym-fac isomers having different numbers of coordinated nitrogen and oxygen atoms of [Co$(dien)_2]^{3+}$, [Co(edma)(dien)]$^{2+}$, [Co(ida)(dien)]$^{+}$, [Co(ida)(edma)], and [Co$(ida)_2]^{-}$. The intensities of the Raman bands above 600 cm^{-1} of the sym-fac and unsym-fac isomers are intensified with the increasing numbers of the coordinated oxygen atoms, whereas those at ca. 550 and 460 cm^{-1} become weaker with the decreased numbers of the coordinated nitrogen atoms. Furthermore, the polarized bands at ca. 550 cm^{-1} of the fac isomers of [Co(ida)(dien)]$^{+}$ and [Co$(dien)_2]^{3+}$ exhibit a shift (about 20 cm^{-1}) to lower frequency upon the deuteration of the amino nitrogen protons. Accordingly, the

Raman bands above 600 cm^{-1} have largely Co-O stretching character and those at ca. 460 and 550 cm^{-1} Co-N stretching character. This fact can be correlated to the Raman spectra of the tris(bidentate)cobalt(III) complexes, which have the bands due to the gly and ox ligands at 564 - 608 cm^{-1} and those due to the en ligand at 521 - 542 cm^{-1} (V-B-1). That is, it is considered that the Raman bands due to Co-N stretching appear at lower frequency region than those due to Co-O stretching.

It is observed that the numbers of the Raman bands in the skeletal breathing mode region increase with increasing the numbers of the coordinated oxygen atoms; $[Co(dien)_2]^{3+}$ and $[Co(edma)(dien)]^{2+}$ exhibit only one Raman band in this region while $[Co(ida)(dien)]^{+}$, $[Co(ida)(edma)]$, and $[Co(ida)_2]^{-}$ two Raman bands. This fact may suggest that the complexes, which have close numbers of the coordinated oxygen and nitrogen atoms each other, have lower symmetry for skeletal vibration compared with the complexes, which have the predominant numbers of the coordinated nitrogen atoms.

The Raman spectra of the isomers of $[Co(ida)(dien)]^{+}$ can be regarded as a superposision of those of $[Co(dien)_2]^{3+}$ and $[Co(ida)_2]^{-}$ (Figs. 27, 29, and 32). Moreover, as shown in Fig. 36, the Raman spectra of the isomers of $[Co(edma)_2]^{+}$ can also be correlated to those of $[Co(ida)(dien)]^{+}$. That is, the Raman spectral patterns of sym-fac-$[Co(ida)(dien)]^{+}$ and sym-fac-cis(N_t)-$[Co(edma)_2]^{+}$ and those of unsym-fac-

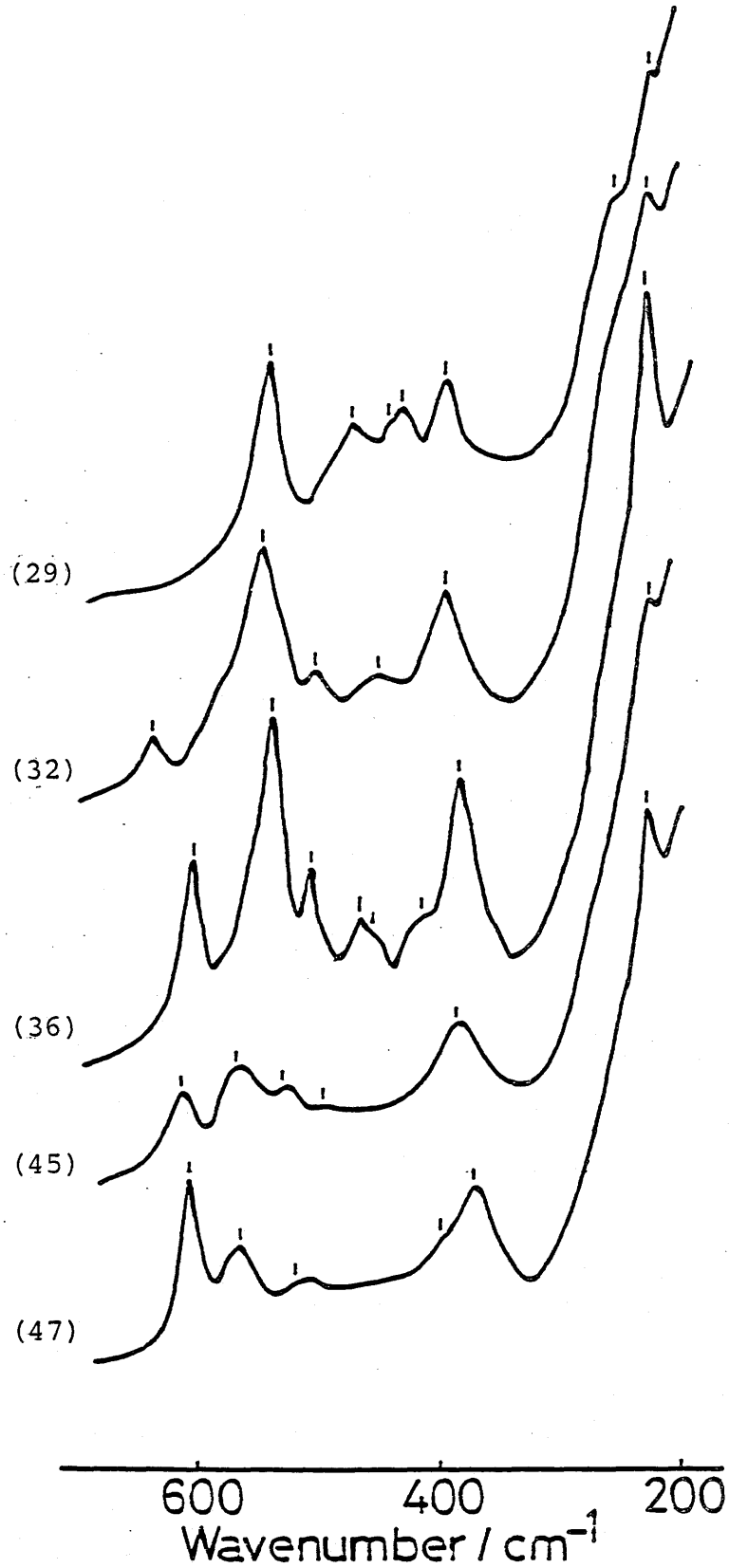

Figure 34. Raman spectra of sym-fac isomers of $[Co(dien)_2]^{3+}$, $[Co(edma)(dien)]^{2+}$, $[Co(ida)(dien)]^{+}$, $[Co(ida)(edma)]$, and $[Co(ida)_2]^{-}$. Numbers in parentheses correspond to those in Table 11.

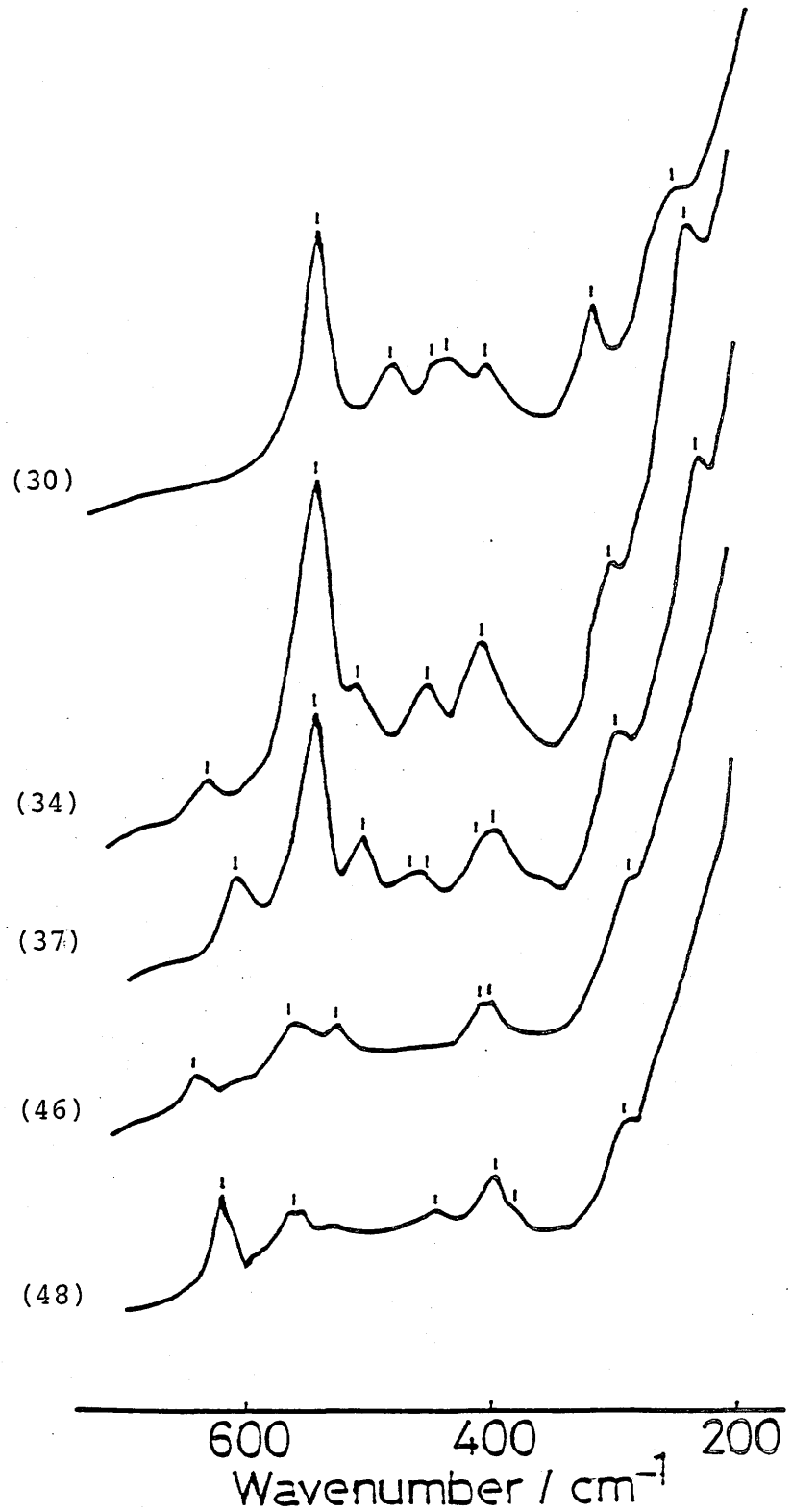

Figure 35. Raman spectra of unsym-fac isomers of $[Co(dien)_2]^{3+}$, $[Co(edma)(dien)]^{2+}$, $[Co(ida)(dien)]^{+}$, $[Co(ida)(edma)]$, and $[Co(ida)_2]^{-}$. Numbers in parentheses correspond to those in Table 11.

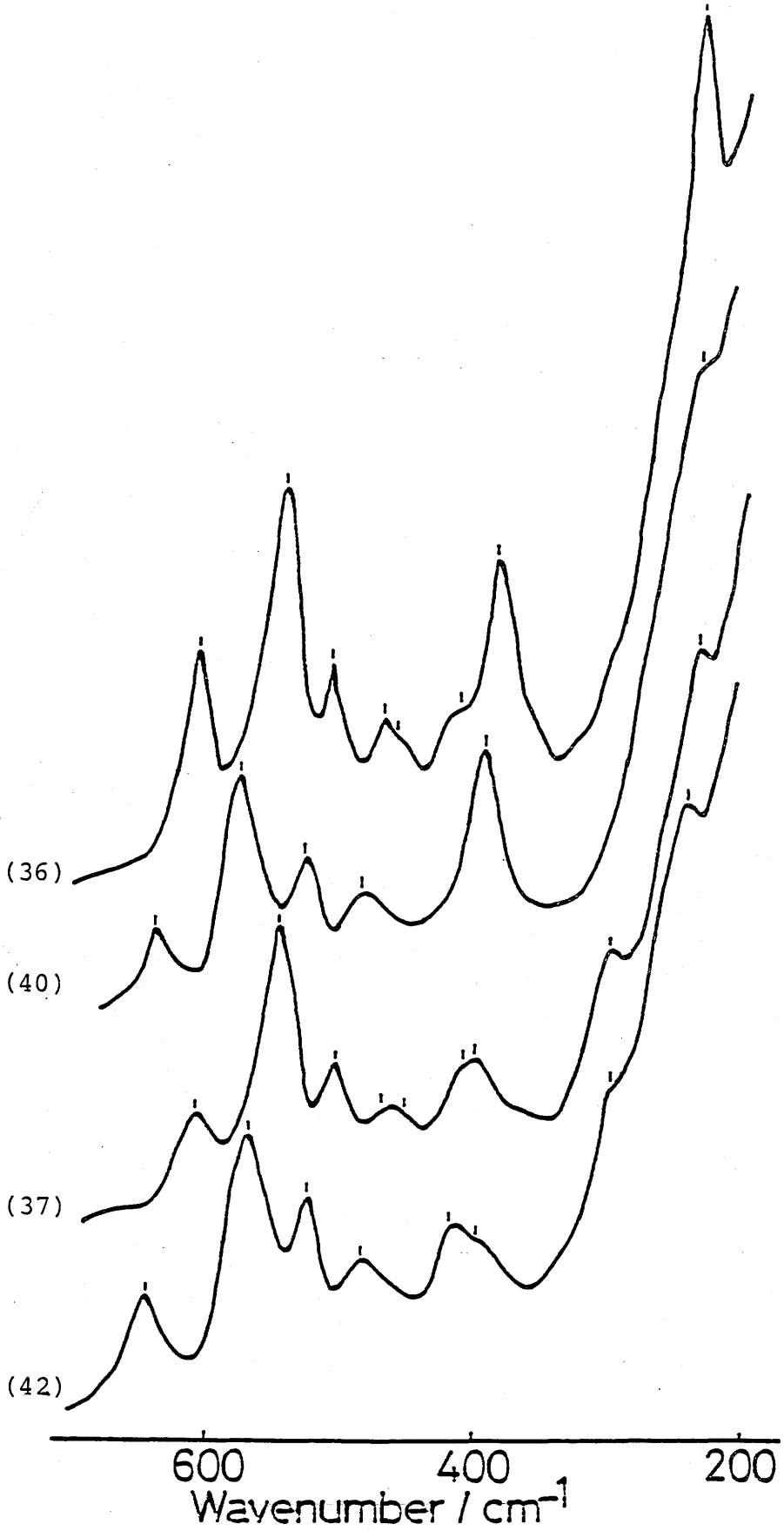

Figure 36. Raman spectra of sym-fac-$[Co(ida)(dien)]^+$, sym-fac-cis(N_t)-$[Co(edma)_2]^+$, unsym-fac-$[Co(ida)(dien)]^+$, and unsym-fac-cis(N_t)cis(O)-$[Co(edma)_2]^+$. Numbers in parentheses correspond to those in Table 11.

$[Co(ida)(dien)]^+$ and unsym-fac-cis(N_t)cis(O)-$[Co(edma)_2]^+$ are similar to each other on the whole spectral region except for a somewhat high frequency shift in the Raman bands of $[Co(edma)_2]^+$ in comparison with those of $[Co(ida)(dien)]^+$ and the difference in the degree of depolarization ratios of Raman bands at ca. 500 - 530 cm^{-1}. It is not surprising that $[Co(edma)_2]^+$ can be considered to have both of the spectral features of the corresponding isomers of $[Co(dien)_2]^{3+}$ and $[Co(ida)_2]^-$, because the Raman spectral characteristics of the bis(terdentate)cobalt(III) complexes having the same numbers of the coordinated nitrogen and oxygen atoms depend mainly on the arrangement of the chelate ring around the central metal atom. In other words, the Raman spectra of the cobalt(III) complexes having the same coordinated atoms are not so much influenced by the variety of ligands.

On the contrary, the Raman bands above 600 cm^{-1}, which have largely Co-O stretching character (vide supra), appear at ca. 615 cm^{-1} for the ida complexes and at ca. 640 cm^{-1} for the edma complexes. This feature can be used as one of the vibrational criteria for differentiating complexes containing either ida or edma, except for [Co(ida)(edma)] which shows the characteristic Raman band at 618 cm^{-1} for sym-fac isomer and at 645 cm^{-1} for unsym-fac-mer(N) one owing to intensification of the one at the sacrifice of the other.

V-B-4. Raman Spectra of Cobalt(III) Complexes with

Terdentate Ligands Containing N-Methyl Group.

The Raman spectra of $[Co(edma)(mdien)]^{2+}$, $[Co(ida)(mdien)]^{+}$, [Co(mida)(edma)], $[Co(ida)(mida)]^{-}$, $[Co(mida)(mdien)]^{+}$, and $[Co(mida)_2]^{-}$ are shown in Figs. 37 - 42, respectively, and the Raman spectral numerical data of these complexes are summarized in Table 12. The Raman bands in the skeletal bending deformation mode region, which are observed on the unsym-fac isomers of $[Co(edma)(dien)]^{2+}$, $[Co(ida)(dien)]^{+}$, and [Co(ida)(edma)] (Figs. 28, 29, and 31), are no longer present in the Raman spectra of unsym-fac-mer(N_t)-$[Co(edma)(mdien)]^{2+}$, unsym-fac-$[Co(ida)(mdien)]^{+}$, and unsym-fac-fac(N)-[Co(mida)(edma)] (Figs. 37 - 39). By contrast, two Raman bands are observed in the skeletal bending deformation mode region for the unsym-fac-fac(N_t) isomer of $[Co(edma)(mdien)]^{2+}$. These evidences may be related to change in the O-Co-N_c angles owing to a steric interaction between the methyl group of the mdien ligand and the methylene group of the edma ligand. With all these differences, the cobalt(III) complexes with terdentate ligands, mdien and mida, exhibit the Raman spectral feature corresponding to that of the cobalt(III) complexes with terdentate ligands, dien, edma, and ida. Accordingly, the Raman bands of the cobalt(III) complexes containing N-methyl group can also be classified into the five vibrational modes; polarized bands in the 520 - 650 cm^{-1} region due to the totally symmetric stretching vibration mode, depolarized bands in the 410 - 520 cm^{-1}

region due to the stretching vibration mode excluding the totally symmetric one, polarized bands in the 360 - 450 cm^{-1} region due to the skeletal breathing vibration mode, depolarized bands in the 270 - 380 cm^{-1} region due to the skeletal bending deformation mode, and polarized bands in the 220 - 290 cm^{-1} region due to the chelate ring deformation mode.

The Raman spectra of the cobalt(III) complexes containing N-methyl group also show some characteristic behaviors. First, the strongest Raman bands due to the totally symmetric stretching vibration in the Raman spectra of cobalt(III) complexes containing N-methyl group, except mer-$[Co(ida)(mdien)]^+$ and mer-$[Co(mida)(mdien)]^+$, appear at the lower frequency region compared with the Raman spectra of the corresponding cobalt(III) complexes containing no N-methyl group. This fact suggests the existence of the mass effect in the totally symmetric stretching vibration mode owing to the replacement of a hydrogen atom on the imino nitrogen by a methyl group, similar to the isotope shifts, and/or the difference in the central metal-donor atom bond strength which can be related to the ligand field strength. In fact, the first and the second absorption maxima shift to the lower energy side when the methyl group is introduced on the central donor atom of the terdentate ligands (Table 13). Incidentally, because of specificity of mer isomers for skeletal vibration, it may be considered that mer-$[Co(ida)(mdien)]^+$ and mer-$[Co(mida)(mdien)]^+$ do not exhibit similar behavior to the other complexes. Thus, the Raman

bands in the totally symmetric stretching vibration mode may be regarded as the most sensitive bands for the mass effect and/or the central metal-donor atom bond strength. However, such a distinct relation could not be found on other vibrational modes. The coordinated mida and mdien ligands are characteristic in that their conformations are somewhat restricted by the methyl group on imino nitrogen; the replacement of hydrogen atom on the imino nitrogen by a methyl group causes a marked change in the Raman spectral characteristics rather than the spectral shift anticipated in the case of the deuteration of the amino protons.

Second, the mer isomers of the cobalt(III) complexes containing N-methyl group also exhibit a spectral feature appreciably different from that of the fac isomers. That is, the Raman spectra of the mer isomers have the sharp Raman bands at the higher frequency region in the skeletal breathing vibration mode and have no Raman bands in the chelate ring deformation mode region, except mer-$[Co(mida)_2]^-$ and mer-$[Co(mida)(mdien)]^+$ containing two terdentate ligands having N-methyl group. Furthermore, the Raman bands above 600 cm^{-1} region appear at ca. 615 cm^{-1} for the ida complexes and at ca. 640 cm^{-1} for the edma complexes. The cobalt(III) complexes containing mida ligand ($[Co(mida)(mdien)]^+$, $[Co(mida)(edma)]$, and $[Co(ida)(mida)]^-$) exhibit several Raman bands in the skeletal breathing vibration mode region. This fact may be correlated to increase of the numbers of the coordinated oxygen atoms.

These features are in line with the general characteristic of the Raman spectra of the cobalt(III) complexes containing no N-methyl group. However, the Raman spectra in the stretching vibration region of the mer isomers for $[Co(edma)(mdien)]^{2+}$, $[Co(ida)(mdien)]^{+}$, $[Co(ida)(mida)]^{-}$, $[Co(mida)(mdien)]^{+}$, and $[Co(mida)_2]^{-}$ exhibit depolarized bands. These spectral characteristics differ somewhat from the Raman spectra of the mer isomers for the cobalt(III) complexes containing no N-methyl group, which give only polarized bands except mer-$[Co(edma)_2]$. These findings suggest that the skeletal vibration characteristics of the mer isomers for the mida or mdien cobalt(III) complexes are mainly regulated by the linked chelate rings, which are folded by the restriction imposed by the methyl group on imino nitrogen. Furthermore, mer-$[Co(mida)(mdien)]^{+}$ and mer-$[Co(mida)_2]^{-}$ with two terdentate ligands containing N-methyl group exhibit the Raman bands in the chelate ring deformation mode and sym-fac-$[Co(mida)(mdien)]^{+}$ and fac-$[Co(mida)_2]^{-}$ do not exhibit the Raman bands above 600 cm^{-1}. It seems that these facts suggest new vibrational characteristic appearance owing to two methyl groups. Specifically, the fact that mer-$[Co(mida)_2]^{-}$ and mer-$[Co(mida)(mdien)]^{+}$ have the Raman bands in the chelate ring deformation mode, may have a relation with high stability of these complexes; for example, mer-$[Co(mida)_2]^{-}$ has been found stable even in a weakly basic aqueous solution compared to mer-$[Co(ida)(mida)]^{-}$ [23,24].

Table 12. Raman Spectral Data of Cobalt(III) Complexes With Terdentate Ligands Containing N-Methyl Group.

No.	Complexes	Raman frequency / cm^{-1} a)				
51	sym-fac-[Co(edma)(mdien)]$^{2+}$	643 w(p) 554 sh(-) 529 s(p)	466 sh(-) 443 m(dp)	401 m(p)		235 s(p)
52	unsym-fac-fac(Nt)-[Co(edma)(mdien)]$^{2+}$	637 vw(-) 555 m(-) 527 s(p)	450 m(dp)	403 w(-)	346 m(-) 289 vw(-)	249 w(-)
53	unsym-fac-mer(Nt)-[Co(edma)(mdien)]$^{2+}$	636 w(p) 585 vw(-) 529 s(p)	450 w(dp) 417 vw(dp)	378 vw(-)		237 vw(-)
54	mer-[Co(edma)(mdien)]$^{2+}$	631 vw(-) 533 s(p)	503 sh(-)	442 s(p) 417 m(-)	373 vw(-) 326 vw(-) 279 sh(-)	
55	sym-fac-[Co(ida)(mdien)]$^{+}$	614 w(p) 529 s(p)	518 w(dp) 471 vw(-) 442 w(-)	390 m(p)		225 vw(p)
56	unsym-fac-[Co(ida)(mdien)]$^{+}$	617 w(p) 533 s(p)	517 w(dp) 450 w(-)	403 w(-)		237 vw(p)
57	mer-[Co(ida)(mdien)]$^{+}$	538 m(p)	499 vw(-)	442 m(p) 386 m(p)		
58	sym-fac-[Co(mida)(edma)]	644 w(p) 569 sh(p) 537 s(p)	498 m(-) 458 vw(-)	406 m(p) 378 m(p)		
59	unsym-fac-fac(N)-[Co(mida)(edma)]	642 vw(-) 534 m(p)	498 vw(-)	413 w(-)		
60	sym-fac-[Co(ida)(mida)]$^{-}$	611 m(p) 546 m(p)	497 w(dp) 450 w(-)	407 w(-) 382 w(-) 361 w(-)		246 m(p)

61 unsym-fac-[Co(ida)(mida)]$^-$	622 w(p) 547 m(p)	495 vw(-) 450 vw(-)	409 w(p) 386 vw(-)	354 vw(dp)	
62 mer-[Co(ida)(mida)]$^-$	533 m(p)	455 vw(-)	407 m(p)		
63 sym-fac-[Co(mida)(mdien)]$^+$	531 s(p)	505 w(dp) 451 vw(-)	405 w(p) 397 w(p) 370 w(p) 361 w(p)		224 m(-)
64 mer-[Co(mida)(mdien)]$^+$	546 sh(p) 535 s(p)	487 w(-)	440 m(p) 392 m(p) 377 sh(p)		254 vw(p)
65 sym-fac-[Co(mida)$_2$]$^-$	541 vw(p)	501 vw(dp)			
66 unsym-fac-[Co(mida)$_2$]$^-$	545 vw(-)	506 vw(-)			
67 mer-[Co(mida)$_2$]$^-$	563 s(p)	504 vw(dp) 465 w(dp)	404 m(p)		259 vw(-)

Assignment [a]	ν_{ts}(Co-L)	ν(Co-L)	ν_{br}	δ_{sbd}(L-Co-L)	δ_{crd}(Co$<^{L}_{L}$)

a) The following abbreviations are used: s, strong; m, medium; w, weak; vw, very weak; sh, shoulder; p, polarized; dp, depolarized; ν_{ts}, totally symmetric stretching vibration mode; ν, stretching vibration mode excluding the totally symmetric stretching character; ν_{br}, skeletal breathing vibration mode; δ_{sbd}, skeletal bending deformation mode; δ_{crd}, chelate rind deformation mode. The Raman band intensities (s, m, w, vw, and sh) are classified by a comparison of all the Raman bands among all the complexes.

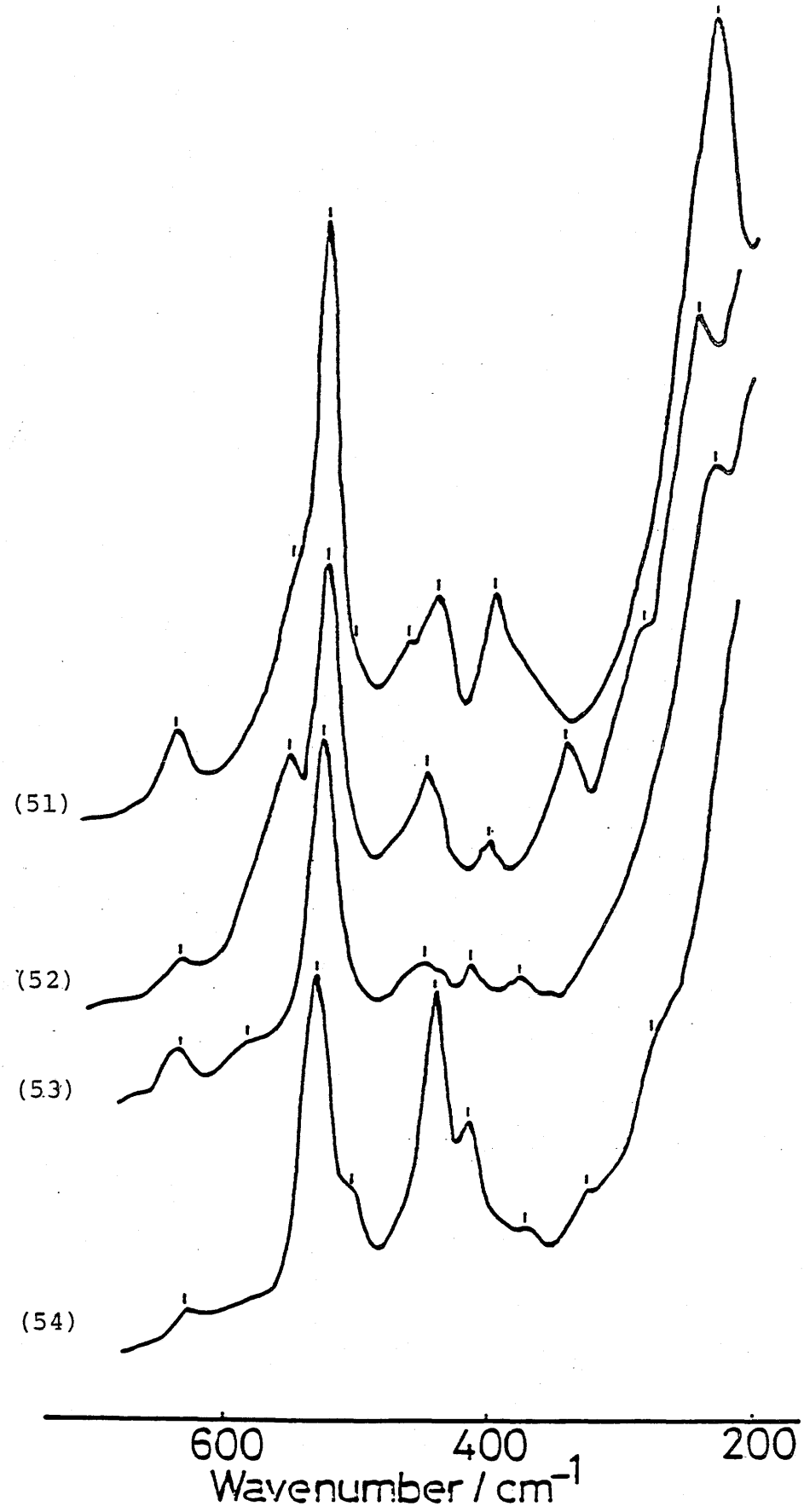

Figure 37. Raman spectra of four geometrical isomers of $[Co(edma)(mdien)]^{2+}$. Numbers in parentheses correspond to those in Table 12.

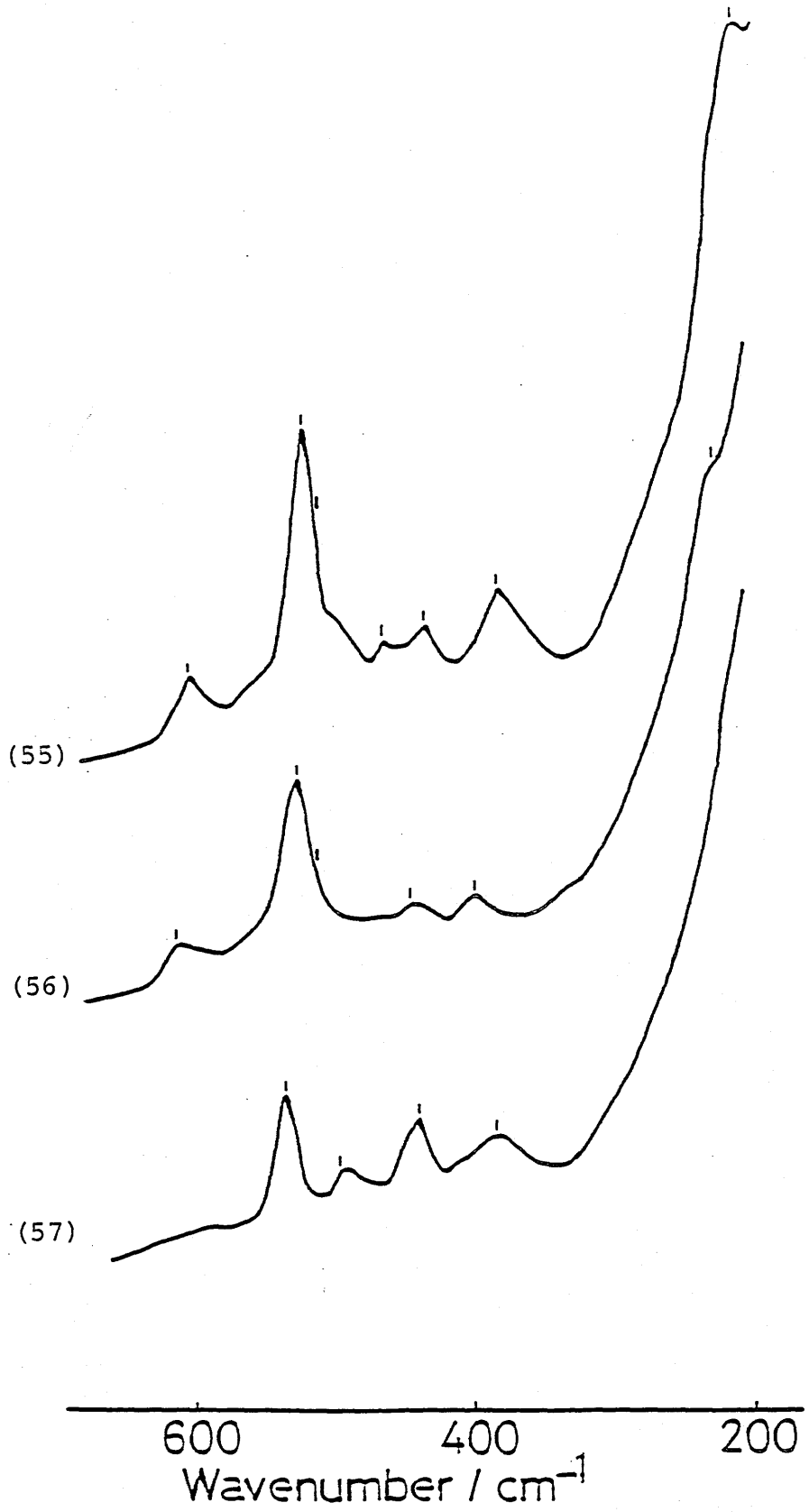

Figure 38. Raman spectra of three geometrical isomers of $[Co(ida)(mdien)]^+$. Numbers in parentheses correspond to those in Table 12.

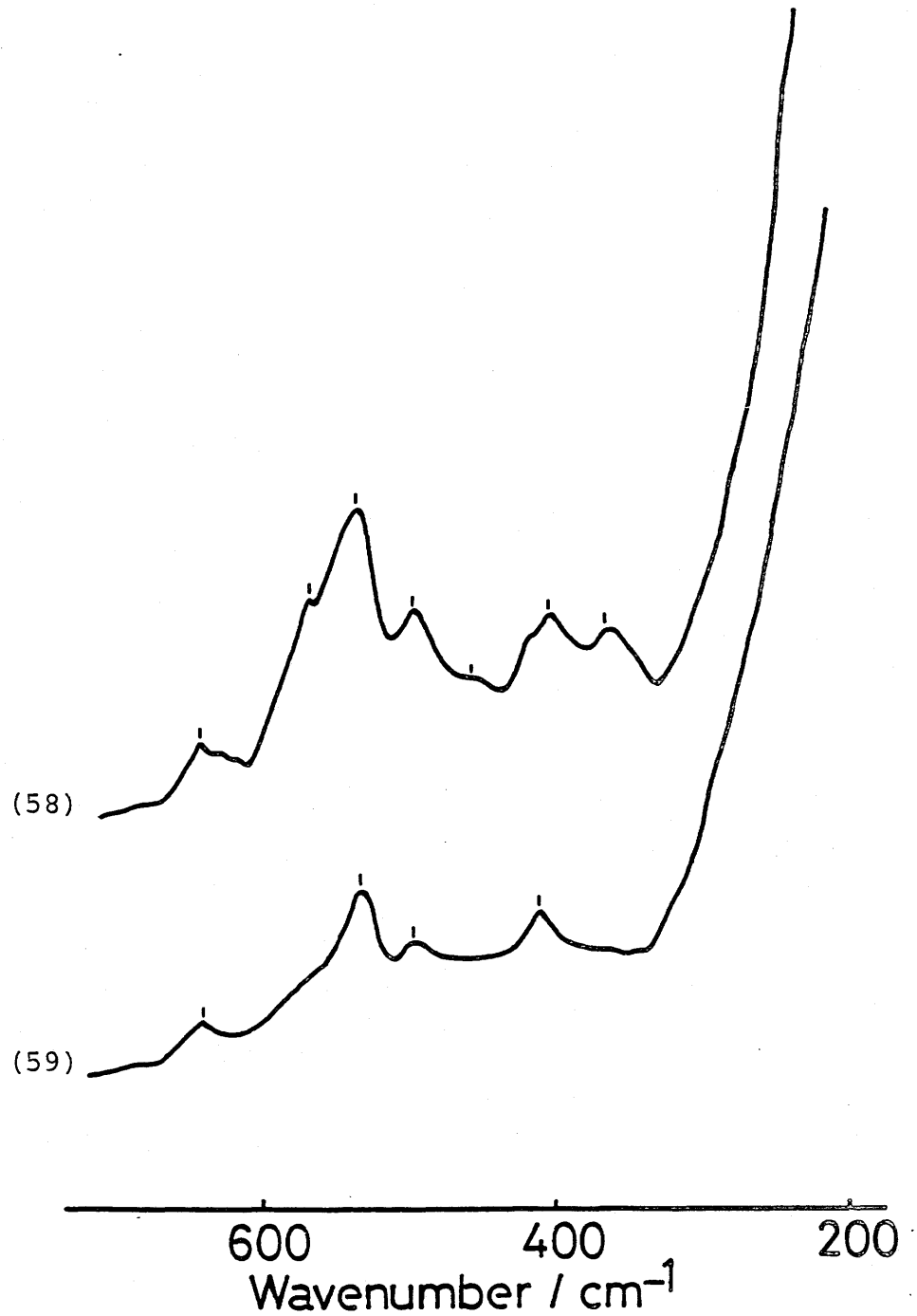

Figure 39. Raman spectra of two geometrical isomers of [Co(mida)(edma)]. Numbers in parentheses correspond to those in Table 12.

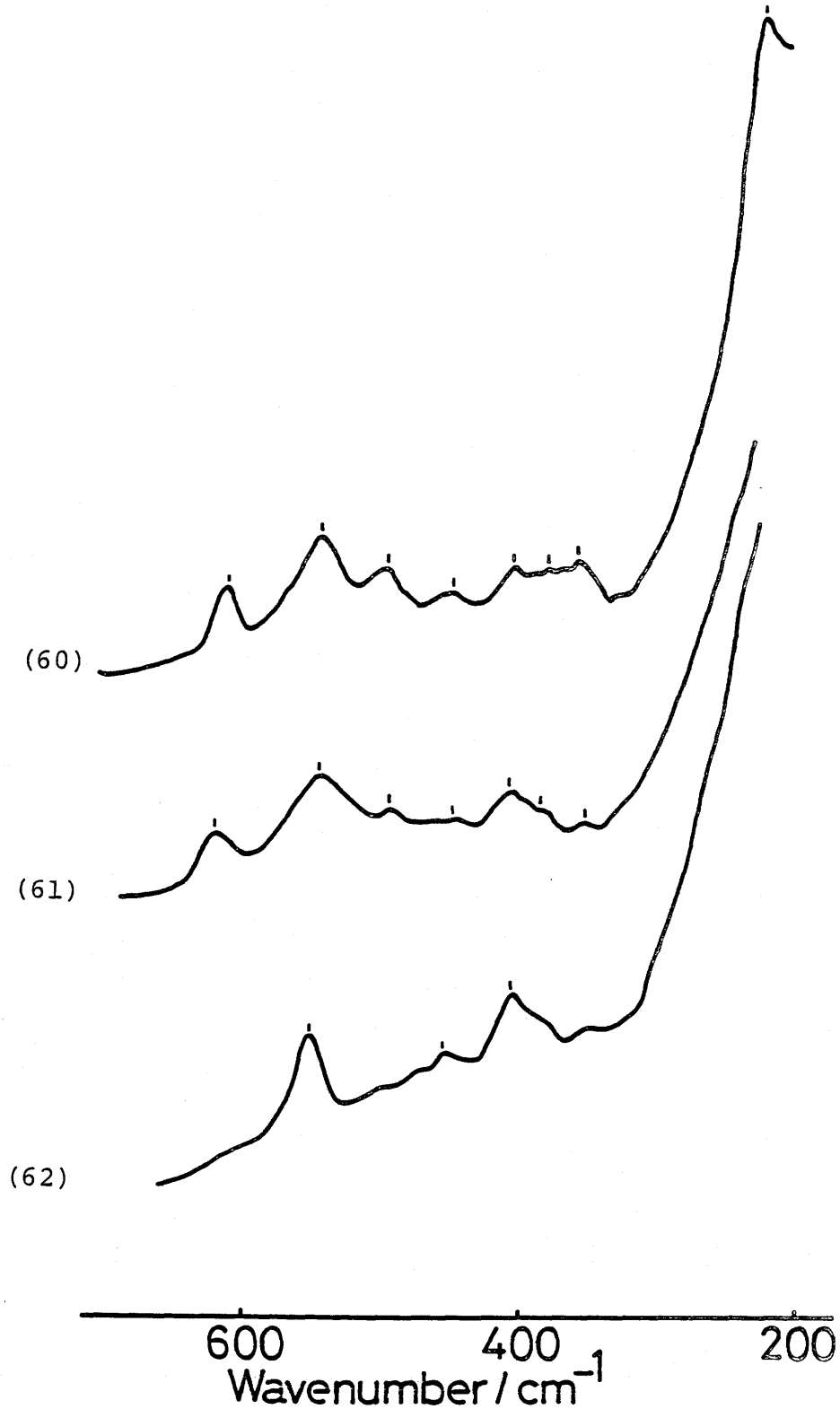

Figure 40. Raman spectra of three geometrical isomers of $[Co(ida)(mida)]^-$. Numbers in parentheses correspond to those in Table 12.

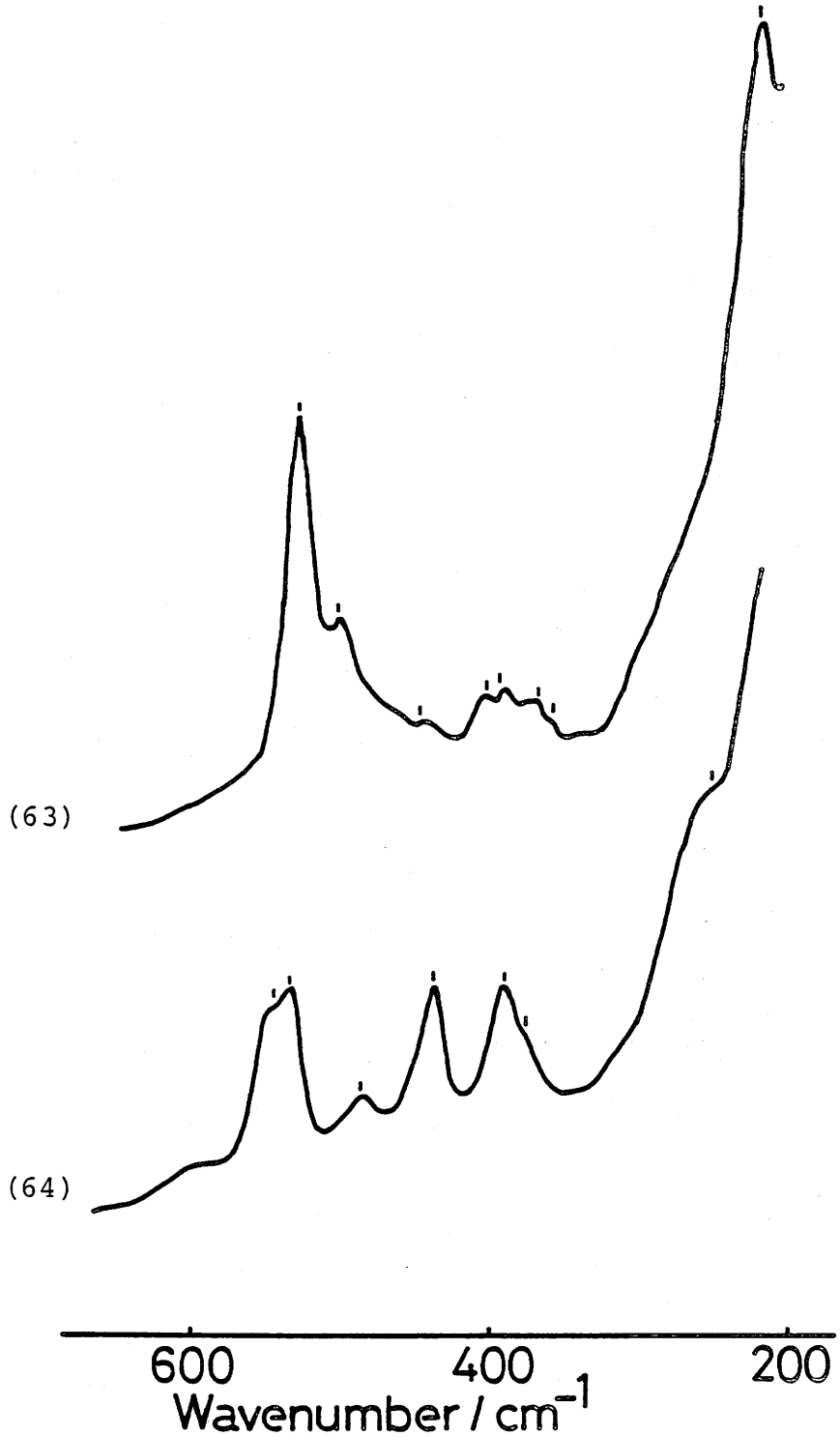

Figure 41. Raman spectra of two geometrical isomers of $[Co(mida)(mdien)]^+$. Numbers in parentheses correspond to those in Table 12.

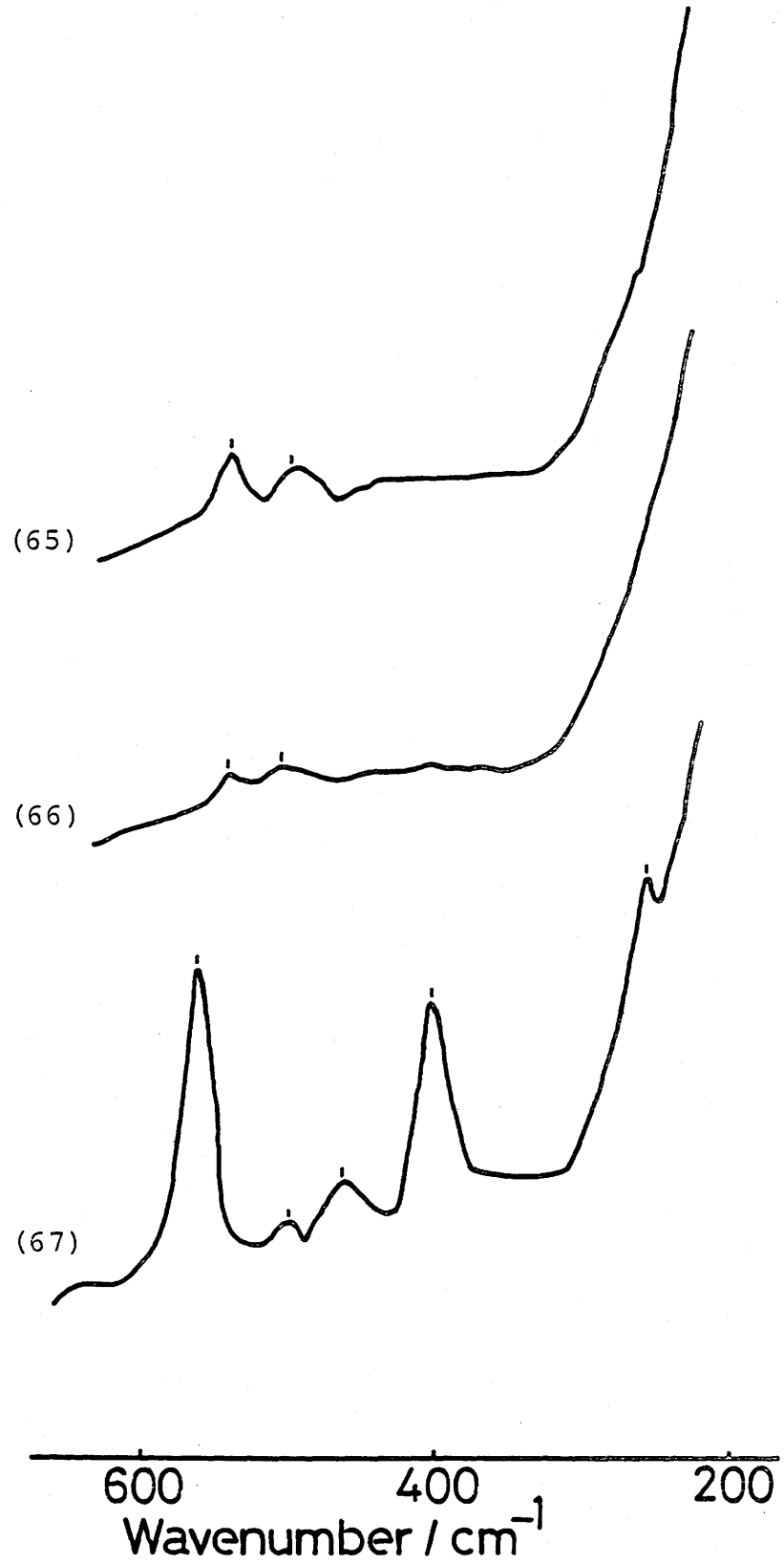

Figure 42. Raman spectra of three geometrical isomers of $[Co(mida)_2]^-$. Numbers in parentheses correspond to those in Table 12.

Table 13. Raman Spectral Data in Totally Symmetric Stretching Vibration Mode and Absorption Data of Cobalt(III) Complexes with Terdentate Ligands

Complex	Raman frequency[a]	Absorption maxima[b] First band	Second band
sym-fac-[Co(edma)(dien)]$^{2+}$	553	21.05	28.99
sym-fac-[Co(edma)(mdien)]$^{2+}$	529	20.81	29.07
unsym-fac-fac(N_t)-[Co(edma)(dien)]$^{2+}$	558	20.66	28.99
unsym-fac-fac(N_t)-[Co(edma)(mdien)]$^{2+}$	527	20.28	28.41
unsym-fac-mer(N_t)-[Co(edma)(dien)]$^{2+}$	547	20.62	28.99
unsym-fac-mer(N_t)-[Co(edma)(mdien)]$^{2+}$	529	19.92	28.49
mer-[Co(edma)(dien)]$^{2+}$	538	21.05	28.65
mer-[Co(edma)(mdien)]$^{2+}$	533	20.45	28.25
sym-fac-[Co(ida)(dien)]$^{+}$	546	20.6	28.6
sym-fac-[Co(ida)(mdien)]$^{+}$	529	20.2	28.4
sym-fac-[Co(mida)(mdien)]$^{+}$	531	20.0	28.4
unsym-fac-[Co(ida)(dien)]$^{+}$	546	19.6	28.2
unsym-fac-[Co(ida)(mdien)]$^{+}$	533	19.1	27.9
mer-[Co(ida)(dien)]$^{+}$	524	19.6	27.8
mer-[Co(ida)(mdien)]$^{+}$	538	19.2	27.6
mer-[Co(mida)(mdien)]$^{+}$	535	18.9	27.0

sym-fac-[Co(ida)(edma)]	573	17.7(sh) 20.7	28.0
sym-fac-[Co(mida)(edma)]	537	17.5(sh) 20.3	28.0
sym-fac-$[Co(ida)_2]^-$	569	16.47 20.18	27.55
sym-fac-$[Co(ida)(mida)]^-$	546	16.69 20.04	27.40
sym-fac-$[Co(mida)_2]^-$	541	16.4(sh) 19.76	27.25
unsym-fac-$[Co(ida)_2]^-$	562	17.83	26.28
unsym-fac-$[Co(ida)(mida)]^-$	547	17.70	26.04
unsym-fac-$[Co(mida)_2]^-$	545	17.24	25.32

a) Wave numbers are given cm^{-1}.

b) Wave numbers are given 10^3 cm^{-1}.

Sh denotes a shoulder.

V-B-5. Raman Spectral Characteristics of Cobalt(III) Complexes with Quadridentate Ligands.

General Aspects.

The Raman spectral data in the skeletal vibration region of cobalt(III) complexes with quadridentate ligands, such as trien, tren, edda, and aeida, are summarized in Table 14.

Figure 43 shows the Raman spectrum of cis-α-$[Co(en)(trien)]^{3+}$ as a typical example of the cobalt(III) complexes with the quadridentate ligand, together with those of unsym-fac-$[Co(dien)_2]^{3+}$, $[Co(en)_3]^{3+}$, and $[Co(NH_3)_6]^{3+}$ (Tables 9, 11, and 14 for numerical data). These complexes equally possess an O_h symmetry with respect to coordinated atoms. From their Raman frequencies and intensities, it seems that the Raman bands at 555, 421 - 498, 354, and 282 cm^{-1} of cis-α-$[Co(en)(trien)]^{3+}$ correspond to those at 546, 434 - 485, 321, and 255 cm^{-1} of unsym-fac-$[Co(dien)_2]^{3+}$ and to those at 525, 440, 378, and 283 cm^{-1} of $[Co(en)_3]^{3+}$, respectively. However, the depolarization ratio of the Raman band at 498 cm^{-1} of cis-α-$[Co(en)(trien)]^{3+}$ is different from that of the corresponding Raman bands of unsym-fac-$[Co(dien)_2]^{3+}$ (485 cm^{-1}), $[Co(en)_3]^{3+}$ (440 cm^{-1}), and $[Co(NH_3)_6]^{3+}$ (440 cm^{-1}) (Tables 9, 11, and 14); the band at 498 cm^{-1} of cis-α-$[Co(en)(trien)]^{3+}$ is polarized, while the band at 485 cm^{-1} of unsym-fac-$[Co(dien)_2]^{3+}$ and the bands at 440 cm^{-1} of $[Co(en)_3]^{3+}$ and $[Co(NH_3)_6]^{3+}$ are depolarized. This spectral feature is unique for the

cobalt(III) complexes with the quadridentate ligands: The polarized Raman bands at 400 - 510 cm^{-1} are regarded as characteristic of the cobalt(III) complexes with the quadridentate ligands, because they were not observed for the tris(bidentate)cobalt(III) complexes and the bis(terdentate)cobalt(III) ones except $[Co(edma)_2]^+$ (vide supra). On the contrary, the polarized Raman bands around 400 cm^{-1}, characteristic for the cobalt(III) complexes with the terdentate ligands, could not be observed for the cobalt(III) complexes with the quadridentate ligands.

It is evident from Fig. 43 and Table 14 that the Raman spectral characteristic of cis-α-$[Co(en)(trien)]^{3+}$ is similar to that of $[Co(en)_3]^{3+}$ rather than that of unsym-fac-$[Co(dien)_2]^{3+}$. Accordingly, the Raman spectrum of cis-α-$[Co(en)(trien)]^{3+}$ can be assigned on the basis of the Raman spectrum of $[Co(en)_3]^{3+}$ except the Raman band at 498 cm^{-1}. This deduction is supported by comparison of the Raman spectra of cis-α-$[Co(edda)(en)]^+$ and trans(O)-$[Co(gly)_2(en)]^+$ having a D_{4h} symmetry with respect to the coordinated atoms (Fig. 44). That is, the Raman bands at 525 - 617, 421 - 461, 349, and 262 cm^{-1} of cis-α-$[Co(edda)(en)]^+$ correspond to those at 523 - 596, 458 - 504, 368, and 275 cm^{-1} of trans(O)-$[Co(gly)_2(en)]^+$, except for the difference in the depolarization ratio between the Raman band at 461 cm^{-1} of the former and that at 504 cm^{-1} of the latter (Tables 9 and 14). Furthermore, taking the Raman frequency and the depolarization ratio into account, it is considered that the polarized band at 498 cm^{-1} of cis-α-

Table 14. Raman Spectral Data of the Cobalt(III) Complexes With Quadridentate Ligands.

No.	Complexes	Raman frequency / cm^{-1} a)			
68	cis-α-[Co(en)(trien)]$^{3+}$	646 vw(-) 555 s(p) 498 m(p)	446 w(-) 421 m(dp)	354 vw(-)	282 m(p)
69	cis-β-[Co(en)(trien)]$^{3+}$	575 m(p) 531 s(p) 507 s(p) 465 w(-) 433 s(p)		385 vw(-) 349 w(-) 318 vw(-)	
70	cis-α-[Co(ox)(trien)]$^{+}$	649 vw(-) 570 s(p) 510 w(p)	429 m(dp)		282 vw(-)
71	cis-β-[Co(ox)(trien)]$^{+}$	589 w(p) 539 s(p) 457 m(p)	428 m(dp)	370 vw(-) 342 w(-)	
72	[Co(en)(tren)]$^{3+}$	605 w(p) 531 s(p) 514 m(p)		442 m(p) b) 419 w(-) 383 w(dp)	265 m(p)
73	[Co(ox)(tren)]$^{+}$	606 w(p) 542 s(p) 475 vw(-)		453 m(p) b) 418 w(-) 370 w(dp)	242 w(-)
74	cis-α-[Co(edda)(en)]$^{+}$	617 m(p) 525 m(p) 461 m(p)	421 vw(dp)	349 w(-)	262 m(-)
75	cis-β-[Co(edda)(en)]$^{+}$	660 w(p) 594 vw(-) 530 m(p) 465 m(p)	438 w(-) 405 w(-)	346 vw(dp) 308 vw(-)	

76	cis-α-[Co(edda)(tn)]$^{+}$	613 m(p) 521 m(p) 478 sh(-) 448 m(p)	390 vw(-)	350 w(-)	
77	cis-β-[Co(edda)(tn)]$^{+}$	655 w(p) 556 vw(-) 530 w(-) 485 s(p) 425 m(p)		313 w(-)	
78	cis-α-[Co(edda)$(NH_3)_2$]$^{+}$	620 m(p) 522 m(p) 470 sh(-) 452 m(p)	398 vw(-)	349 m(-)	260 vw(-)
79	cis-α-[Co(edda)(gly)]	621 s(p) 537 m(p) 473 w(-)	429 w(-)	385 vw(-) 347 w(-)	265 m(-)
80	cis-α-[Co(edda)(β-ala)]	615 m(p) 529 w(p) 452 vw(-)		354 vw(-)	
81	cis-α-[Co(edda)(ox)]$^{-}$	618 m(p) 533 w(p)	417 w(-)	373 vw(-)	
82	cis-β-[Co(edda)(ox)]$^{-}$	662 vw(-) 570 vw(-)	425 vw(-)		
83	trans(O)-[Co(aeida)(en)]$^{+}$	546 w(p) 494 w(-) 449 vw(-)		400 m(p)[b]	
84	cis(O)-[Co(aeida)(en)]$^{+}$	550 m(p) 505 vw(-) 450 m(p)		409 m(-)[b]	245 vw(-)

Assignment[a]	ν_{ts}(Co-L)	ν(Co-L)	δ_{sbd}(L-Co-L)	δ_{crd}(Co$\prec^{L}_{L}$))

a) The following abbreviations are used: s, strong; m, medium; w, weak; vw, very weak; sh, shoulder; p, polarized; dp, depolarized; ν_{ts}, totally symmetric stretching vibration mode; ν, stretching vibration mode excluding the totally symmetric stretching character; δ_{sbd}, skeletal bending deformation mode; δ_{crd}, chelate ring deformation mode. The Raman band intensities (s, m, w, vw, and sh) are classified by a comparison of all the Raman bands among all the complexes.

b) These bands correspond to the breathing vibration mode which is characteristic for the bis-(terdentate)cobalt(III) complexes.

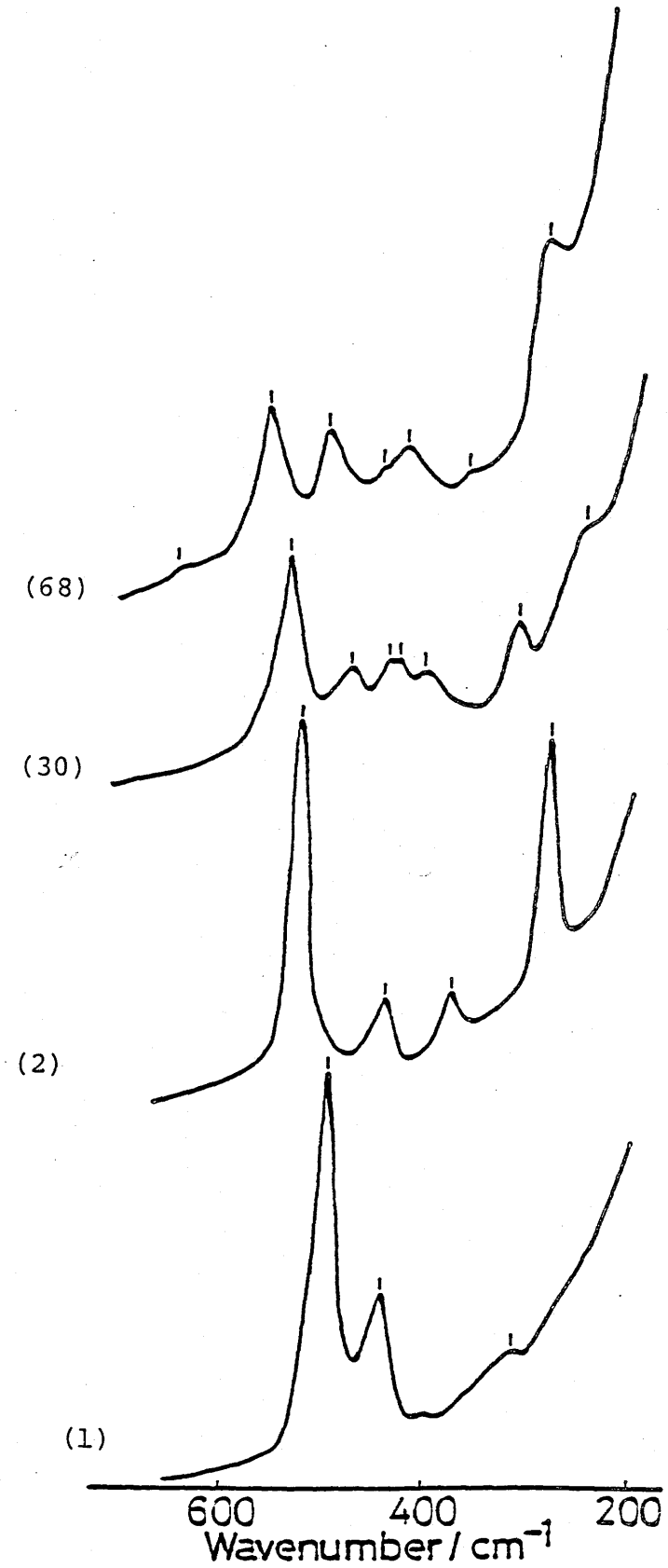

Figure 43. Raman spectra of cis-α-$[Co(en)(trien)]^{3+}$, unsym-fac-$[Co(dien)_2]^{3+}$, $[Co(en)_3]^{3+}$, and $[Co(NH_3)_6]^{3+}$. Numbers in parentheses correspond to those in Tables 9, 11, and 14.

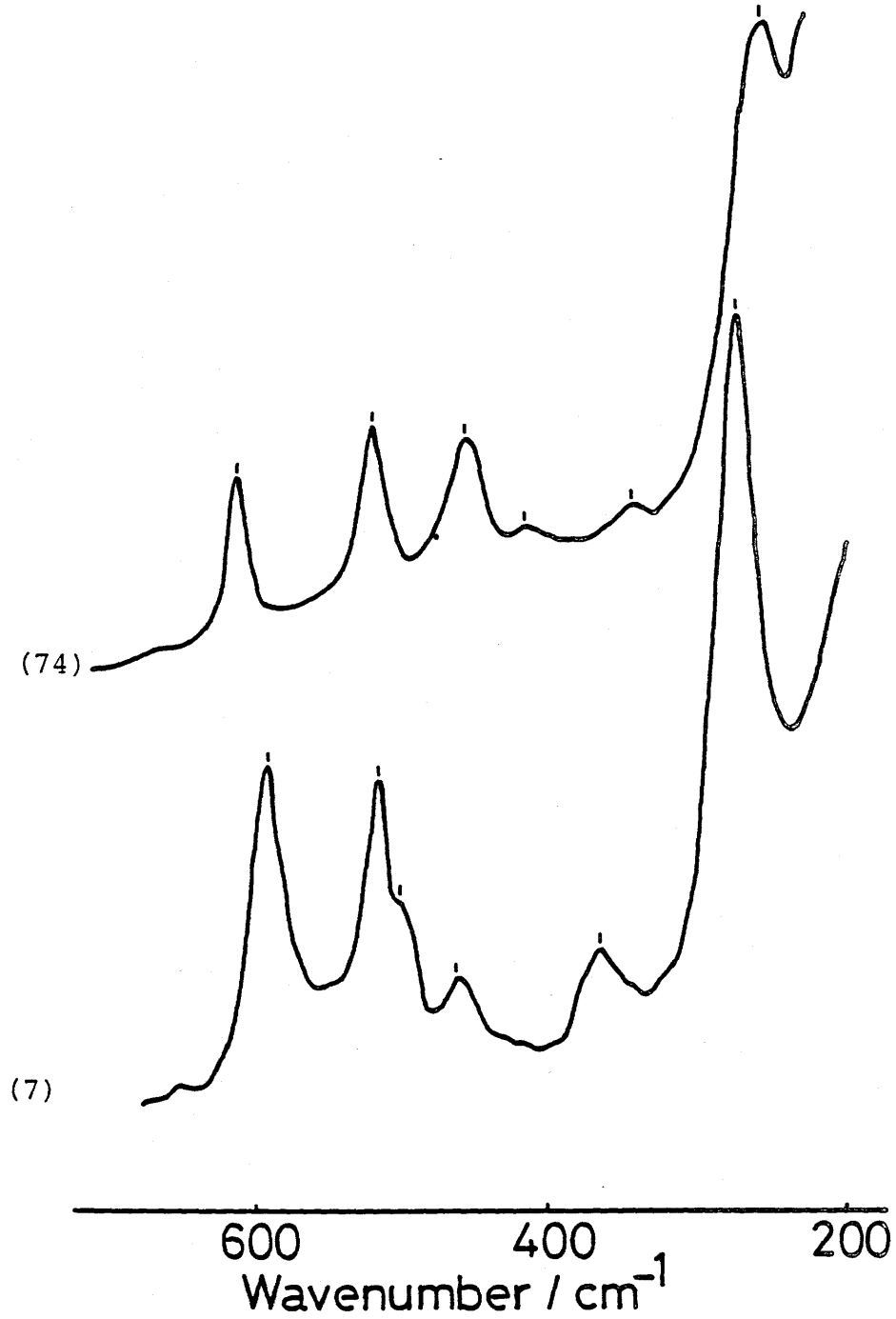

Figure 44. Raman spectra of cis-α-$[Co(edda)(en)]^+$ and trans(O)-$[Co(gly)_2(en)]^+$. Numbers in parentheses correspond to those in Tables 9 and 14.

$[Co(en)(trien)]^{3+}$ and that at 461 cm^{-1} of cis-α-$[Co(edda)(en)]^{+}$ can be assigned to the totally symmetric stretching vibration mode.

On the basis of these observations and the Raman spectral characteristics summarized in Table 14, it can be concluded that the Raman spectra of cobalt(III) complexes with quadridentate ligands are classified into four categories similar to those of tris(bidentate)cobalt(III) complexes. Accordingly, the polarized bands in the 420 - 670 cm^{-1} region, the depolarized ones in the 390 - 450 cm^{-1} region, the depolarized ones in the 300 - 420 cm^{-1} region, and the polarized ones in the 240 - 290 cm^{-1} region can be assigned to the totally symmetric stretching vibration mode, the stretching vibration mode excluding the totally symmetric one, the skeletal bending deformation mode, and the chelate ring deformation mode, respectively.

Raman Spectra of [Co(trien)(bidentate)]- and [Co(tren)(bidentate)]-Type Complexes.

Figure 45 shows the Raman spectra of the two geometrical isomers of $[Co(en)(trien)]^{3+}$, together with that of $[Co(en)(tren)]^{3+}$. It can be seen from Fig. 45 and Table 14 that cis-α- and cis-β-$[Co(en)(trien)]^{3+}$ show different Raman spectral feature in each skeletal vibration region. Further, the Raman spectrum of cis-β-$[Co(en)(trien)]^{3+}$ is similar to that of $[Co(en)(tren)]^{3+}$ rather than that of the cis-α isomer. The significant aspect in structures of cis-

β-[Co(en)(trien)]$^{3+}$ and [Co(en)(tren)]$^{3+}$ is that the coordinated N-N-N portion of the quadridentate ligands (trien and tren) have equally meridional configuration toward the central metal atom. It is not surprising that this meridional configuration greatly influences normal vibration modes in the skeletal vibration region of the Raman spectra of cis-β-[Co(en)(trien)]$^{3+}$ and [Co(en)(tren)]$^{3+}$, since the mer isomers of the bis(terdentate)cobalt(III) complexes have shown the Raman spectral feature quite different from that of the fac isomers. This sort of Raman spectral feature can also be observed for the two geometrical isomers of [Co(ox)(trien)]$^{+}$ and [Co(ox)(tren)]$^{+}$; the Raman spectrum of cis-β-[Co(ox)(trien)]$^{+}$ can not be correlated to that of cis-α isomer, but, that of [Co(ox)(tren)]$^{+}$ (Fig. 46).

As shown in Figs. 45 and 46, the cobalt(III) complexes with the quadridentate ligands, cis-β-[Co(en)(trien)]$^{3+}$, cis-β-[Co(ox)(trien)]$^{+}$, [Co(en)(tren)]$^{3+}$, and [Co(ox)(tren)]$^{+}$, which have equally meridional configuration with respect to the coordinated N-N-N portion in the quadridentate ligands, exhibit multiple polarized bands in the stretching vibration region, which is characteristic for the mer isomers of bis(terdentate)cobalt(III) complexes. These findings suggest that their Raman spectra are mainly regulated by the normal vibrational modes of meridional configuration of the quadridentate ligands. Especially, the polarized Raman bands around 450 cm^{-1} are regarded as characteristic for cis-β isomers of the

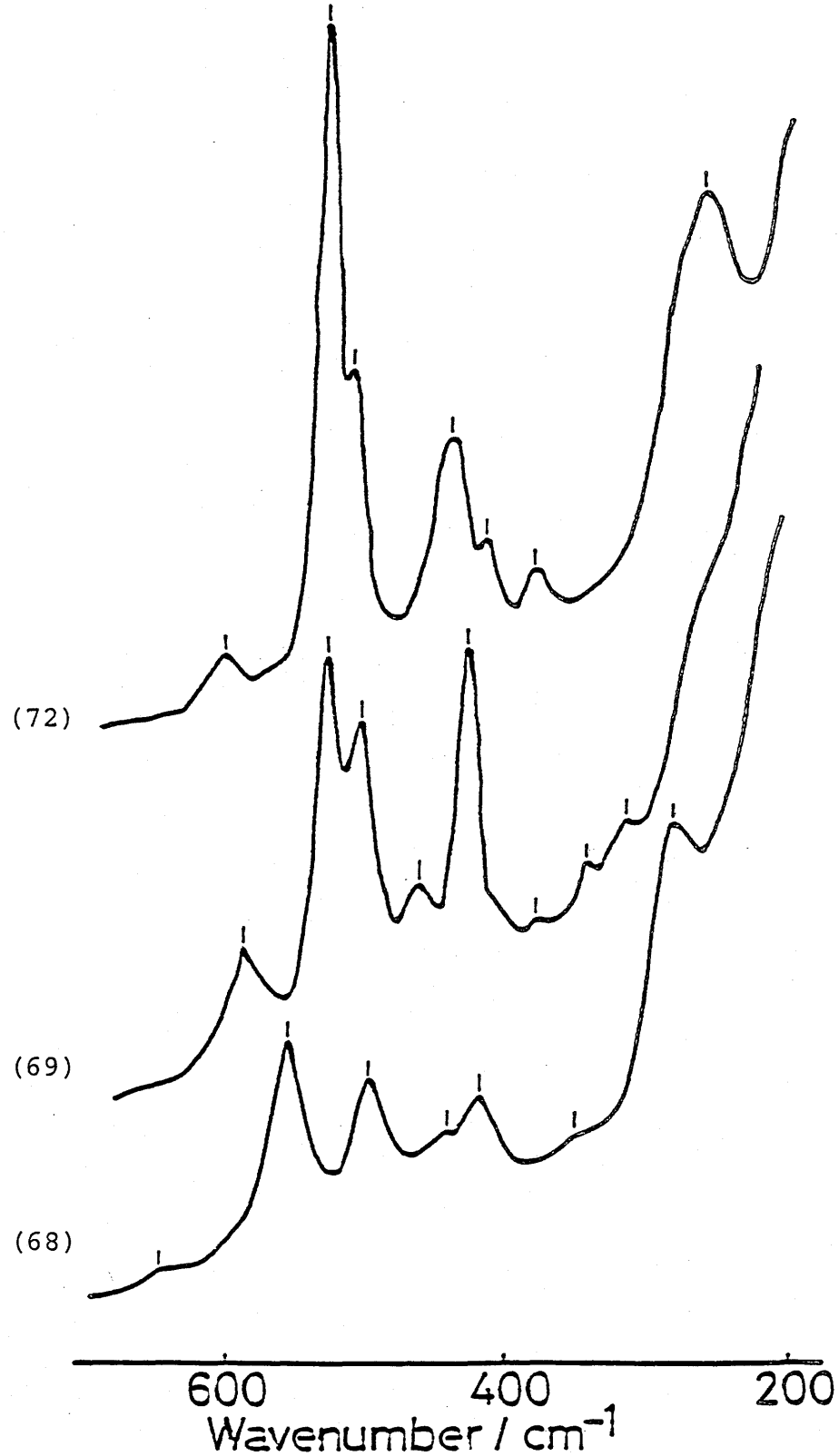

Figure 45. Raman spectra of cis-α- and cis-β-$[Co(en)(trien)]^{3+}$ and $[Co(en)(tren)]^{3+}$. Numbers in parentheses correspond to those in Table 14.

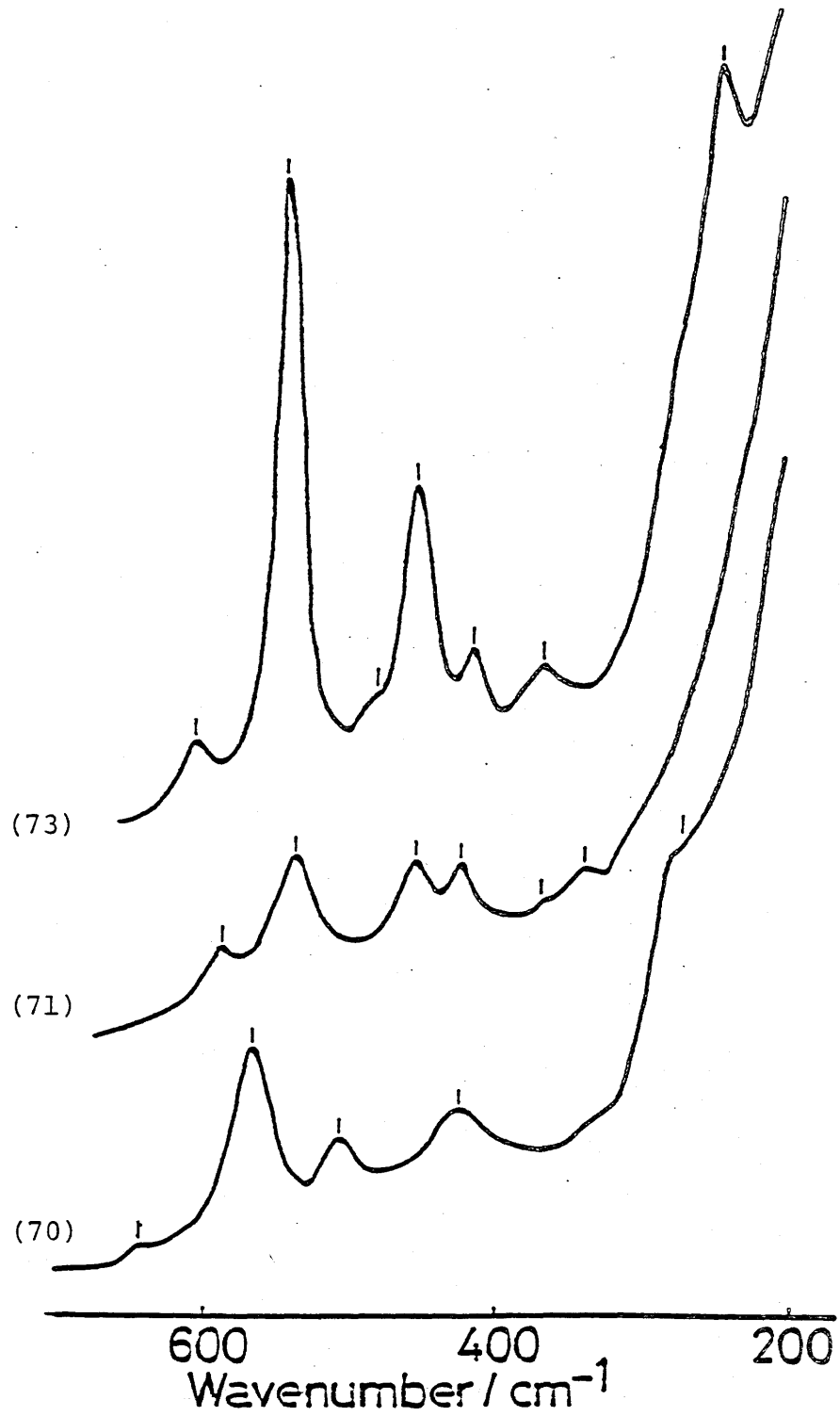

Figure 46. Raman spectra of cis-α- and cis-β-$[Co(ox)(trien)]^+$ and $[Co(ox)(tren)]^+$. Numbers in parentheses correspond to those in Table 14.

[Co(trien)(bidentate)]- and [Co(tren)(bidentate)]-type complexes since the corresponding bands could not be observed in the spectra of the tris(bidentate)cobalt(III) complexes and the fac isomers of the bis(terdentate)cobalt(III) complexes. Further, the Raman bands at ca. 530 and ca. 450 cm^{-1} of these complexes can be correlated with the characteristic Raman bands (ca. 520 and ca. 440 cm^{-1}) for the mer isomers of the bis(terdentate)cobalt(III) complexes.

Hence, in the cobalt(III) complexes with trien and tren ligands, so far as skeletal vibrations are concerned, the Raman spectra of the cis-α isomers can be correlated with those of the tris(bidentate)cobalt(III) complexes, and those of the cis-β isomers and the complexes with the tripodlike quadridentate ligands can be correlated with those of the mer isomers of the bis(terdentate)cobalt(III) complexes, respectively. Accordingly, the Raman spectra can be used for the differenciation of the cis-α and cis-β isomers of the [Co(trien)(bidentate)]-type complexes.

Raman Spectra of [Co(edda)(bidentate)]-Type and $[Co(aeida)(en)]^+$ Complexes.

Figure 47 shows the Raman spectra of cis-α and cis-β isomers of $[Co(edda)(en)]^+$ and $[Co(edda)(tn)]^+$. In view of the Raman spectra of the tris(bidentate)cobalt(III) and bis(terdentate)cobalt(III) complexes, the Raman band at 617 cm^{-1} of the cis-α isomer of $[Co(edda)(en)]^+$ and that at 660

cm^{-1} of the cis-β isomer are closely associated with coordinated oxygen atom. Furthermore, the shift of these bands is most prominent for the Raman spectra of cis-α- and cis-β-$[Co(edda)(en)]^+$ and is useful for the differentiation of the cis-α and cis-β isomers. A similar feature is also observed for the Raman spectra of the cis-α and cis-β isomeric pairs of $[Co(edda)(tn)]^+$ (Fig. 47) and $[Co(edda)(ox)]^-$ (Fig. 48).

The Raman spectra of trans(O)- and cis(O)-$[Co(aeida)(en)]^+$ exhibit unique differences around 400 cm^{-1} from the Raman spectrum of cis-β-$[Co(edda)(en)]^+$ with the different chelate ring structure (Figs. 47 and 49); the trans(O) and cis(O) isomers of $[Co(aeida)(en)]^+$ show polarized bands at 400 and 409 cm^{-1}, respectively, but the cis-β isomer of $[Co(edda)(en)]^+$ shows no polarized band in the corresponding region. These polarized bands around 400 cm^{-1} can be assigned to the skeletal breathing mode on the basis of the Raman spectral characteristics of the mer isomers of the bis(terdentate)cobalt(III) complexes (Tables 11, 12, and 14). The skeletal breathing mode of the cobalt(III) complexes with tripodlike quadridentate ligand, $[Co(en)(tren)]^{3+}$ and $[Co(ox)(tren)]^+$, are also detectable at 442 and 453 cm^{-1} by comparison with the mer isomers of the bis(terdentate)cobalt(III) complexes (Figs. 45 and 46 and Tables 11, 12, and 14).

Role of Bidentate Ligands.

It can be seen by comparison of Figs. 45 and 46 that

cis-α-[Co(en)(trien)]$^{3+}$ and [Co(en)(tren)]$^{3+}$ exhibit Raman spectral characteristics quite similar to cis-α-[Co(ox)(trien)]$^{+}$ and [Co(ox)(tren)]$^{+}$, respectively. Furthermore, the Raman spectral behaviors of the same geometrical isomers of the cobalt(III) complexes with edda ligands in the higher frequency region resemble each other as shown in Figs. 48 and 50. That is, all the cis-α isomers exhibit characteristic polarized Raman bands around 615 cm^{-1}, which shift to around 655 cm^{-1} in the cis-β isomer. These bands can be used for differentiation of the cis-α from the cis-β ones in the cobalt(III) complexes with the edda ligands. Hence, it is evident that the Raman spectra of the [Co(quadridentate)(bidentate)]-type complexes depend mainly on the configuration of the quadridentate ligands and the role of the bidentate ligands is of minor importance. However, closer examination of Fig. 50 discloses the minor role of the bidentate ligands in the 445 - 465 cm^{-1} region; each of the complexes containing NH_3, tn, and en has polarized Raman bands (at 452 cm^{-1} for NH_3, 448 cm^{-1} for tn, and 461 cm^{-1} for en), which does not appear for the spectra of the complexes containing gly, β-ala, and ox. This fact may reflect that the difference of the coordinated atoms (oxygen and nitrogen) in the bidentate ligands influences the Raman bands in this region.

V-B-6. Raman Spectra of the Cobalt(III) Complexes with Sulfur-Containing Ligands.

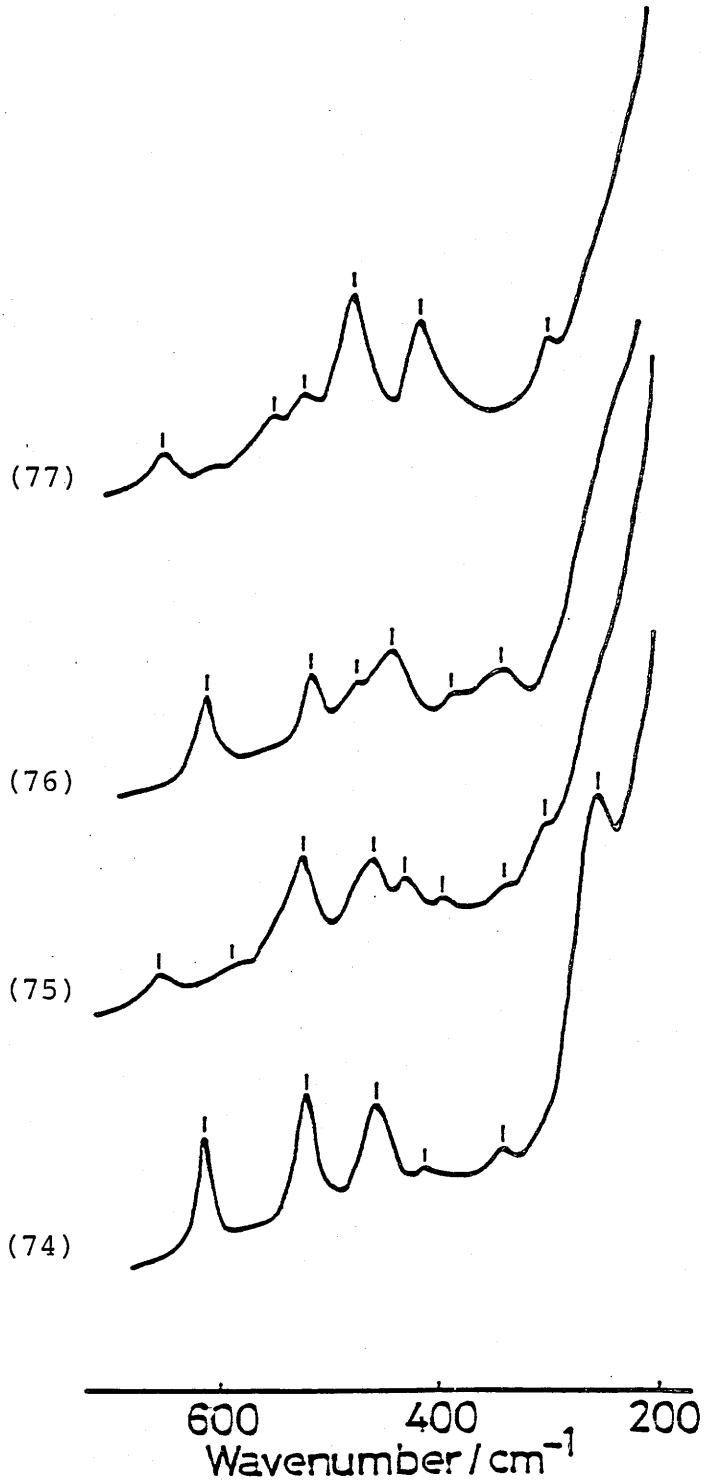

Figure 47. Raman spectra of cis-α and cis-β isomers of $[Co(edda)(en)]^+$ and of $[Co(edda)(tn)]^+$. Numbers in parentheses correspond to those in Table 14.

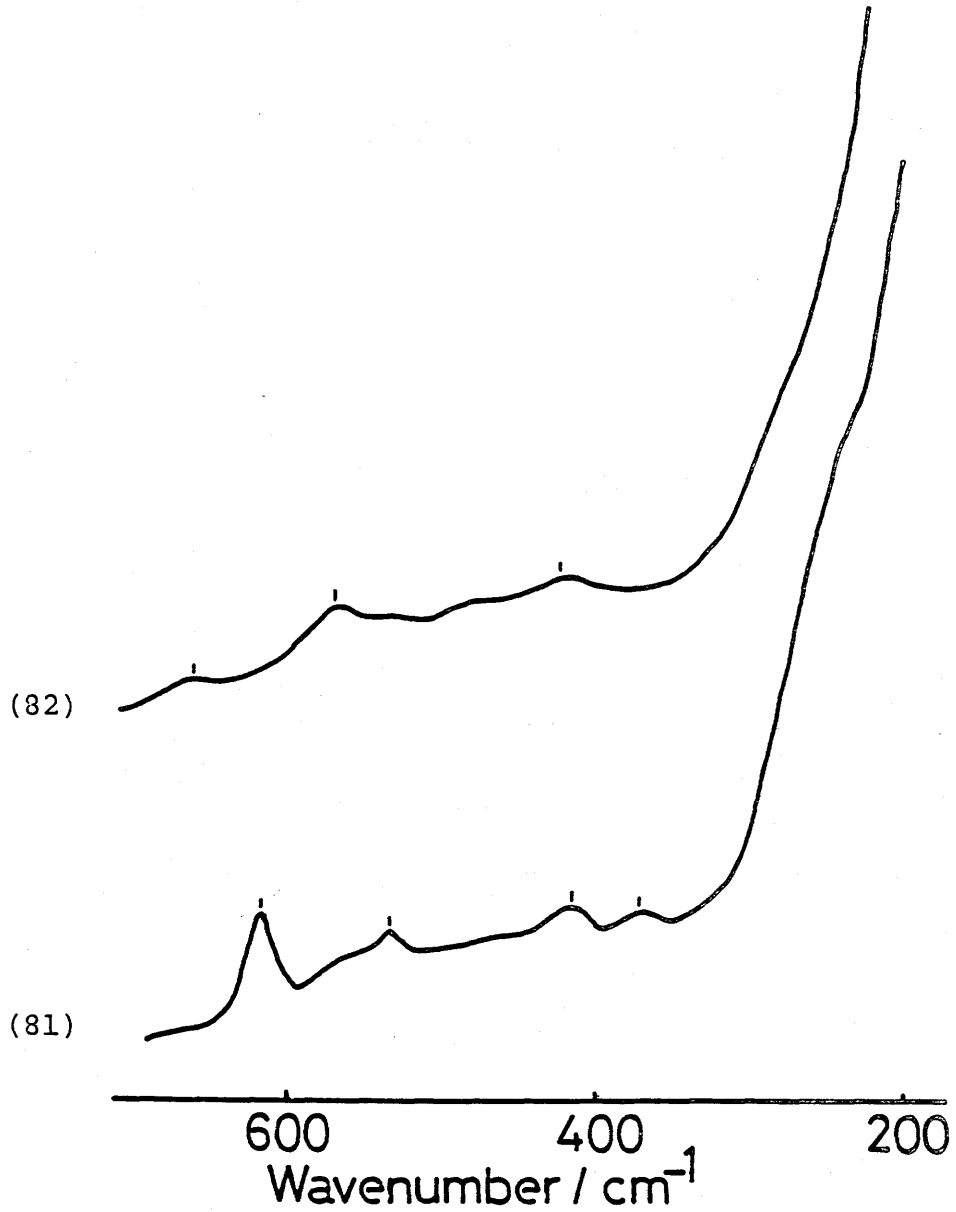

Figure 48. Raman spectra of two geometrical isomers of $[Co(edda)(ox)]^-$. Numbers in parentheses correspond to those in Table 14.

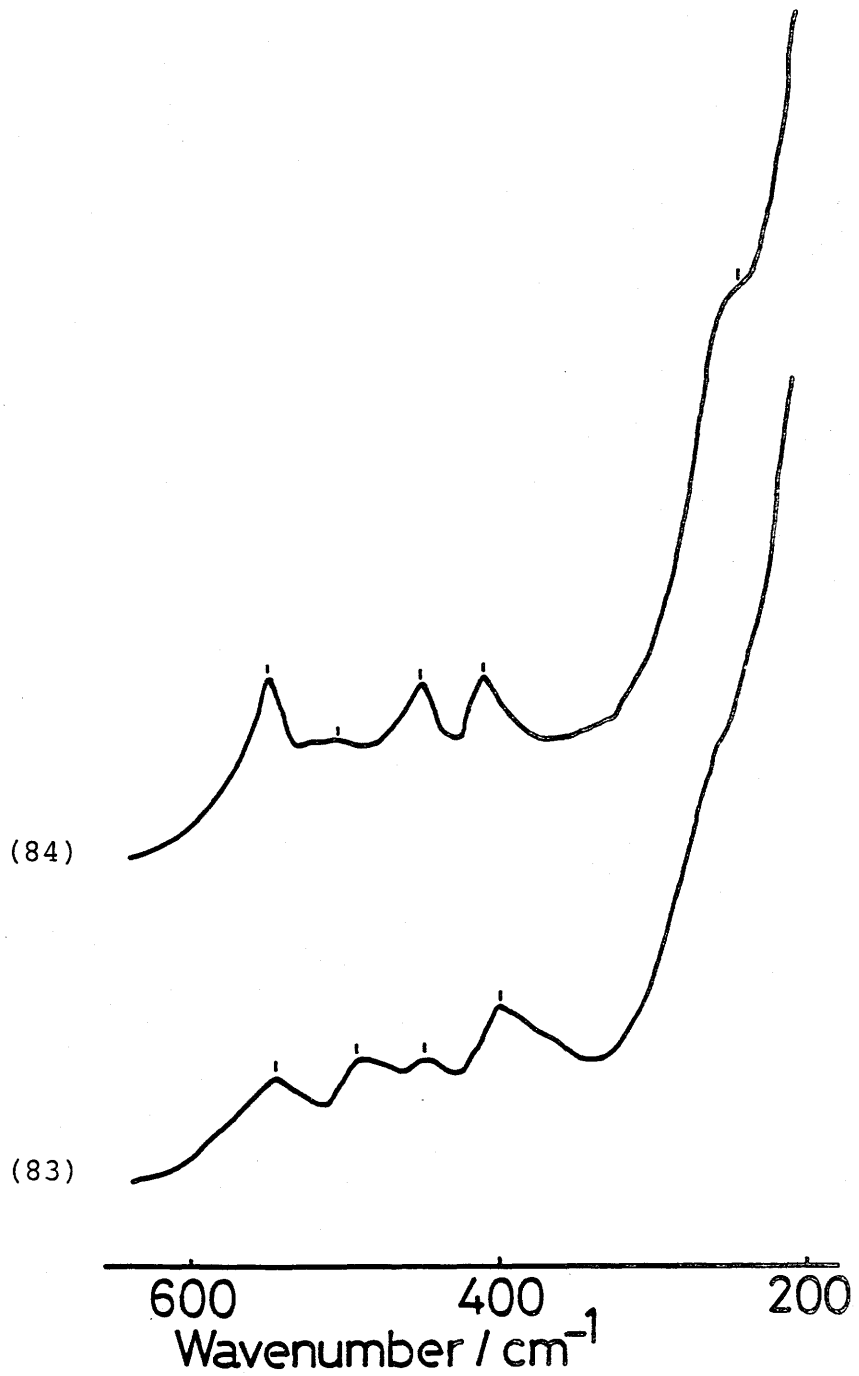

Figure 49. Raman spectra of two geometrical isomers of $[Co(aeida)(en)]^+$. Numbers in parentheses correspond to those in Table 14.

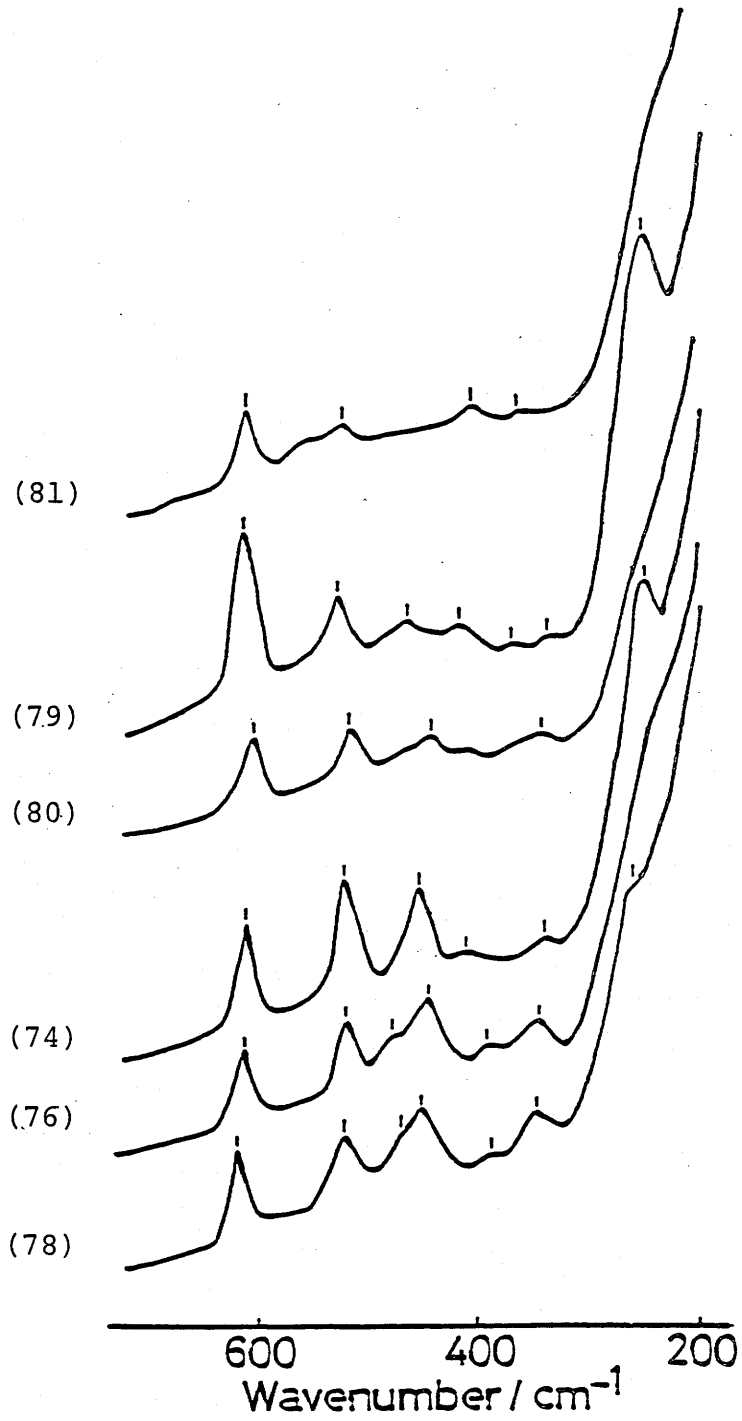

Figure 50. Raman spectra of cis-α isomers of $[Co(edda)(ox)]^-$, $[Co(edda)(gly)]$, $[Co(edda)(\beta\text{-ala})]$, $[Co(edda)(en)]^+$, $[Co(edda)(tn)]^+$, and $[Co(edda)(NH_3)_2]^+$. Numbers in parentheses correspond to those in Table 14.

Figure 51 shows the Raman spectra of the bis(1,2-ethanediamine)cobalt(III) complexes containing a thiolato ligand, 2-aminoethanethiolato or 2-mercaptoacetato, ($[Co(aet)(en)_2]^{2+}$ or $[Co(SCH_2COO)(en)_2]^{+}$) together with that of $[Co(en)_3]^{3+}$. Their Raman frequencies, intensities, and depolarization ratios (Table 15) indicate that $[Co(aet)(en)_2]^{2+}$ and $[Co(SCH_2COO)(en)_2]^{+}$ have the same spectral characteristics as $[Co(en)_3]^{3+}$; the Raman bands at 510, 450, and 384 cm^{-1} of $[Co(aet)(en)_2]^{2+}$ and those at 514, 465, and 381 cm^{-1} of $[Co(SCH_2COO)(en)_2]^{+}$ correspond to those at 525, 440, and 378 cm^{-1} of $[Co(en)_3]^{3+}$, respectively. Hence, the Raman spectra of the cobalt(III) complexes, in which either of the N and O donor atom is substituted by sulfur, can also be treated as in the case of the tris(bidentate)cobalt(III) complexes with the N and/or O donor atoms. The Raman bands of $[Co(aet)(en)_2]^{2+}$ and $[Co(SCH_2COO)(en)_2]^{+}$ can be assigned to the totally symmetric stretching vibration mode, the stretching vibration mode excluding the totally symmetric one, the skeletal bending deformation mode, and the chelate ring deformation mode from the higher frequency region. However, the Raman bands in the totally symmetric stretching vibration mode region of $[Co(aet)(en)_2]^{2+}$ and $[Co(SCH_2COO)(en)_2]^{+}$ appear at the lower frequency compared with that of $[Co(en)_3]^{3+}$. This fact suggests the existence of the mass effect owing to distinction between nitrogen and sulfur donor atoms and/or the difference in the central metal-donor atom bond strength. This is supported by the Raman spectrum of

$[Co(aet)_3]$; this complex exhibits three main lines (ca. 420, 360, and 350 cm^{-1}) and it is thought that the Raman bands at 420 and 360 cm^{-1} correspond to the totally symmetric stretching vibration mode.[66]

The frequencies, intensities, and depolarization ratios of the Raman bands in the totally symmetric stretching vibration mode region of $[Co(aet)(en)_2]^{2+}$, $[Co(aese)(en)_2]^{2+}$, $[Co(aesi)(en)_2]^{2+}$, and $[Co(mea)(en)_2]^{3+}$ are similar to one another (Fig. 52). Furthermore, the number of Raman bands of $[Co(aet)(en)_2]^{2+}$ is fewer than those of the other complexes. This fact indicates that $[Co(aet)(en)_2]^{2+}$ have a higher symmetry for skeletal vibration because of no substituent groups on the sulfur donor atom. On the other hand, the distinct difference between $[Co(aese)(en)_2]^{2+}$ and $[Co(aesi)(en)_2]^{2+}$ is observed at 400 - 500 cm^{-1} and that between $[Co(aesi)(en)_2]^{2+}$ and $[Co(mea)(en)_2]^{3+}$ at ca. 650 cm^{-1}. The Raman band at 653 cm^{-1} of $[Co(mea)(en)_2]^{3+}$ may be correlated to the nature of the sulfur donor atom: the thiolato, sulfenato, and sulfinato ligands have a formal negative charge, while the thioether one is electrically neutral and the structure of the thioether complex is devoid of a significant structural trans effect.[39] Moreover, since the band at 653 cm^{-1} exhibit little spectral shift upon deuteration, this band may originate from ν(Co-SMe). The shift to the higher frequency of the Raman band due to ν(Co-SMe) may be concerned with the increase of the value of force constant

Table 15. Raman Spectral Data of Cobalt(III) Complexes With Sulfur Containing Ligands.

No.	Complex	Raman frequency / cm^{-1} a)			
85	$[Co(aet)(en)_2]^{2+}$	510 m(p)	450 vw(-)	384 w(dp) 305 vw(-)	
86	$[Co(SCH_2COO)(en)_2]^{+}$	514 w(p)	465 vw(-)	381 w(-) 316 vw(-)	239 vw(-)
87	$[Co(aese)(en)_2]^{2+}$	513 m(p)	414 vw(dp)	346 vw(dp)	229 vw(-)
88	$[Co(aesi)(en)_2]^{2+}$	522 s(p)	441 vw(dp) 419 w(dp)	387 vw(-)	246 w(-) 237 w(-)
89	$[Co(mea)(en)_2]^{2+}$	653 w(p) 586 vw(-) 520 s(p)	459 m(dp) 433 m(dp)	394 w(dp) 295 w(-)	245 w(-)
	Assignment[a)]	ν_{ts}(Co-L)	ν(Co-L)	δ_{sbd}(L-Co-L)	δ_{crd}(Co$\langle^{L}_{L}$)

a) The following abbreviations are used: s, strong; m, medium; w, weak; vw, very weak; sh, shoulder; p, polarized; dp, depolarized; ν_{ts}, totally symmetric stretching vibration mode; ν, stretching vibration mode excluding the totally symmetric stretching character; δ_{sbd}, skeletal bending deformation mode; δ_{crd}, chelate ring deformation mode. The Raman band intensities (s, m, w, vw, and sh) are classified by a comparison of all the Raman bands among all the complexes.

Figure 51. Raman spectra of $[Co(en)_3]^{3+}$, $[Co(aet)(en)_2]^{2+}$, and $[Co(SCH_2COO)(en)_2]^{+}$. Numbers in parentheses correspond to those in Tables 9 and 15.

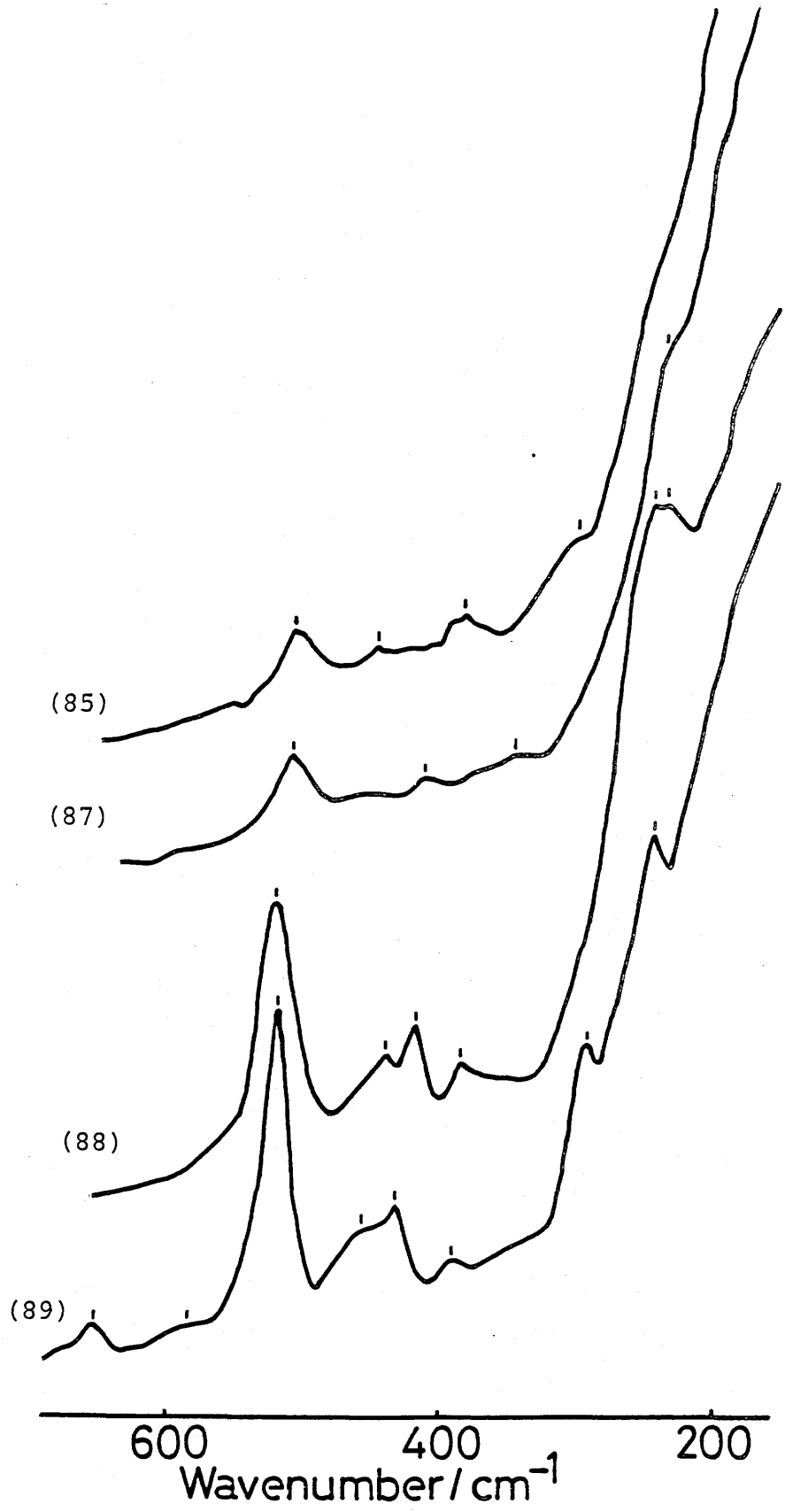

Figure 52. Raman spectra of $[Co(aet)(en)_2]^{2+}$ $[Co(aese)(en)_2]^{2+}$, $[Co(aesi)(en)_2]^{2+}$, and $[Co(mea)(en)_2]^{3+}$. Numbers in parentheses correspond to those in Table 15.

by an electronic donative methyl group.

V-B-7. Raman Spectra of the Cobalt(III) Complexes with Branched Terdentate Ligands.

Figures 53 and 54 show the Raman spectra of [Co(DL-asp)(dien)]$^{+}$ and [Co(DL-asp)$_2$]$^{-}$, respectively. Most serious difference between the cobalt(III) complexes with the branched terdentate ligands and those with the linear terdentate ligands (V-2-C) in their Raman spectra is that the complexes with the branched terdentate ligands have no Raman bands due to the skeletal breathing vibration mode (Tables 11 and 16). Furthermore, it can be seen from Fig. 55 that the Raman spectral characteristic of [Co(DL-asp)$_2$]$^{-}$ is distinct from that of [Co(ida)$_2$]$^{-}$ having the same donor atoms even in the stretching vibration region. It seems that the cobalt(III) complexes with the branched terdentate ligands, when considered with these results, have a character for the skeletal vibration close to the cobalt(III) complexes with the bidentate ligands rather than those with the linear terdentate ligands. Accordingly, the cobalt(III) complexes with the branched terdentate ligands are regarded as quite different species from those with the linear terdentate ligands for the skeletal vibration. However, on the basis of frequencies, intensities, and depolarization ratios, the Raman bands at 509 - 627 cm^{-1} of [Co(DL-asp)(dien)]$^{+}$ and those at 525 - 637 cm^{-1} of [Co(DL-asp)$_2$]$^{-}$ can be assigned to the totally symmetric stretching vibration mode.

Three geometrical isomers of $[Co(DL\text{-}asp)(dien)]^+$ and of $[Co(DL\text{-}asp)_2]^-$ exhibit the Raman spectral characteristics similar to each other. The difference of chelate ring arrangement have no marked influence on the Raman spectra of $[Co(DL\text{-}asp)(dien)]^+$ and $[Co(DL\text{-}asp)_2]^-$. Especially, three isomers of $[Co(DL\text{-}asp)_2]^-$ exhibit three lines, which have similar frequencies and intensities each other, at higher frequency side (520 - 640 cm^{-1}). Moreover, these bands reveal similar spectral shift upon deuteration; the Raman bands at 625 - 637 cm^{-1} and 525 - 553 cm^{-1} are shifted low frequency side by ca. 30 cm^{-1}, while the bands at 562 - 575 cm^{-1} by ca. 10 cm^{-1}. Accordingly, the Raman bands at 625 - 637 and 525 - 553 cm^{-1} may be mainly correlated with the Co-N totally symmetric stretching vibration mode.

The cobalt(III) complexes with the branched terdentate ligands containing sulfur donor atoms ($[Co(L\text{-}smc)_2]^+$ and $[Co(L\text{-}met)_2]^+$) also do not exhibit the Raman bands due to the skeletal breathing vibration mode (Figs. 56 and 57). The skeletal breathing vibration mode is considered a characteristic one for the Raman spectra of cobalt(III) complexes with the linear terdentate ligands.

In view of frequencies, intensities, and depolarization ratios, the Raman bands at 434 - 655 cm^{-1} of $[Co(L\text{-}smc)_2]^+$ and those at 525 - 663 cm^{-1} of $[Co(L\text{-}met)_2]^+$ can be assigned to the totally symmetric stretching vibration mode. Furthermore, the Raman bands at ca. 615 and 510 cm^{-1} of $[Co(L\text{-}smc)_2]^+$ and at ca. 600 and 530 cm^{-1} of $[Co(L\text{-}met)_2]^+$

exhibit a large spectral shift (about 25 cm^{-1}) upon deuteration and the Raman bands at ca. 650 cm^{-1} of $[Co(L\text{-}smc)_2]^+$ and $[Co(L\text{-}met)_2]^+$ exhibit a little shift (about 5 cm^{-1}). Accordingly, the bands at 598 - 618 cm^{-1} and at 505 - 537 cm^{-1} may be mainly correlated with $\nu_{ts}(Co\langle^{N}_{O}\rangle)$ and $\nu_{ts}(Co\langle^{N}_{S}\rangle)$, respectively, compared from the Raman spectra of tris(bidentate)cobalt(III) (V-B-1) and the cobalt(III) complexes with sulfur-containing ligands (V-B-6). The bands at ca. 650 cm^{-1} may be correlated with ν(Co-SMe) in comparison with the Raman spectrum of $[Co(mea)(en)_2]^{3+}$ and the origin of these bands is different from that of the Raman bands at 630 cm^{-1} of $[Co(DL\text{-}asp)_2]^-$.

The Raman spectra among the geometrical isomers of $[Co(L\text{-}smc)_2]^+$ and of $[Co(L\text{-}met)_2]^+$ do not exhibit a marked difference, like the geometrical isomers of $[Co(DL\text{-}asp)_2]^-$. On the other hand, some differences between the Raman spectra of $[Co(L\text{-}smc)_2]^+$ and $[Co(L\text{-}met)_2]^+$ are observed, as is shown in Fig. 58. That is, the Raman bands of $[Co(L\text{-}smc)_2]^+$ appear at ca. 615 and 510 cm^{-1}, but those of $[Co(L\text{-}met)_2]^+$ appear at ca. 600 and 530 cm^{-1}. Moreover, $[Co(L\text{-}smc)_2]^+$ has the Raman bands at ca. 440 cm^{-1}, but $[Co(L\text{-}met)_2]^+$ has those at ca. 490 cm^{-1}. Thus, absorption spectra do not indicate a regular difference between the corresponding geometrical isomers of $[Co(L\text{-}smc)_2]^+$ and $[Co(L\text{-}met)_2]^+$,[42,43] but the Raman spectra can be used to distinguish clearly between $[Co(L\text{-}smc)_2]^+$ and $[Co(L\text{-}met)_2]^+$.

Table 16. Raman Spectral Data of Cobalt(III) Complexes With Branched Terdentate Ligands.

No.	Complex	Raman frequency / cm^{-1} a)			
90	sym-cis-[Co(DL-asp)(dien)]$^+$	550 m(p) 509 w(p)	447 vw(dp)	387 vw(-)	259 vw(-)
91	unsym^1-cis-[Co(DL-asp)(dien)]$^+$	622 vw(-) 551 m(p) 510 vw(-)	462 vw(-) 445 vw(-)	389 w(-)	
92	unsym^2-cis-[Co(DL-asp)(dien)]$^+$	627 vw(-) 555 m(p)	459 vw(dp) 404 vw(dp)	313 vw(-)	
93	trans(N)-[Co(DL-asp)$_2$]$^-$	625 vw(-) 562 w(p) 525 m(p)			
94	cis(N)trans(O_5)-[Co(DL-asp)$_2$]$^-$	637 w(p) 575 sh(p) 543 m(p)			
95	cis(N)trans(O_6)-[Co(DL-asp)$_2$]$^-$	628 vw(-) 572 w(p) 553 m(p)		360 vw(-)	
96	trans(N)-[Co(L-smc)$_2$]$^+$	651 w(p) 613 m(p) 505 m(p) 442 w(p)	418 vw(-)	309 w(dp)	
97	trans(O)-[Co(L-smc)$_2$]$^+$	655 w(p) 618 m(p) 511 m(p) 434 w(p)		382 vw(-) 354 w(dp)	241 vw(-)

98	trans(S)-$[Co(L\text{-}smc)_2]^+$	655 vw(-) 618 w(p) 525 m(p) 434 vw(-)		362 vw(-) 295 m(dp)	
99	trans(N)-$[Co(L\text{-}met)_2]^+$	644 vw(-) 601 m(p) 525 w(p)	491 vw(dp) 418 vw(dp)	354 vw(-) 309 vw(dp)	281 vw(-)
100	trans(O)-$[Co(L\text{-}met)_2]^+$	642 vw(-) 602 w(p) 531 m(p)	489 w(dp) 474 w(dp)	418 vw(-) 395 vw(-) 346 vw(-)	287 w(-)
101	trans(S)-$[Co(L\text{-}met)_2]^+$	663 vw(-) 598 w(-) 537 w(-)	495 vw(-) 476 vw(-)	314 vw(-)	282 vw(-)

Assignment[a]	ν_{ts}(Co-L)	ν(Co-L)	δ_{sbd}(L-Co-L)	$\delta_{crd}(Co\langle^{L}_{L})$

a) The following abbreviations are used: s, strong; m, medium; w, weak; vw, very weak; sh, shoulder; p, polarized; dp, depolarized; ν_{ts}, totally symmetric stretching vibration mode; ν, stretching vibration mode excluding the totally symmetric stretching character; δ_{sbd}, skeletal bending deformation mode; δ_{crd}, chelate ring deformation mode. The Raman band intensities (s, m, w, vw, and sh) are classified by a comparison of all the Raman bands among all the complexes.

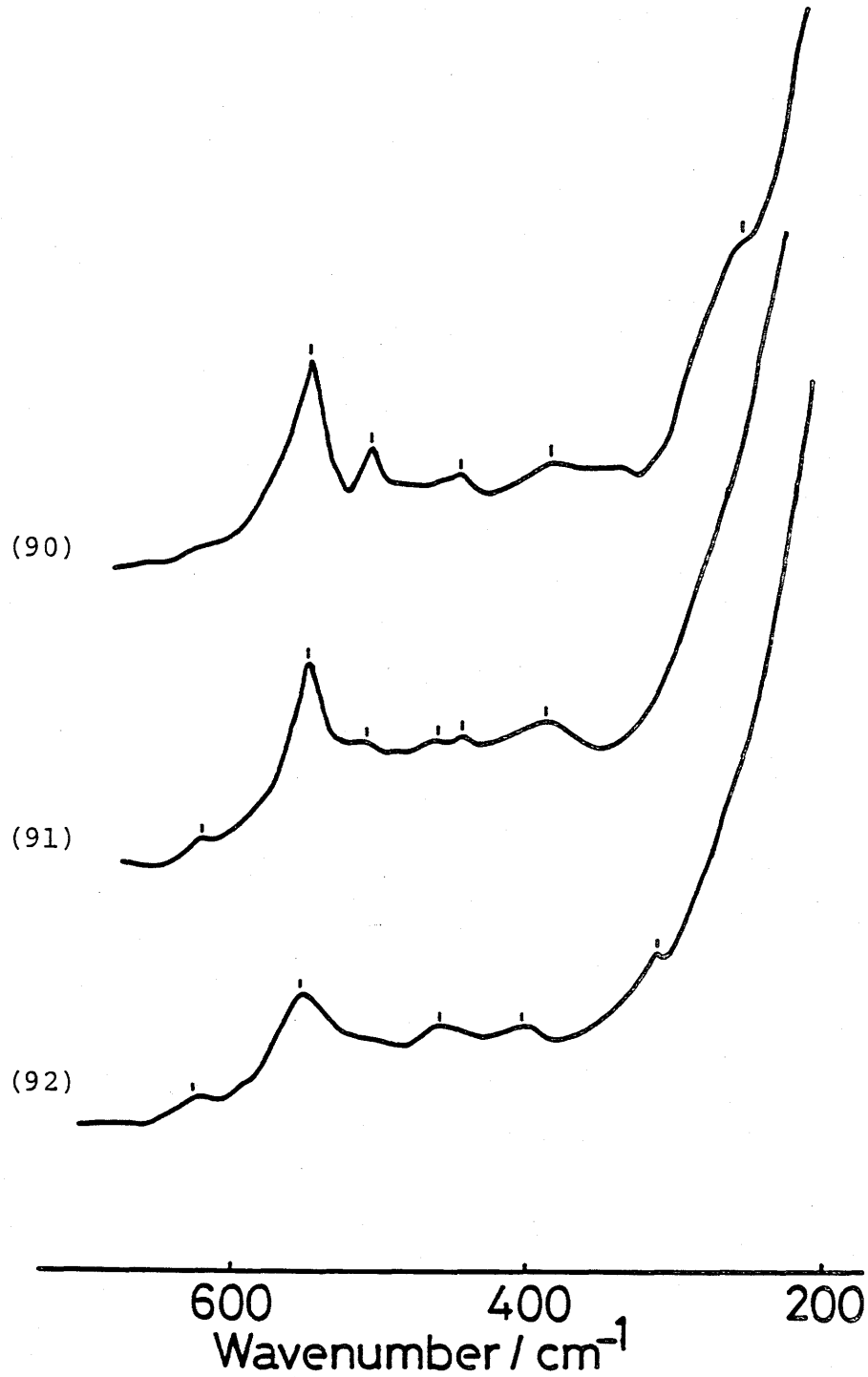

Figure 53. Raman spectra of three geometrical isomers of $[Co(DL\text{-}asp)(dien)]^+$. Numbers in parentheses correspond to those in Table 16.

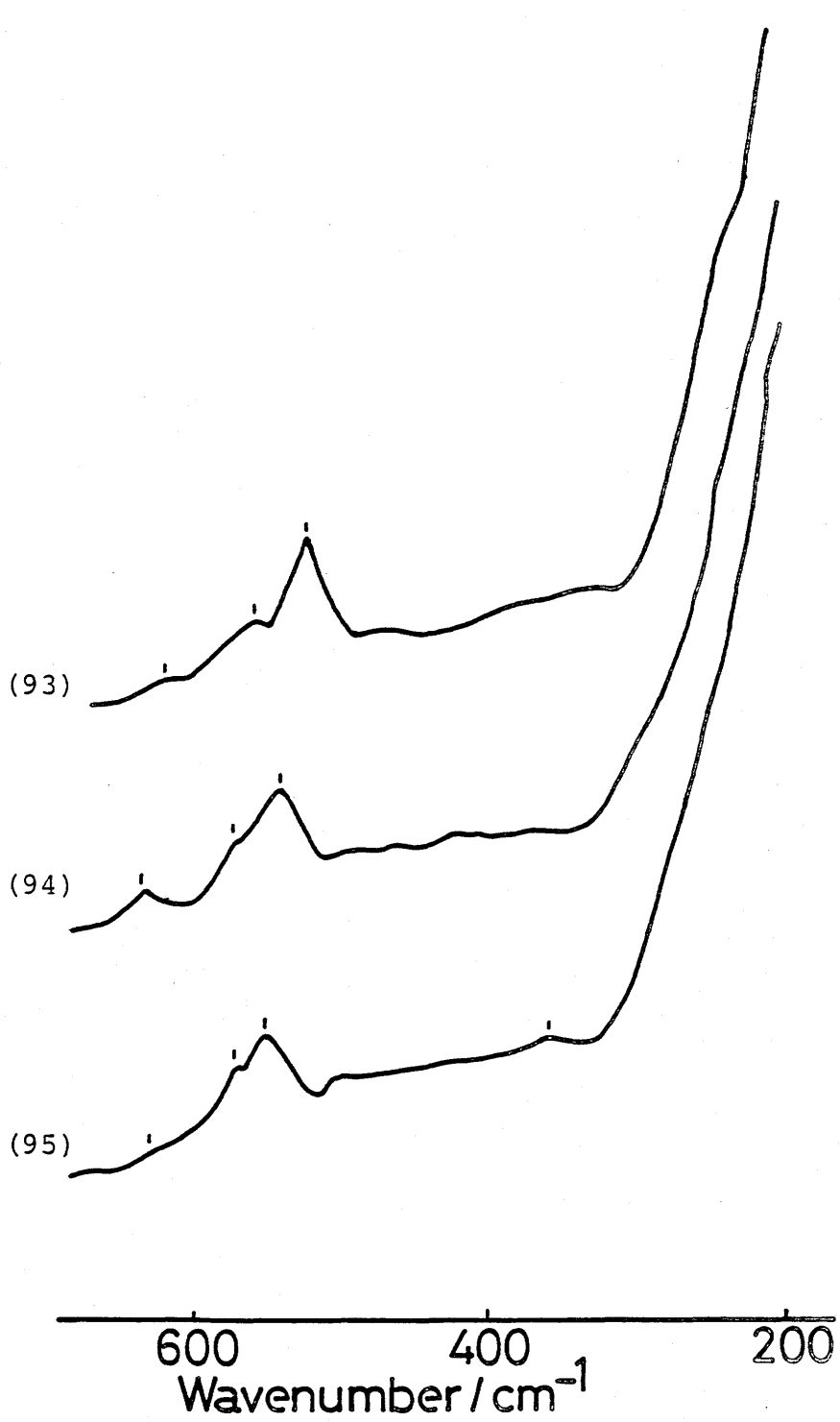

Figure 54. Raman spectra of three geometrical isomers of $[Co(DL\text{-}asp)_2]^-$. Numbers in parentheses correspond to those in Table 16.

Figure 55. Raman spectra of sym-cis-[Co(DL-asp)(dien)]$^{+}$, sym-fac-[Co(ida)(dien)]$^{+}$, trans(N)-[Co(DL-asp)$_2$]$^{-}$, and sym-fac-[Co(ida)$_2$]$^{-}$. Numbers in parentheses correspond to those in Tables 11 and 16.

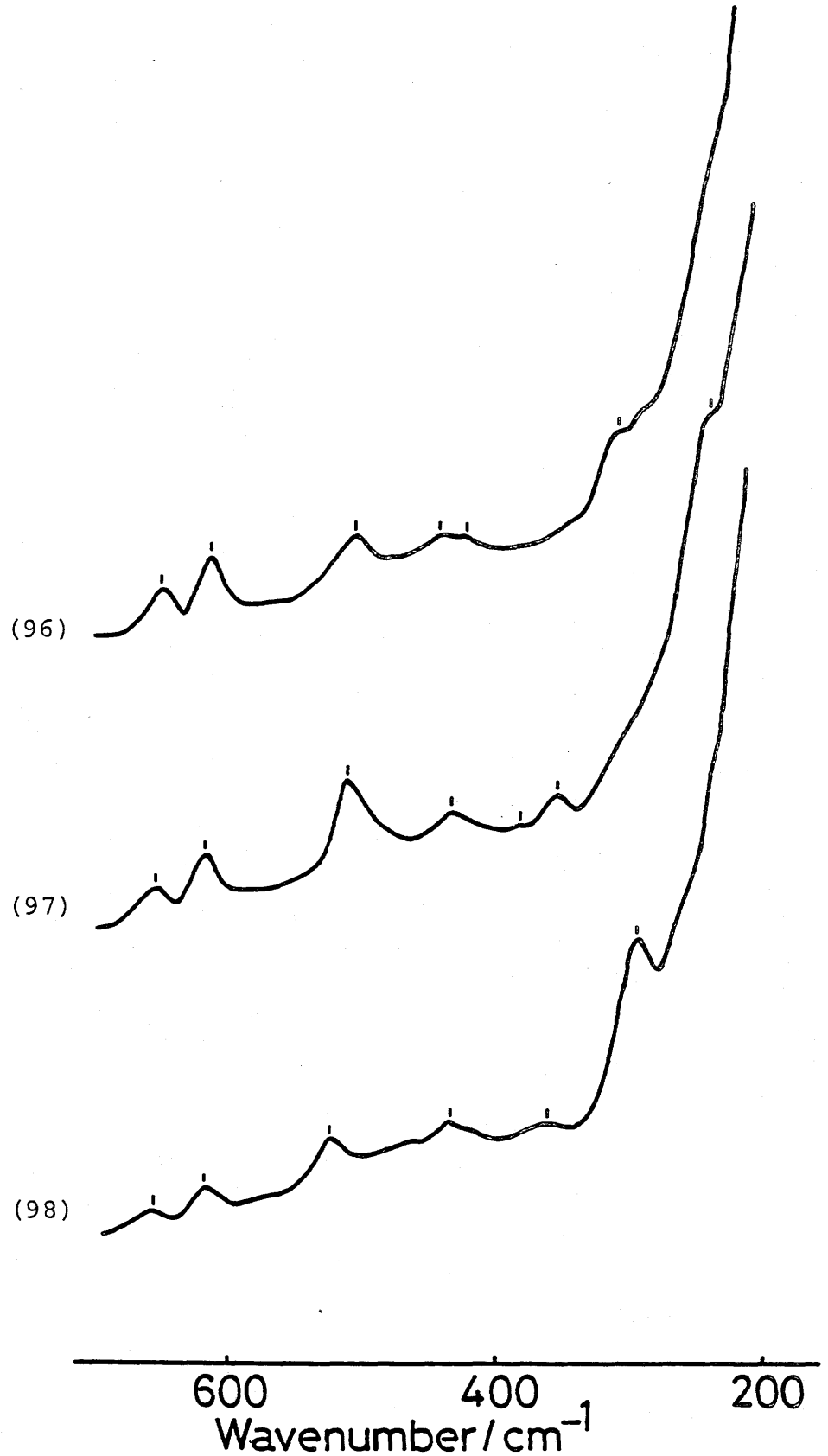

Figure 56. Raman spectra of three geometrical isomers of $[Co(L\text{-}smc)_2]^+$. Numbers in parentheses correspond to those in Table 16.

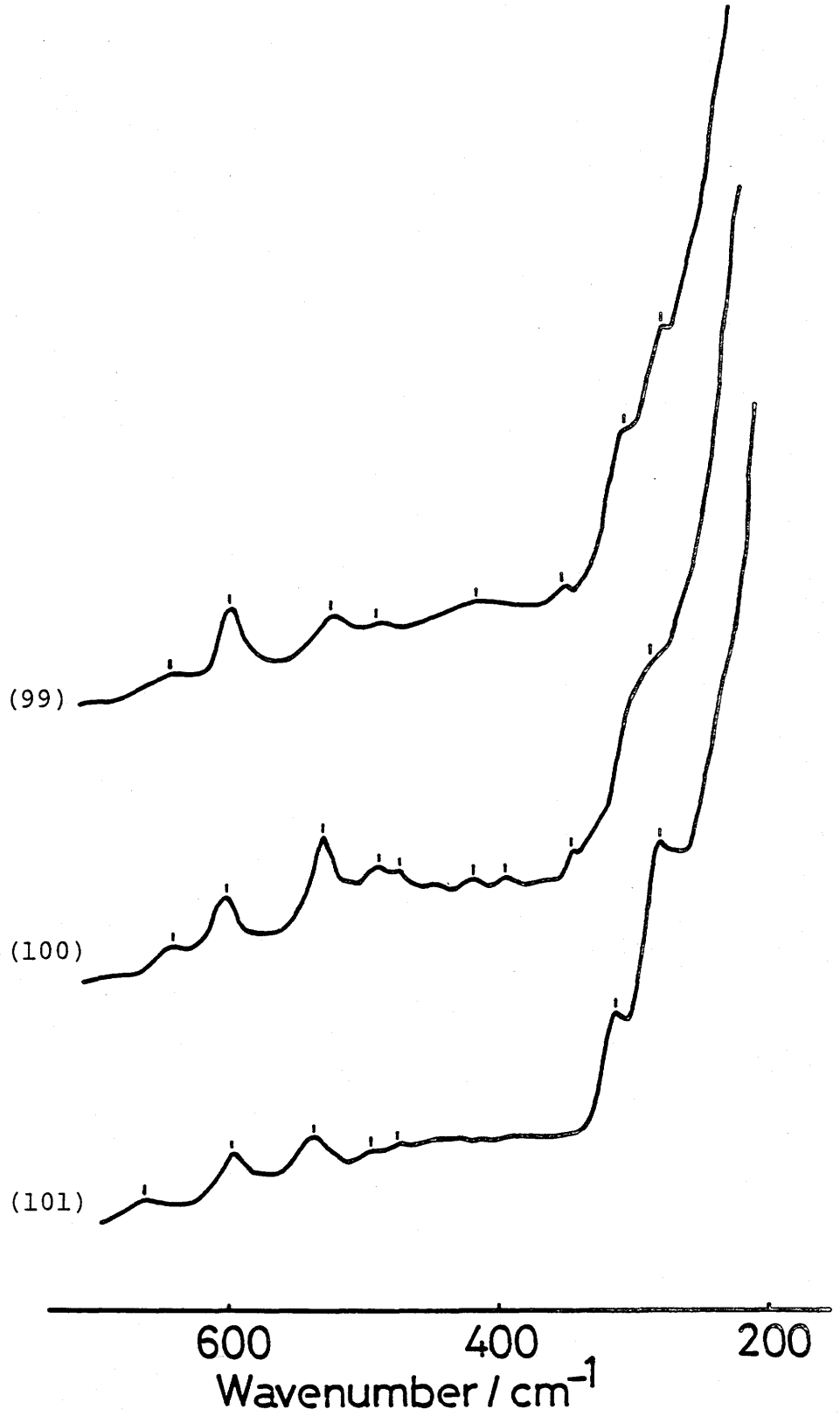

Figure 57. Raman spectra of three geometrical isomers of $[Co(L\text{-met})_2]^+$. Numbers in parentheses correspond to those in Table 16.

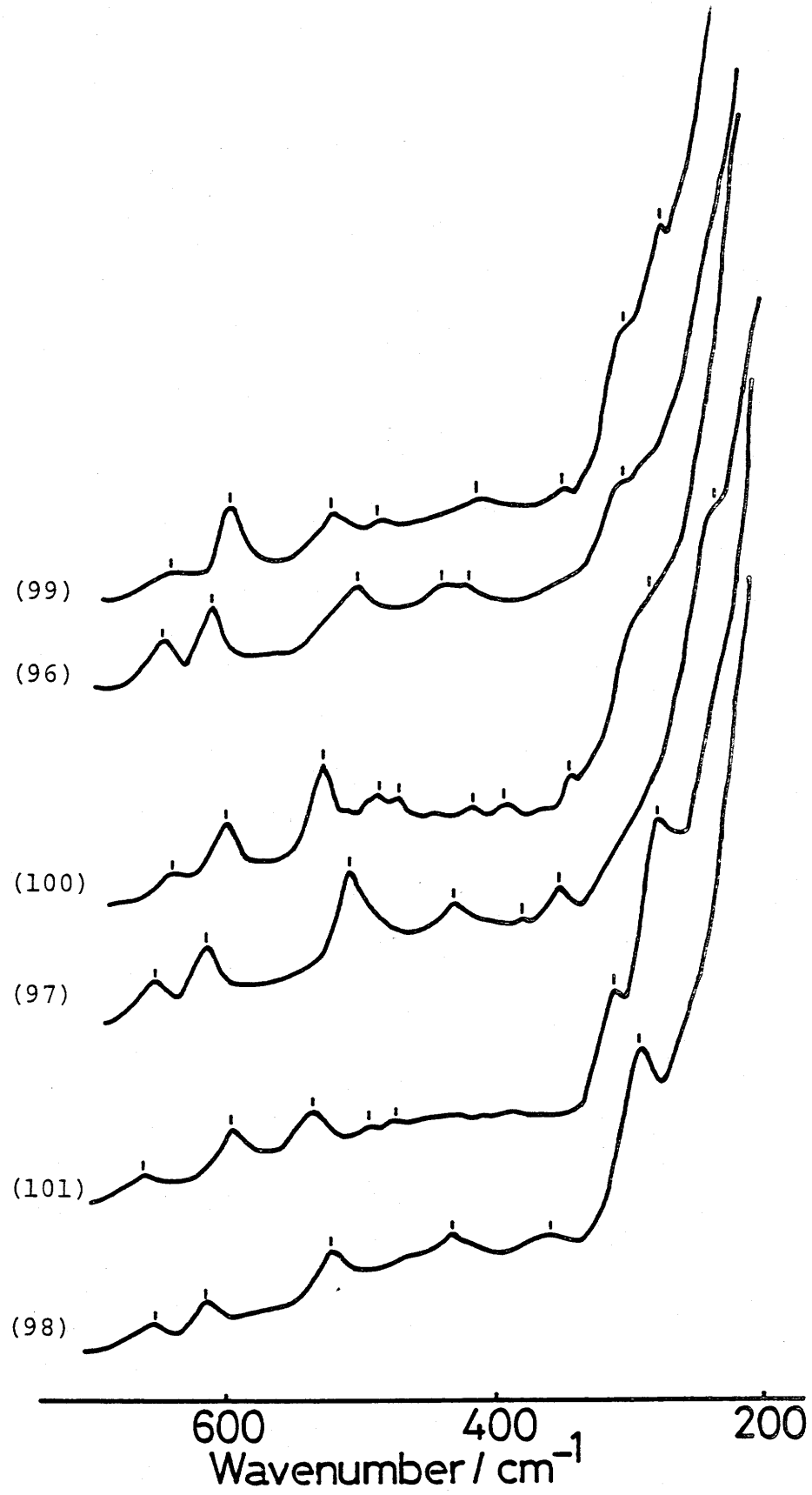

Figure 58. Raman spectra of trans(N), trans(O), and trans(S) isomers of $[Co(L\text{-}smc)_2]^+$ and $[Co(L\text{-}met)_2]^+$. Numbers in parentheses correspond to those in Table 16.

Chapter VI. Concluding Remarks

The object of this work is to deduce a general rule on the relation between the coordination stereochemistry and the Raman spectral characteristics. For this purpose, the cobalt(III) complexes, which have various structures, were prepared by the literature procedures, by the modified methods of the literatures, and in this work for the first time, and systematic investigations were carried out by comparison of the Raman spectra of these complexes. The general rule thus obtained can be summarized as shown below.

(1) The octahedral tris(bidentate)cobalt(III) complexes with five-membered chelate rings show characteristic Raman bands in the skeletal vibration region and these Raman spectra can be mainly treated in terms of the effective symmetry of the complexes. Their Raman bands can be classified into four vibration modes; totally symmetric stretching vibration mode (520 - 610 cm^{-1}), stretching vibration mode excluding the totally symmetric one (i.e., non-totally symmetric one) (400 - 520 cm^{-1}), skeletal bending deformation mode (300 - 400 cm^{-1}), and chelate ring deformation mode (200 - 300 cm^{-1}). The Raman bands of the tris(bidentate)cobalt(III) complexes containing six-membered chelate rings can also be classified into four categories. However, there is a significant distinction between the Raman spectral characteristics of the cobalt(III) complexes containing the six-membered chelate rings and those with the five-membered chelate rings; on

going from the latter to the former, the number of the Raman bands is increased, and the bands are shifted to lower frequencies. This Raman spectral evidence demonstrates that the six-membered chelate rings are more flexible than the five-membered chelate rings.

(2) Raman spectral characteristics of the geometrical isomers of the tris(bidentate)cobalt(III) complexes with the five-membered chelate rings are noticed in the stretching vibration mode excluding the totally symmetric one, while those of the complexes with the six-membered chelate rings appear in the totally symmetric stretching vibration mode. For example, the depolarized bands caused by the stretching vibration can be used for the differentiation of the C_1-cis and C_2-cis isomers of $[Co(gly)_2(en)]^+$ and $[Co(gly)_2(ox)]^-$. The C_1-cis(O) and C_2-cis(O) isomers of $[Co(\beta\text{-ala})_2(tn)]^+$ can be differentiated on the basis of a comparison of the Raman bands in the totally symmetric stretching vibration mode.

(3) Raman bands of the cobalt(III) complexes with the linear terdentate ligands can be classified into five vibration modes; totally symmetric stretching vibration mode (510 - 650 cm^{-1}), stretching vibration mode excluding the totally symmetric one (i.e., non-totally symmetric one) (430 - 540 cm^{-1}), skeletal breathing vibration mode (370 - 490 cm^{-1}), skeletal bending deformation mode (290 - 420 cm^{-1}), and chelate ring deformation mode (220 - 270 cm^{-1}). Especially, the skeletal breathing vibration

is regarded as characteristic of the mono and bis(terdentate)cobalt(III) complexes.

(4) An important Raman spectral characteristic for the geometrical isomers of the cobalt(III) complexes with the linear terdentate ligands lies in the fact that the mer isomer of each complex gives Raman spectra clearly different from those of the fac isomers in the stretching vibration region. This Raman spectral characteristic can be used for the differentiation of the fac and mer isomers. This feature can be ascribed to the difference of the strain energy in the skeletal vibrational motion between the ligand of the meridional arrangement and that of the facial one. Further, the differences for chelate ring arrangement between the Raman spectra of sym-fac and unsym-fac isomers are observed in the skeletal bending deformation mode. On the other hand, the Raman spectra of the cobalt(III) complexes having the same coordinated atoms are not so much influenced by the variety of the ligands. Hence, it can be considered that, so far as the bis(terdentate)cobalt(III) complexes having the same numbers of the coordinated nitrogen and oxygen donor atoms are concerned, the Raman spectral characteristics depend mainly on the arrangement of the chelate ring around the central metal atom.

(5) Raman bands of the cobalt(III) complexes with the terdentate ligands containing an N-methyl group can also be classified into five vibration modes, like those of the cobalt(III) complexes with the terdentate ligands containing no N-methyl group. One of the most significant

characteristics in the Raman spectra of the cobalt(III) complexes containing an N-methyl group is that the strongest Raman bands attributable to the totally symmetric stretching vibration appear at a lower frequency region compared with the Raman spectra of the corresponding cobalt(III) complexes containing no N-methyl group. This fact suggests the existence of a mass effect in the totally symmetric stretching vibration mode as a result of the replacement of a hydrogen atom on the imino nitrogen by a methyl group and/or the difference in the central metal-donor atom bond strength. However, such a distinct relation can not be found on other vibrational modes. Hence, the replacement of hydrogen atom on the imino nitrogen by a methyl group causes a marked change in the Raman spectral characteristics rather than the spectral shift anticipated in the case of the deuteration of the amino protons.

(6) Raman bands of the cobalt(III) complexes with the quadridentate ligands are classified into four categories similar to those of the tris(bidentate)cobalt(III) complexes: totally symmetric stretching vibration mode (420 - 670 cm^{-1}), stretching vibration mode excluding the totally symmetric one (i.e., non-totally symmetric one) (390 - 450 cm^{-1}), skeletal bending deformation mode (300 - 420 cm^{-1}), and chelate ring deformation mode (240 - 290 cm^{-1}). The polarized Raman bands at 400 - 510 cm^{-1} are regarded as characteristic of the cobalt(III) complexes with the quadridentate ligands, because they are not observed for

the tris(bidentate)cobalt(III) complexes and the bis(terdentate)conbalt(III) ones.

(7) The cis-α and cis-β isomers of the [Co(trien)(bidentate)]-type complexes show different Raman spectral feature in each skeletal vibration region and the Raman spectra of the cis-β isomers are similar to those of the [Co(tren)(bidentate)]-type complexes. This fact suggests that the Raman spectra of the cis-β isomers of the [Co(trien)(bidentate)]-type complexes and those of the [Co(tren)(bidentate)]-type complexes are mainly regulated by the normal vibrational modes of meridional configuration of the quadridentate ligands. On the other hand, the Raman spectra of the cis-α isomers of the [Co(trien)(bidentate)]-type complexes are similar to each other. Moreover, the cis-α isomers of the [Co(edda)(bidentate)]-type complexes also exhibit the Raman spectral characteristics similar to each other. Hence, we can state that the Raman spectra of the [Co(quadridentate)(bidentate)]-type complexes depend mainly on the configuration of the quadridentate ligands.

(8) The Raman spectra of the bis(1,2-ethanediamine)cobalt(III) complexes containing sulfur donor atoms can be treated as in the case of the tris(bidentate)cobalt(III) complexes with the N and/or O donor atoms. Their Raman bands can be assigned to the totally symmetric stretching vibration mode, the stretching vibration mode excluding the totally symmetric one (i.e., non-totally symmetric one), the skeletal bending deformation mode, and the chelate ring deformation mode from the higher

frequency region. The Raman bands in the totally symmetric stretching vibration mode region appear at the lower frequency compared with that of $[Co(en)_3]^{3+}$. This fact suggests the existence of the mass effect owing to distinction between nitrogen and sulfur donor atoms and/or the difference in the central metal-donor atom bond strength.

(9) The cobalt(III) complexes with the branched terdentate ligands have no Raman bands caused by the skeletal breathing vibration mode which are regarded as characteristic bands for the cobalt(III) complexes with the linear terdentate ligands. It seems that the cobalt(III) complexes with the branched terdentate ligands have a character for the skeletal vibration close to the cobalt(III) complexes with the bidentate ligands rather than those with the linear terdentate ligands. The three geometrical isomers for each of $[Co(DL\text{-}asp)(dien)]^+$, $[Co(DL\text{-}asp)_2]^-$, $[Co(L\text{-}smc)_2]^+$ and $[Co(L\text{-}met)_2]^+$ exhibit the Raman spectral characteristics similar to one another. The difference of the chelate ring arrangement have no marked influence on the Raman spectra of the cobalt(III) complexes with the branched terdentate ligands.

In conclusion, Raman spectroscopy is considered very useful spectroscopic method for the investigation of stereochemistry and differentiation between the geometrical isomers of cobalt(III) complexes.

References

1) E. B. Wilson, Jr., J. C. Decius, and P. C. Cross, "Molecular Vibrations - The Theory of Infrared and Raman vibrational Spectra," McGraw-Hill, New York, 1955.

2) a) T. Shimanouchi and I. Nakagawa, Spectrochim. Acta, 18, 89, (1962).

b) T. Shimanouchi, Pure and Appl. Chem., 7, 131 (1963).

c) T. Shimanouchi and I. Nakagawa, Inorg. Chem., 3, 1805 (1964).

d) I. Nakagawa and T. Shimanouchi, Spectrochim. Acta, 22, 759 (1966).

e) I. Nakagawa and T. Shimanouchi, Spectrochim. Acta, 22, 1707 (1966).

f) I. Nakagawa and T. Shimanouchi, Spectrochim, Acta, Part A, 23, 2099 (1967).

g) I. Nakagawa, Bull. Chem. Soc. Jpn., 46, 3690 (1973).

3) T. Shimanouchi, J. Chem. Soc. Jpn., Pure Chem. Sec. 74, 266 (1953).

4) W. A. Yeranos, Inorg. Chem., 7, 1259 (1968).

5) K. H. Schmidt and A. Müller, J. Mol. Struct., 22, 343 (1974).

6) H. Ogino and J. Fujita, Bull. Chem. Soc. Jpn., 48, 1836 (1975).

7) J. C. Bailar, Jr. and J. B. Work, J. Am. Chem. Soc., 68, 232 (1946).

8) G. R. Brubaker and D. P. Schaefer, Inorg. Chem., 10, 2170 (1971).

9) M. Ogawa, Y. Shimura, and R. Tsuchida, Nippon Kagaku

Zasshi, 81, 72 (1960).

10) N. Matsuoka, J. Hidaka, and Y. Shimura, Bull. Chem. Soc. Jpn., 45, 2491 (1972).

11) M. B. Ćelap, S. R. Niketić, T. J. Janjić, and V. N. Nikolić, Inorg. Chem., 6. 2063 (1967).

12) F. R. Keen and G. H. Seale, Inorg. Chem., 11, 148 (1972).

13) Y. Yoshikawa and K. Yamasaki, Bull. Chem. Soc. Jpn., 45, 179 (1972).

14) T. Yasui, T. Shikiji, N. Koine, T. Ama, and H. Kawaguchi, Bull. Chem. Soc. Jpn., 60, 595 (1987).

15) K. Okamoto, J. Hidaka, and Y. Shimura, Bull. Chem. Soc. Jpn., 48, 2456 (1975).

16) a) T. Yasui, H. Kawaguchi, and T. Ama, Chem. Lett., 1983, 1277.

b) T. Ama, H. Kawaguchi, T. Yasui, K. Matsumoto, and S. Ooi, Bull. Chem. Soc. Jpn., 58, 2561 (1985).

17) T. Ama, H. Kawaguchi, and T. Yasui, Bull. Chem. Soc. Jpn., 59, 1471 (1986).

18) J. Hidaka, Y. Shimura, and R. Tsuchida, Bull. Chem. Soc. Jpn., 35, 567 (1962).

19) K. Okamoto, J. Hidaka, and Y. Shimura, Bull. Chem. Soc. Jpn., 46, 3134 (1973).

20) Presented at the Symposium by the Chemical Society of Japan, Kochi, 1984, Abstract, p. 91.

21) T. Ama, R. Niiyama, H. Kawaguchi, and T. Yasui, Bull. Chem. Soc. Jpn., 60, 119 (1987).

22) T. Yasui, H. Kawaguchi, N. Koine, and T. Ama, Bull. Chem. Soc. Jpn., 56, 127 (1983).

23) H. Kawaguchi, T. Ama, and T. Yasui, Bull. Chem. Soc. Jpn., 57, 2422 (1984).

24) T. Ama, H. Kawaguchi, and T. Yasui, Chem. Lett., 1981, 323.

25) D. P. Schaefer and G. R. Brubaker, Inorg. Chem., 8, 1794 (1969).

26) Y. Yoshikawa, N. Kato, Y. Kimura, S. Utsuno, and G. N. Natu, Bull. Chem. Soc. Jpn., 59, 2123 (1986).

27) G. R. Brubaker and D. P. Schaefer, Inorg. Chem., 10, 968 (1971).

28) a) G. A. Bottomley, L. G. Glossop, B. W. Skelton, and A. H. White, Aust. J. Chem., 32, 285 (1979).
b) K. Akamatsu, T. Komorita, and Y. Shimura, Bull. Chem. Soc. Jpn., 54, 3000 (1981).

29) J. I. Legg and D. W. Cooke, Inorg. Chem., 4, 1576 (1965).

30) J. I. Legg, D. W. Cooke, and B. E. Douglas, Inorg. Chem., 6, 700 (1967).

31) H. Nakazawa, H. Ohtsuru, and H. Yoneda, Bull. Chem. Soc. Jpn., 60, 525 (1987).

32) P. F. Coleman, J. I. Legg, and J. Steele, Inorg. Chem., 9, 937 (1970).

33) K. Akamatsu, T. Komorita, and Y. Shimura, Bull. Chem. Soc. Jpn., 55, 2390 (1982).

34) T. Konno, Ph. D. Thesis, University of Tsukuba, 1985.

35) R. C. Elder, L. R. Florian, R. E. Lake, and A. M.

Yacynych, Inorg. Chem., 12, 2690 (1973).

36) K. Hori, Bull. Chem. Soc. Jpn., 48, 2209 (1975).

37) I. K. Adzamli, K. Libson, J. D. Lydon, R. C. Elder, and E. Deutsch, Inorg. Chem., 18, 303 (1979).

38) B. A. Lange, K. Libson, E. Deutsch, and R. C. Elder, Inorg. Chem., 15, 2985 (1976).

39) R. C. Elder, G. J. Kennard, M. D. Payne, and E. Deutsch, Inorg. Chem., 17, 1296 (1978).

40) J. I. Legg and D. W. Cooke, J. Am. Chem. Soc., 89, 6854 (1967).

41) S. Yamada, J. Hidaka, and B. E. Douglas, Inorg. Chem., 10, 2187 (1971).

42) K. Okamoto, K. Wakayama, H. Einaga, S. Yamada, and J. Hidaka, Bull. Chem. Soc. Jpn., 56, 165 (1983).

43) J. Hidaka, S. Yamada, and Y. Shimura, Chem. Lett., 1974, 1487.

44) T. Shimanouchi, "Computer Programs for Normal Coordinate Treatment of Polyatomic Molecules" The University of Tokyo, 1968.

45) a) Y. Omura, I. Nakagawa, and T. Shimanouchi, Spectrochim. Acta, Part A, 27, 2227 (1971).

b) M. M. Chamberlain and J. C. Bailar, Jr., J. Am. Chem. Soc., 81, 6412 (1959).

c) P. E. Merritt and S. E. Wiberley, J. Phys. Chem., 59, 55 (1955).

d) M. L. Morris and D. H. Busch, J. Am. Chem. Soc., 82, 1521 (1960).

e) M. E. Baldwin, J. Chem. Soc., 1960, 4369.

f) M. N. Hughes and W. R. McWhinnie, J. Inorg. Nucl. Chem., 28, 1659 (1966).

46) G. Borch, P. H. Nielsen, and P. Klaeboe, Acta Chem. Scand., Series A, 31, 109 (1977).

47) K. Hakamata, A. Urushiyama, J. Degen, H. Kupka, and H. -H. Schmidtke, Inorg. Chem., 22, 3519 (1983).

48) a) K. Krishnan and R. A. Plane, Inorg. Chem., 5, 852 (1966).

b) P. Stein, V. Miskowski, W. H. Woodruff, J. P. Griffin, K. G. Werner, B. P. Gaber, and T. G. Spiro, J. Chem. Phys., 64, 2159 (1976).

49) J. Gouteron-Vaissermann, Compt. Rend. Acad. Sci. Paris, Ser. B, 275, 149 (1972).

50) K. Rasmussen, Spectrochim. Acta, Part A, 30, 1763 (1974).

51) K. Nakamoto, "Infrared and Raman Spectra of Inorganic and Coordination Compounds," 3rd ed, Wiley-Interscience, New York (1977), Part III.

52) K. Kanamori and K. Kawai, Bull. Chem. Soc. Jpn., 53, 2520 (1980).

53) K. Kanamori and K. Kawai, Bull. Chem. Soc. Jpn., 55, 764 (1982).

54) K. Kanamori, H. Ichinose, and K. Kawai, Bull. Chem. Soc. Jpn., 55, 1315 (1982).

55) K. Kanamori, I. Bansho, K. Kawai, K. Akamatsu, and Y. Shimura, Bull. Chem. Soc. Jpn., 58, 943 (1985).

56) K. Kanamori, Y. Nunomura, M. Takashima, K. Nagata, K.

Kawai, and J. Hidaka, Bull. Chem. Soc. Jpn., 58, 92 (1985).

57) K. Kanamori, T. Morikawa, and K. Kawai, Bull. Chem. Soc. Jpn., 53, 2787 (1980).

58) K. Kanamori, and K. Kawai, Inorg. Chem., 25, 3711 (1986).

59) T. F. Maruyama, K. Okamoto, J. Hidaka, and H. Einaga, Bull. Chem. Soc. Jpn., 56, 2610 (1983).

60) T. Nomura, F. Marumo, and Y. Saito, Bull. Chem. Soc. Jpn., 42, 1016 (1969).

61) P. G. Beddoe, M. J. Harding, S. F. Mason, and B. J. Peart, J. Chem. Soc., Chem. Commun., 1971, 1283.

62) J. B. Work, Inorg. Synth., 2, 221 (1946).

63) J. Bjerrum and J. P. McReynolds, Inorg. Synth., 2, 216 (1946).

64) M. Kobayashi, F. Marumo, and Y. Saito, Acta Crystallogr., Sect. B, 28, 470 (1972).

65) K. Okiyama, S. Sato, and Y. Saito, Acta Crystallogr., Sect. B, 35, 2389 (1979).

66) K. Kanamori, unpublished results.

67) T. E. Haas and J. R. Hall, Spectrochim. Acta, 22, 988 (1966).

68) H. Siebert and H. H. Eysel, J. Mol. Struct., 4, 29 (1969).

69) T. W. Swaddle, P. J. Craig, and P. M. Boorman, Spectrochim. Acta, Part A, 26, 1559 (1970).

Acknowledgement

The author wishes to express his deepest gratitude to Professor Jinsai Hidaka for his expert guidance and constant warm encouragement during this work. He is also grateful to Dr. Hisahiko Einaga and Dr. Ken-ichi Okamoto for their many helpful discussions and advices. He wishes to thank Professor Takaji Yasui, Dr. Kan Kanamori, and Dr. Takumi Konno for their several helpful discussions. He also wishes to thank Dr. Masayo Nomoto and Mrs. Youko Koizumi for their warm moral support and encouragement.

He would also like to thank all his collaborators who contributed to this work with their assistances and advices.